Identification of novel nuclear factors required for chloroplast gene expression and photosystem I assembly

Dissertation

zur Erlangung des Doktorgrades der Fakultät für Biologie

der Ludwig-Maximilians-Universität München

vorgelegt von

Lina Lezhneva

aus Minsk, Weißrußland

2005

1. Gutachter: Prof. Dr. Reinhold G. Herrmann

2. Gutachter: Prof. Dr. H. Scheer

Tag der mündlichen Prüfung: 14.07.2005

Abbreviations

μE	microeinstein (1 E = 1 mol of photons)
Å	Ångstrom
A_0	PSI primary electron acceptor composed of chlorophyll *a*
A_1	PSI secondary electron acceptor composed of phylloquinone
ATP	adenosine 5′-triphosphate
bp	base pairs
BSA	bovine serum albumin
cDNA	complementary DNA
CES	control by epistasy of synthesis
Ci	Curie
cpm	counts per minute
DNA	deoxyribonucleic acid
dNTPs	deoxynucleoside triphosphates
EDTA	ethylenediaminetetraacetic acid
EGTA	ethylene glycol-bis(2-aminoethylether)-*N*,*N*,*N*_,*N*_-tetraacetic acid
EMS	ethyl methanesulfonate
ESTs	expressed sequence tags
F_A	[4Fe-4S] cluster on PsaC subunit
F_B	[4Fe-4S] cluster on PsaC subunit
FTR	ferredoxin-thioredoxin reductase
F_x	interpolypeptide [4Fe-4S] cluster between PsaA and PsaB subunits
g	gravity force, gramme
GTP	guanosine 5′-triphosphate
hcf	high chlorophyll fluorescence
HEPES	N-[2-Hydroxyethyl]piperazine-N'-[2-ethanesulfonic acid]
K	Kelvin
kb	kilobases
kDa	kilodalton
LHCI	chlorophyll-binding PSI light-harvesting complex
Mb	megabases
MES	2-Morpholinoethanesulfonic acid
MOPS	3-[N-Morpholino]propanesulfonic acid

mRNA	messenger RNA
$NADP^+$	nicotinic adenine dinucleotide phosphate
NPQ	non-photochemical chlorophyll *a* fluorescence quenching
P700	PSI primary electron donor chlorophyll *a*
PAM	pulse amplitude–modulated fluorometer
PCR	polymerase chain reaction
PEG	polyethylene glycol
PSI	photosystem I
PSII	photosystem II
PVDF	polyvinylidene difluoride
qP	photochemical chlorophyll *a* fluorescence quenching
RF	release factor
RNA	ribonucleic acid
rpm	revolutions per minute
rRNA	ribosomal RNA
RT-PCR	reverse transcription PCR
S	svedberg unit
SD	standard deviation
SDS	sodium dodecyl sulfate
SDS-PAGE	SDS-polyacrylamide gel electrophoresis
SSLP	simple sequence length polymorphism
Suc	sucrose
T-DNA	transferred DNA
Tricine	N-Tris-(hydroxymethyl)-methylglycine
Tris	Tris-(hydroxymethyl)-aminomethane
tRNA	transfer RNA
Tween	polyoxyethylenesorbitan monolaurate
U	unit, enzyme activity
UTR	untranslated region
v/v	volume per volume
w/v	weight per volume

Contents

1 Introduction

1.1 Evolution, development and function of chloroplasts

Chloroplasts or related organelles are the characteristic organelles of photoautotrophic eukaryotes. Performing important reactions of nitrogen, sulphur and lipid metabolism as well as photosynthesis, the process of transformation of light energy into chemical energy of hydrocarbonate bonds of sugars accompanied by carbon dioxide fixation and evolvement of molecular oxygen in the biosphere, chloroplasts form the basis of life on Earth.

1.1.1 Evolution of chloroplasts

Phylogenetically chloroplasts of green algae and land plants evolved through the engulfment of an ancestor of presently-living cyanobacteria by a phagotrophic host resulting in primary endosymbiosis and eukaryotism (Mereschkowsky 1905; Herrmann 1997; Douglas 1998; Martin *et al*., 1998; McFadden 2004). Genome sequencing projects provided data on comparisons of gene sequences, gene content and gene arrangement in chloroplasts, cyanobacteria and eukaryotes supporting the idea of single (monophyletic) primary endosymbiosis against the hypothesis of multiple (polyphyletic) partnerships between a prokaryote and an eukaryote (McFadden 2004). On the other hand, many algae and even presently non-photosynthetic lineages acquired chloroplasts indirectly through multiply occurring secondary endosymbiosis, when the products of primary endosymbiosis were engulfed by phagotrophic eukaryotes (Herrmann 1997; Douglas 1998; Palmer 2003; Forth and McFadden, 2003).

During the course of evolution, the endosymbionts lost their independence and were converted to plant organelles. Multiple gene transfers from the genome of the endosymbiont to the host nucleus occurred (Herrmann 1997; Martin and Herrmann, 1998; Martin *et al*., 1998; Richly and Leister, 2004; Timmis *et al*., 2004) establishing genetic and biochemical interdependence of the compartmentalized genetic systems of chloroplasts, mitochondria and nucleus (Herrmann *et al*., 2003). The nucleus plays a major regulatory role in the newly arisen integrated system (Herrmann 1997; Barkan and Goldschmidt-Clermont, 2000; Herrmann and Westhoff, 2001; Rochaix 2004). However, organelles also contribute to the intergenomic communication (Roussell *et al*., 1991; Martinez-Zapater *et al*., 1992; Sakamoto *et al*., 1996;

Hedtke *et al*., 1999; Peltier and Cournac, 2002; Raghavendra and Padmasree, 2003; Gray *et al*., 2003). The genome interdependence must have put constraints on evolutionary changes of the whole genetic system since mutational pressure on one genetic compartment could cause alterations in the whole system, and mutation could only be selected if it was favourable for functioning of all genetic compartments (Herrmann *et al*., 2003). Subtle and specific interaction of genetic compartments during co-evolution of the genome and plastome (plastid genome) could contribute to the origin of cross-barriers between species and lead finally to speciation (Herrmann *et al*., 2003; Stubbe 1989). At the plastome level, regions coding for structural genes are highly conserved.

Plastids are inherited according to non-Mendelian rules, uniparentally in most of species or biparentally (e.g. in *Oenothera*, *Pelargonium*; Hagemann 1992; Birky 2001), their proliferation occurs exclusively by division of pre-existing plastids and never *de novo* (Butterfass 1980).

1.1.2 Plastid development

Ontogenetically chloroplasts of higher plants are formed in the presence of light from undifferentiated types of plastids, proplastids, located in meristematic cells of etioplasts. In the absence of light, proplastids develop into etioplasts which turn into chloroplasts under illumination. Developed chloroplasts possess a complex thylakoid membrane system consisting of grana stacks interconnected by unstacked stroma lamellae. Proplastids can also give rise to chromoplasts, responsible mainly for coloration, or leucoplasts, storage forms of plastids, which can be differentiated further on to amyloplasts, proteinoplasts or elaioplasts based on the substance stored (Schnepf 1980; Vothknecht and Westhoff, 2001).

1.1.3 Function of plastids

A major function of chloroplasts is photosynthesis. This process consists of two sequential stages, primary photochemical reactions occurring in the specialized protein complexes located in the thylakoids and biochemical dark reactions occurring in the stroma. Beyond that, metabolism of amino acids, fatty acids and lipids as well as nitrate and sulfate assimilation, biosynthesis of carotenoids and tetrapyrrols and synthesis of plant hormones, nucleotides and vitamins occur in plastids.

1.2 Biogenesis and structure of photosynthetic complexes of thylakoid membranes

The light stage of photosynthesis involves the functioning of multisubunit complexes of photosystem (PS) I and II with associated light-harvesting antennae, cytochrome b_6f complex, ATP synthase and NAD(P)H dehydrogenase (NDH) complex (Shikanai *et al*., 1998; Wollman *et al*., 1999; Herrmann and Westhoff, 2001).

1.2.1 Photosystem I

The pigment-protein complex operates as a light-driven plastocyanin-ferredoxin oxidoreductase in cyanobacteria, algae and vascular plants. During oxygenic photosynthesis, PSI is involved in cyclic and non-cyclic electron transport (Chitnis 2001; Munekage *et al*., 2002, 2004). Resolving the crystal structure of cyanobacterial (2.5 Å) and plant (4.4 Å) PSI showed quite similar core complex composition (Ben-Shem *et al*., 2003; Jordan *et al*., 2001). In higher plants 15 subunits which are highly conserved among photosynthetic organisms comprise PSI (Figure 1). In contrast, the structure of the peripheral antennae and the supercomplex organisation are completely different between eukaryotes and cyanobacteria. Whereas cyanobacterial PSI complexes form a trimer, the eukaryotic complex is present as a monomer associated to the outer chlorophyll-binding antenna proteins Lhca1-Lhca4 (Baymann *et al*., 2001; Scheller *et al*., 2001; Germano *et al*., 2002). Recently, additional Lhca5 protein was shown to be also associated with PSI (Ganeteg *et al*., 2004).

The functions of various PSI subunits have been identified (Scheller *et al*., 2001). Two major subunits, PsaA and PsaB, are plastid-encoded, form the central heterodimer and serve as anchors for binding cofactors necessary for light absorbance and the primary photochemical reactions. PsaA and PsaB bind pairs of the primary electron donor and acceptor chlorophylls, P700 and A_0, respectively, the phylloquinone A_1 and the [4Fe-4S] cluster F_x. The other two [4Fe-4S] clusters (F_A and F_B) are bound to plastid-encoded PsaC and transfer electrons from F_x to ferredoxin. Additional chlorophyll molecules are associated with the core complex and the outer antenna proteins Lhca1-Lhca4 and involved in light absorbing and energy transfer (Saenger *et al*., 2002; Golbeck, 2003).

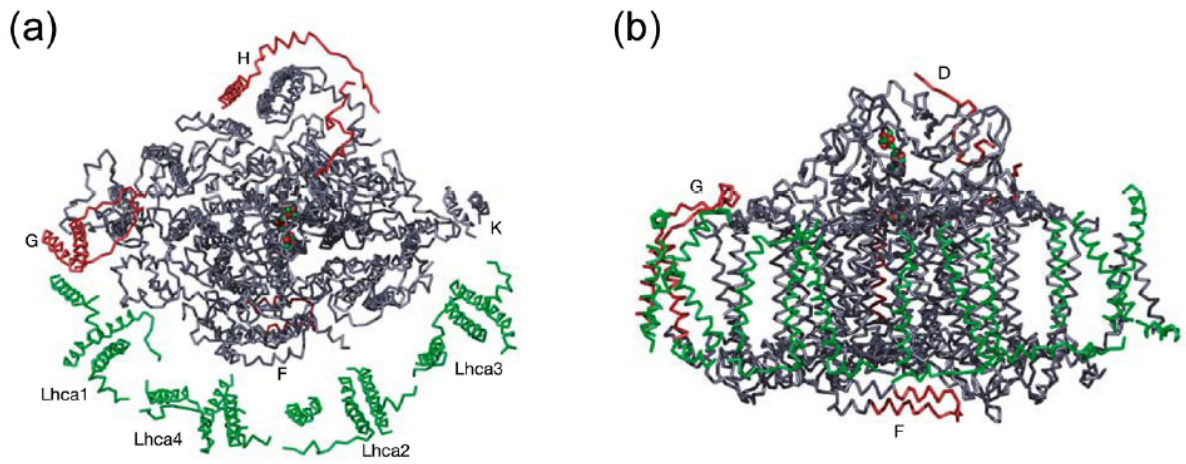

Figure 1. The structural model of PSI organisation in plants (Ben-Shem *et al*., 2003). In grey - conserved subunits of the reaction centre. In red – structural elements that are not present in cyanobacteria. In green - the four subunits of the PSI light harvesting complex (LHCI) Lhca1–Lhca4. Red and green balls - the Fe and S atoms of the three [4Fe-4S] clusters, respectively. D, F, G, H and K represent the PsaD, PsaF, PsaG, PsaH and PsaK subunits of the reaction centre. **(a)** View from the stromal side of the thylakoid membrane. **(b)** View from the LHCI side.

Disruption of either the PsaA or PsaB subunit leads to loss of PSI activity and rapid degradation of other subunits within the core complex (Smart *et al*., 1991; Smart and McIntosh, 1993; Redding *et al*., 1999). The lack of PsaC causes a loss of PsaD and PsaE subunits in *Synechocystis* (Yu *et al*., 1995) and complete PSI deficiency in *Chlamydomonas* (Takahashi *et al*., 1991; Redding *et al*., 1999).

The correct association of chlorophyll and the three [4Fe-4S] clusters in PSI is critical for the function and the stability of the PSI reaction centre (Eichacker *et al*., 1990; Mullet *et al*., 1990; Smart *et al*., 1993; Kim *et al*., 1994; Mehari *et al*., 1995; Rodday *et al*., 1995; Yu *et al*., 1997). Site-directed mutagenesis has shown that only those PsaC proteins that bind the two [4Fe-4S] clusters are capable of assembling into PSI cores *in vivo* (Jung *et al*., 1997; Yu *et al*., 1997). However, the biosynthesis of timeric P700-A_1 cores in cyanobacteria can occur also in the absence of the three [4Fe-4S] clusters (Shen *et al*., 2002).

Several proteins that do not constitute structural compounds of PSI but play important roles in the stability or assembly of PSI have been identified (Schwabe and Kruip, 2000; Rochaix *et al*., 2004). Among those are RubA (Shen *et al*., 2002), Ycf3 (Boudreau *et al*., 1997; Ruf *et al*., 1997), Ycf4 (Boudreau *et al*., 1997), Ycf37 (Wilde *et al*., 2001), BtpA (Zak and Pakrasi, 2000), and Chl27, Crd1 and Cth1 (Moseley *et al*., 2002; Tottey *et al*., 2003).

1.2.2 Photosystem II, cytochrome b_6f and chloroplast ATP synthase complexes

PSII is a dimeric multisubunit pigment-protein complex performing light-induced electron transfer to plastoquinone and photosynthetic water-splitting reactions leading to oxygen evolution (Hankamer *et al*., 1997). The crystal structure of the cyanobacterial PSII complex at 3.7 Å resolution (Kamiya and Shen, 2003) and high-resolution electron microscopy of chloroplast PSII at 6 Å resolution (Rhee, 2001) showed that the primary organisation of PSII between cyanobacteria and higher plants is also basically conserved. Differences are observed in some peripheric PSII subunits as well as in the antenna and water splitting complex composition (Hankamer *et al*., 2001; Barber and Nield, 2002; Kashino *et al*, 2002). The crystal structure of plant major light-harvesting complex has recently been resolved at 2.72 Å (Liu *et al*., 2004).

The electron flow between the two photosystems is mediated by the pigment-protein cytochrome b_6f complex which functions as a plastoquinol-plastocyanin-oxidoreductase. Cytochrome b_6f contributes also to the formation of the proton gradient used to synthesize ATP and is involved in cyclic electron transport around PSI. In cyanobacteria but probably not in higher plants, plastocyanin can be substituted by cytochrome c_6 (Weigel *et al*., 2003). The crystal structure of the cytochrome b_6f complex has been resolved for unicellular algae (Stroebel *et al*., 2003) and cyanobacteria (Kurisu *et al*., 2003), and a revealed dimeric structure is essentially the same in both organisms.

Light-dependent electron transport from water to $NADP^+$ creates the potential energy which is stored in a transmembrane electrochemical proton gradient and used by the chloroplast ATP synthase to produce ATP (photophosphorylation). The basic organization, structure and composition of the ATP synthase protein complex are vastly conserved between eubacteria, mitochondria and plastids (Strotmann *et al*., 1998; Groth and Pohl, 2001), whereas the regulation of the enzymatic activity of chloroplast ATP synthase from higher plants and green algae differs form its prokaryotic and mitochondrial counterparts (Strotmann *et al*., 1998; Groth and Strotmann, 1999).

1.3 Role of nuclear-encoded factors in the expression of chloroplast genes

In contrast to the protein structure of the photosynthetic complexes which is basically conserved between chloroplasts and cyanobacteria, mRNA processing of chloroplasts

changed dramatically during integration of chloroplasts into new regulatory networks which arose between compartments of the eukaryotic cell. In particular, chloroplast transcripts undergo extensive post-transcriptional modifications, e.g. splicing and editing, some of them new. Also, although chloroplasts overtook from prokaryotes processes of exo- and endoribonucleolytic cleavage and modulation of mRNA stability, these processes acquired a number of new features in plastids. Thus, gene expression of chloroplasts differs significantly from that of both prokaryotes and eukaryotes.

As a result of the endosymbiotic gene transfer, protein complexes of the photosynthetic membrane system consist of subunits encoded by the plastid and nuclear genomes. Therefore, biosynthesis, assembly and association of these chimeric protein complexes with cofactors require the coordinated expression of chloroplast and nuclear genes. The nuclear genome encodes the majority of chloroplast proteins. Therefore, this genetic compartment plays a principal role in the regulation of chloroplast gene expression (Herrmann and Westhoff, 2001; Rochaix, 2004).

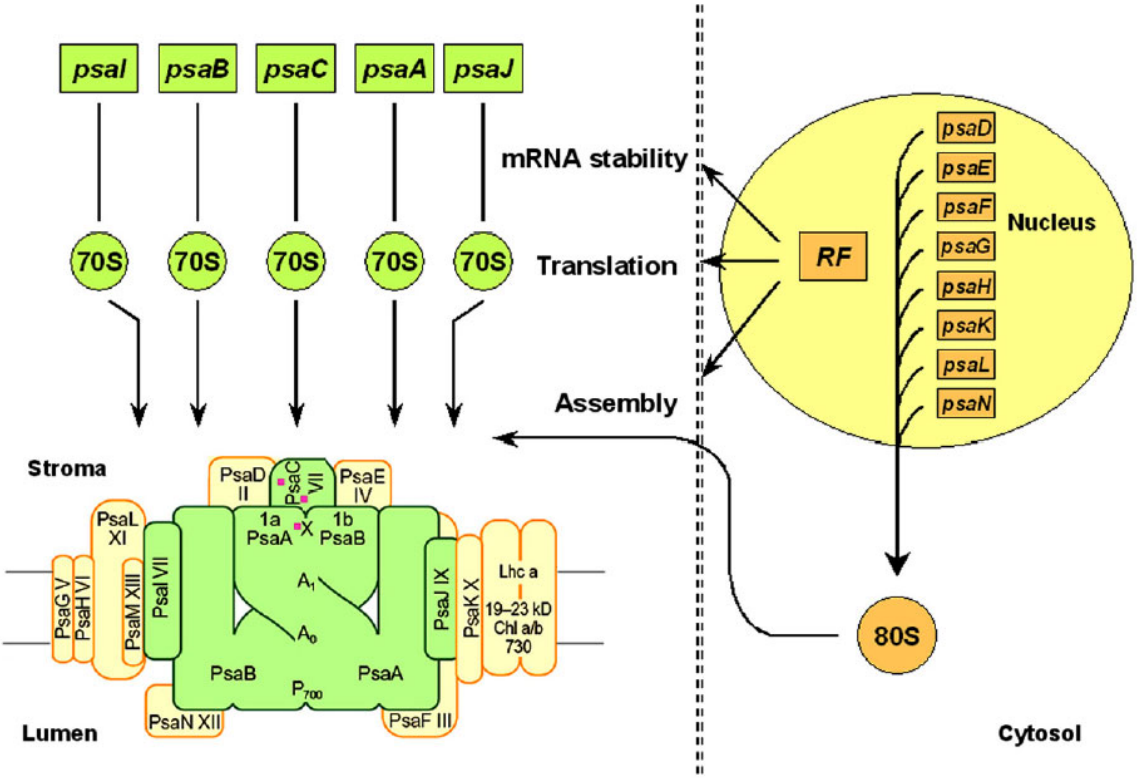

Figure 2. Scheme of PSI biosynthesis. PSI consists of the chloroplast-encoded subunits PsaA, PsaB, PsaC, PsaI and PsaJ (green) and the nuclear-encoded subunits PsaD, PsaE, PsaF, PsaG, PsaH, PsaK, PsaL, PsaN and PsaO (yellow). Nuclear-encoded factors control expression of the chloroplast genes mainly at the post-transcriptional level and regulate assembly of the PSI complex. Pink squares – the three [4Fe-4S] clusters, bound to PsaA, PsaB and PsaC. 70S - chloroplast ribosome; 80S – cytoplasmic ribosome. *RF* – regulatory factors.

Chloroplast development is primarily accompanied by global changes in transcript levels (Gruissem, 1989; Mullet, 1993) which are regulated by both transcription and turn-over rates. Transcription rates depend on light, tissue and cell type and undergo endogenous circadian rhythms and redox controls (Allison, 2000). Nuclear-encoded sigma-like transcription factors appear to regulate the activity of the plastid-encoded RNA polymerase (Allison, 2000; Tanaka *et al*., 1996), and nuclear-encoded phage-type RNA polymerases are involved in the regulation of plastid transcription (Hedtke *et al*., 2002).

mRNA stability is regulated for fine tuning of transcript levels (Barkan and Goldschmidt-Clermont, 2000; Monde *et al*., 2000), during development (Klaff and Gruissem, 1991; Rapp *et al*., 1992; Baumgartner *et al*., 1993), by the redox state (Salvador and Klein, 1999), magnesium concentration (Horlitz and Klaff, 2000), light and endogenous rhythms (Salvador *et al*., 1993), heat-bleaching (Thomas and Ortiz, 1995), or by the cell type (Kubicki *et al*., 1994).

mRNA stability is often mediated by untranslated regions (UTRs) of the messages (Monde *et al*., 2000). Through biochemical assays, RNA binding proteins and multisubunit complexes possessing mRNA processing activities and/or interacting with 5' UTRs, 3' UTRs or poly(A) tails of mRNA were reported (Alexander *et al*., 1998; Baginsky *et al*., 2001; Schuster and Bock, 2001; Sugita and Sugiura, 1996; Yang *et al*., 1996). Nonetheless, the ability to bind transcripts does not provide clues to the precise function of the protein.

First nuclear genes involved in plastid mRNA stability have been isolated only recently (Boudreau *et al*., 2000; Vaistij *et al*., 2000a; Felder *et al*., 2001; reviewed in Nickelsen 2003). The two orthologous gene products of *hcf107* and *mbb1* in *Arabidopsis* (Felder *et al*., 2001) and *Chlamydomonas* (Vaistij *et al*., 2000a), respectively, and the Nac2 protein (Boudreau *et al*., 2000) contain tetratricopeptide repeat motifs, which are supposed to mediate protein-protein interactions, indicating that protein complexes appear to play substantial roles in both stabilisation of plastid transcripts and translation (Nickelsen *et al*., 1999; Ossenbühl and Nickelsen, 2000).

1.4 Chloroplast translation

The chloroplast translation machinery is quite complex. On the one hand, it has inherited a number of prokaryotic components, such as ribosomal proteins and rRNAs, tRNAs, aminoacyl tRNA synthetases, initiation (IF1-3) and elongation factors (EF-Tu and

EF-G) from cynobacterial ancestors (Sugiura *et al*., 1998). A chloroplast ribosome recycling factor is functional also in *Escherichia coli* (Rolland *et al*., 1999). On the other hand, several features differ in the plastid translation system from that of eubacteria: (i) novel subunits specific for chloroplast ribosomes have been identified (Yamaguchi and Subramanian, 2000, 2003); (ii) Shine-Dalgarno sequences are often missing in 5' UTRs of plastid transcripts (Sugiura *et al*., 1998); (iii) translationally competent monocistronic transcripts are produced by extensive intramolecular cleavage of polycistronic transcripts as well as by splicing and editing events (Barkan and Goldschmidt-Clermont, 2000); (iv) nuclear-encoded protein factors specifically regulate translational processes of plastid messages (McCormac and Barkan 1999; Rattanachaikunsopon *et al*., 1999; Zerges, 2000; Cohen *et al*., 2001; Dauvillée *et al*., 2003; Zerges *et al*., 2003); (v) chloroplast translation is light-dependent (Bruick and Mayfield, 1999) and mediated by a number of mRNA-binding proteins (Fedoroff, 2002); (vi) the CES (control by epistasy of synthesis) process during which chloroplast translation is regulated by the assembly of thylakoid membrane complexes has been described from *Chlamydomonas* chloroplasts (Stampacchia et al., 1997; Choquet and Wollman 2002; Wostrikoff *et al*., 2004).

Furthermore, the proposed ribosomal scanning on the 5′ UTRs of plastid transcripts, the assumed interaction of chloroplast transcript extremities and the presence in chloroplast of poly(A) binding protein of eukaryotic origin interacting with the 5′ UTRs of plastid mRNAs (Yohn *et al*., 1998) demonstrate similarities between the plastid and eukaryotic translation systems (Zerges 2000).

1.5 *Arabidopsis thaliana* is a model organism for the study of chloroplast biogenesis

To identify nuclear factors specifically involved in the control of chloroplast gene expression and organell biogenesis, powerful genetic approaches in the organisms *Chlamydomonas*, maize and *Arabidopsis* are available (Meurer *et al*., 1996b; Barkan and Goldschmidt-Clermont, 2000).

Arabidopsis thaliana, a member of the mustard (*Brassicaceae*) family, has become a very popular model for plant cellular and molecular biology studies. Its small size, a short life cycle (6 - 8 weeks), the ability to self-fertilize and to produce a large number of seeds make possible easy cultivation of large progeny in restricted space and time.

Due to a relatively small genome size (five chromosomes comprising 125 Mb), *Arabidopsis* was the first plant chosen for complete sequencing of a plant nuclear genome. The sequenced regions of the genome (115.4 Mb) contain 25,498 genes encoding proteins which belong to 11,000 families (Arabidopsis Genome Initiative, 2000). The number of partial *Arabidopsis* cDNA sequences, or expressed sequence tags (ESTs) amounts 322,651 (December 10, 2004).

To understand, which genes are important for chloroplast functioning, a forward genetics approach linking a phenotype of interest to a corresponding genotype is widely pursued. For this purpose a large, steadily growing number of mutants has been induced chemically, (e.g. via ethyl methanesulfonate [EMS] treatment) or via tagging with mutagenic DNA elements (T-DNA and transposons; Feldmann 1991; Meurer *et al*., 1996b; Martienssen 1998; Krysan *et al*., 1999; Szabados *et al*., 2002; Alonso *et al*., 2003; Kuromori *et al*., 2004). T-DNAs and transposons carrying strong enhancers or promoters are also used for activation tagging and generation of gain-of-function mutants (Ichikawa *et al*., 2003; Nakazawa *et al*., 2003). A system of promoter trapping generates loss-of-function mutations and allows to identify genes by activation of a promoter-less reporter gene by the tagged gene promoter (Alvarado et al., 2004; Lindsey et al., 1993).

The available sequence information has provided means for generation of a large collection of PCR-based molecular markers (Konieczny and Ausubel, 1993; Lukowitz *et al*., 2000; Schmid *et al*., 2003) that can be used for positional (map-based) cloning of mutations.

Improved techniques for *Agrobacterium*-mediated nuclear transformation (Bechtold and Pelletier 1998; Clough and Bent, 1998) and selection of transformants (Hadi *et al*., 2002) allow functional complementation of a mutation with a wild-type genomic DNA or cDNA.

To assess gene function, information provided by EST- and genome sequencing can be used for large scale expression studies at the transcript and protein levels using transcriptomics (real-time RT-PCR, microarrays and gene chips) and proteomics (two-dimentional polyacrylamide gel electrophoresis and mass-spectrometry) approaches, respectively (Richmond and Somerville, 2000; Schubert *et al*., 2002; Zhu 2003; Buckhout and Thimm, 2003; Richly *et al*., 2003; Czechowski *et al*., 2004; Kleffmann *et al*., 2004;).

Sequencing of the *Arabidopsis* genome figured out that about 30% of the predicted gene products have no assigned function, therefore, reverse genetics approaches are widely used. Loss- or gain-of-function mutants of a gene of interest are searched for in already available mutant collections. In addition, corresponding antisense and over-expression lines are generated and powerful RNA interference (RNAi) gene silencing approaches are used to

obtain mutant phenotypes (Guo *et al*., 2003; Horiguchi *et al*., 2004). In addition, the TILLING (Targeting Induced Local Lesions in Genomes) strategy becomes a general approach for high-throughput identification of chemically-induced mutations in genes of interest (Henikoff *et al*., 2004).

In order to dissect chloroplast regulatory networks, it is profitable to evaluate several model organisms in parallel since differences in regulation of plastid gene expression are expected not only in phylogenetically unrelated material but also in closely related species (Stubbe 1989; Kushnir *et al*., 1991). Inactivation of homologous genes in *Chlamydomonas* and *Arabidopsis* can lead to quite different phenotypes (Vaistij *et al*., 2000a; Felder *et al*., 2001). Moreover, the pathways of regulation of chloroplast gene expession in lower and higher photoautotrophic eukaryotes appear to be substantially different in a number of instances (Nickelsen 1999).

1.6 Goals of the project

The aim of this work was to extend knowledge of the biogenesis of photosynthetic complexes and especially of PSI. Although some aspects of the structural organization of PSI and functions of the PSI subunits have been evaluated, molecular mechanisms of synthesis and assembly of the complex are largely unknown. The latter processes are extensively regulated at the post-transcriptional level by numerous nuclear-encoded factors. Therefore, a forward genetics approach was chosen. Since most, if not all nuclear genes encoding structural compounds of PSI are known (Legen *et al*., 2001), it is often possible to suggest already after initial mapping, whether the affected gene encodes an unknown regulatory protein.

The nuclear mutants of *Arabidopsis, hcf145, hcf109 and hcf101*, affected in photosynthesis were used as objects of my study. It was necessary (i) to identify and characterize the mutant phenotypes, (ii) to determine at which level of chloroplast gene expression the mutants were affected, (iii) to identify and characterize the nuclear-encoded product, and (iv) to perform functional analyses of the components.

2 Materials and methods

2.1 Materials

2.1.1 Chemicals, enzymes, radioactive substances, working materials and devices

Chemicals used in this work were usually of p.a. quality and, if not mentioned, were purchased from the following companies: Applichem (Darmstadt, Germany), Biozym (Oldendorf, Germany), Fluka (Steinhein, Germany), ICN Biomedicals GmbH (Eschwege, Germany), Merck (Darmstadt, Germany), Pharmacia (Uppsala, Sweden), Roth (Karlsruhe, Germany), Serva (Heidelberg, Germany), Sigma-Aldrich Chemie GmbH (Taufkirchen, Germany), and USB (Cleveland, USA).

Enzymes were obtained from Clontech (Palo Alto, USA), Invitrogen (Karlsruhe, Germany), MBI Fermentas (St. Leon-Rot, Germany), New England Biolabs (Frankfurt/Main, Germany), Promega (Mannheim, Germany), Qiagen (Hilden; Germany), Roche Diagnostics (Mannheim, Germany), and Stratagene (Heidelberg, Germany).

Radioactive nucleotides and [^{35}S]-methionine were purchased from Amersham Biosciences Europe GmbH (Freiburg, Germany).

Other materials were obtained from Biomol (Hamburg, Germany), Eppendorf (Hamburg, Germany), Greiner Bio-One GmbH (Frickenhausen, Germany), Millipore (Eschborn, Germany), Pall Bio Support Division (Dreieich, Germany), Qiagen (Hilden, Germany), and Schleicher and Schüll (Dassel, Germany). The manufacturers of commercial devices are mentioned in the text.

2.1.2 Plant material

The *hcf145* line, accession Wassilewskija, was originally identified in a T-DNA collection (Feldmann 1991) obtained from the Arabidopsis Biological Resource Centre (Ohio State University, Columbus, USA). The seeds of *Arabidopsis thaliana* mutants *hcf109* and *hcf101*, accession Columbia, were obtained from the EMS mutant collection of Dr. Jörg Meurer (Meurer *et al*., 1996a). Seeds of *Arabidopsis* ecotypes Columbia, Landsberg erecta and Wassilewskija, were obtained from Dr. Meurer as well.

2.1.3 Bacterial strains and vectors

E. coli DH5α (Bethesda Res. Lab., 1986)

Agrobacterium tumefaciens GV3101 (pMP90RK) (Koncz *et al*., 1994)

The vector pBluescript KSII+ (Stratagene, Heidelberg) was used for standard cloning. The plant binary expression vector pSEX001-VS (Reiss *et al*., 1996) was used for cloning of cDNAs under the control of the 35S RNA promoter of *Cauliflower mosaic virus* in complementation studies (Figure 3).

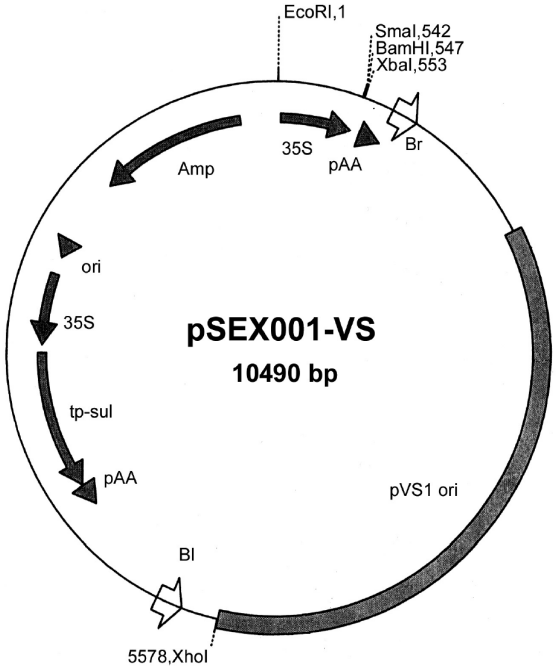

Figure 3. Map of the plant binary expression vector pSEX001-VS. EcoRI,1 – EcoRI site at nucleotide position 1; SmaI,542 – SmaI site at nucleotide position 542; BamHI,547 – BamHI site at nucleotide position 547; XbaI,552 – XbaI site at nucleotide position 552; 5578,XhoI – XhoI site at nucleotide position 5578; Br and Bl – *Agrobacterium* T-DNA right and left border sequences, respectively; 35S – CaMV 35S RNA promoter; pAA – polyadenylation signal from CaMV; ori – *E. coli* origin of replication; tp-sul – sulfonamide-resistance gene equipped with a chloroplast targeting peptide; Amp – ampicillin-resistance gene; pVS1 – *Agrobacterium* origin of replication.

2.1.4 Hybridisation probes

Hybridization probes are listed in Table 1. Additional plastid DNA probes were generated by amplifying specific regions of the *Arabidopsis* plastid chromosome (Table 2) using oligonucleotide primers synthesized by MWG-Biotech (Ebersberg, Germany).

Table 1. Hybridisation probes used for Northern analysis

Gene	Plasmid	Fragment	Reference
psaA	W3	BamHI/KpnI	Westhoff *et al*., 1991
psaC	pR668HSI	HincII/SspI	Kubicki *et al*., 1996
psaE	103N6T7	SalI/NotI	Arabidopsis Biological Resource Center (ABRC), Ohio State University Columbus, Ohio, USA
psbA	pSoP2520.3	PstI/XbaI	Westhoff *et al*., 1991
psbB	pSoP1927	BamHI/XbaI	Westhoff and Herrmann, 1988
psbK	pSoP3105	EcoRI/XhoII	Westhoff *et al*., 1991
psbZ	KGB2	BamHI/PvuII	Westhoff *et al*., 1991
atpA/trnR/trnG	pSoP1270	SalI/HindIII	P. Westhoff (Heinrich-Heine-Universitat, Düsseldorf, Germany)
ndhF	pR896PS	PstI/XbaI	Kubicki *et al*., 1996
rbcL	pSoP2458	PstI/BamHI	M. Streubel and P. Westhoff

2.1.5 Oligonucleotides

Table 2. Oligonucleotide primers used for amplification of genes and quantification of mRNAs

Experiment	Amplified gene	Primer designation	Primer sequence (5′→3′)
Northern analysis (*hcf145*)	*psaI*	psaI-f psaI-r	ccgcgcgtaatacgactcactataggagtaaatcgaggtacccct agcggatctaaacaatc
	ycf3 coding region	ycf3-f ycf3-r	gctatgcgactagaaattgacccc ctccttgttgaatggcctgttctc
	ycf3 intron	ycf3-intron-f ycf3-intron-r	ttgagcagcggtgtagcatca gagtttcctacctcatacggctcgac

Table 2. Oligonucleotide primers used for amplification of genes and quantification of mRNAs (continued)

Northern analysis (*hcf145*)	*ycf3-psaA* intergenic region	ycf3/psaA-i-f ycf3/psaA-i-r	tagcgcctttacattggtacac atctggtagtctctaggggtaagtagtac
	trnfM	trnfM-f trnfM-r	ttggatttgaaccaatgactcctg cggggtagagcagtttggtag
Northern, *run-on* analyses, real-time RT-PCR (*hcf145*)	*psaA*	A-f A-r	ccaatttctaaacgctggagtagatcc catgaccaataccccagttggtcctatac
	rps14	R14-f R14-r	aaatatcatttgattcgtcgatcctc ctctcggtcttccggtcgaa
Run-on analysis, real-time RT-PCR (*hcf145*)	*psaB*	B-f B-r	gcgtgggcataagggtctttatgacac gcaaaagctcctgtcatgatgaatcctgc
Real-time RT-PCR (*hcf145*)	*psaA* 5′end	A5'-f A5'-r	acccggtcatttctcaagaacaatagc ccatggaaatacatgccactcagcc
	psaA-psaB intergenic region	A/B-f A/B-r	ctcctgctactcagcctagagccttgagca tcatcatgactctcgaagtcatgtgcgg
	rps14 3′end	R14-3'-r	gatcttgttgcccctggcaacaaacatgc
	psaC	psaC-f psaC-r	aggatgtactcaatgtgtccgagc gttggacaggcggattcacatctc
	psbB 3′end	psbB-3'-r	gcaatgttgcatcagactgcttgtcg
Real-time RT-PCR (*hcf145, hcf101*)	*18S rRNA*	18S rRNA-f 18S rRNA-r	gctcaaagcaagcctacgctctgg ggacggtatctgatcgtcttcgagcc
Run-on analysis, real-time RT-PCR (*hcf145*)	*psbB*	psbB-f psbB-r	ggtctttggagttacgaaggggtagc gcgccaaaaccgaagcaagccac
Run-on analysis, (*hcf145*)	*psbA*	psbA-f psbA-r	tggctatacaacggcggtcc aagggagccgccgaatacac

Table 2. Oligonucleotide primers used for amplification of genes and quantification of mRNAs (continued)

Run-on analysis, (*hcf145*)	*rbcL*	rbcL-f rbcL-r	ctagaggatctgcgaatccctcc ctagtatttgcggtgaatccccc
	16S rRNA	16S rRNA-f 16S rRNA-r	taagcatcggctaactctgtgcc tacagcactgcacgggtcgatac
	actin 1	act-f act-r	tcctagtattgtgggtcgtcctcg gctcattctgtcggcgattccagg
Isolation of the *atprfB* cDNA, Northern analysis (*hcf109*)	*atprfB*	atprfB-f atprfB-r	P-atgtccatggagctcaccgttctcggac ctaattggttacagcagaagccatggc
Complementation (*hcf109*)	*atprfB* genomic DNA	atprfB-int2-f atprfB-ex4-r	tttcccagtgaatctgaattctta caagtaaactaacatcagtagagtccat
Complementation, RT-PCR (*hcf109*)	*atprfB* cDNA and genomic DNA	atprfB-ex1-f atprfB-ex3-r	gccggtcggagtttcgcaatcgc cttgagctttagtacgatcatccc
Northern analysis (*hcf109*)	*rps2*	rps2 At-f rps2 At-r	atggcttggttcatgcataaatggcc gaagctatagcgtcatcatttgcgg
	rps16	rps16-At-f rps16 At-r	tcattctgaccgaacctttacgcg cacgttatatacgagtctttcacatcctc
	petL	petL At-f petL At-r	cctgagatagtgcagatgccaaagacg ctgtattgccaatgaatctcaatgacc
	ycf4	ycf4 At-f ycf4 At-r	tggatcatcgtcgggccgatgtctg cttcaattggtacacgcaagaagtaagcc
	atpB	atpB At-f atpB At-r	gtcagatgaatgaaccgccaggagctc gttcgtagccttcgcagtagcttcatcg

Table 2. Oligonucleotide primers used for amplification of genes and quantification of mRNAs (continued)

Northern analysis (*hcf109*)	*atpE*	atpE At-f atpE At-r	catcgatgaagctactgcgaaggctacg attgagagcctcgactcgtgtccgagc
	ndhI	ndhI At-f ndhI At-r	ggtcaacaaaccctacgagctgcaagg tcaattcgtgacgatcataagtgg
	ndhC/K/J	ndhC/K/J-f ndhC/K/J-f	ctatccaactctcgggcattaggatc ccggagttttatctccaattaggaaggggc
Sequencing of the frameshift site	*prfB Synechocystis*	prfB-Syn-f prfB-Syn-r	aaccagggcaatttggaagtcaaagg cgcccttcaatctccaacgtgacg
Isolation of the *HCF101* cDNA	*HCF101*	hcf101-f hcf101-r	gtagcaatgccgcttcttcatccacagtcg tattgttctagactagacttcgactggagacaatggagg
Complementation (*hcf101*)	*HCF101* genomic DNA	hcf101-int-f hcf101-int-r	atgtgccaatgctttttcccttgc caaagtctggaacagggaaataac
Complementation, real-time RT-PCR (*hcf101*)	*HCF101* cDNA and genomic DNA	hcf101-ex-f hcf101-ex-r	cagggcagcttccctttggattatc ggttgcagggtgcagtaagaactcttcgtc

2.1.6 cDNA library

An Uni-ZAP^{TM}XR cDNA library (Stratagene, La Jolla, USA) was prepared from RNA of *Arabidopsis* leaves, ecotype Columbia, according to the manufacturer's instructions and was kindly provided by Dr. Csaba Koncz (Max-Planck-Institut für Züchtungsforschung, Köln, Germany).

2.1.7 Media, solutions and buffers

TE buffer 10 mM Tris-HCl, pH 8.0
1 mM Na_2EDTA

10x TBE buffer:	108 g/l Tris, pH 8.2-8.4
	55 g/l M boric acid
	7.4 g/l Na_2EDTA
MOPS buffer:	20 mM MOPS
	5 mM Na-acetate
	1 mM Na_2EDTA, pH 7.0
20x SSC buffer:	3 M NaCl
	0.33 M Na-citrate, pH 7.0
MS-medium:	1x MS-salts (Murashige and Skoog, 1962)
	1.5% sucrose
	2.5 mM MES-NaOH, pH 5.7
	0.3% gelrite
Infiltration medium:	5% sucrose
	0.05% Silvet L-77 (Clough and Bent, 1998)
YEB medium:	5 g/l beef extract
	5 g/l bacteriological peptone
	1 g/l yeast extract
	5 g/l sucrose
	2 ml 1 M $MgCl_2$
	supplemented with 20 g/l agar for solid medium
LB-medium:	10 g/l bacteriological peptone
	5 g/l yeast extract
	10 g/l NaCl, pH 7.2
	supplemented with 15 g/l agar for solid medium
Hybridisation buffer:	250 mM Na_2HPO_4, pH 7.2
	7% (w/v) SDS
	2.5 mM EDTA (Church and Gilbert, 1984)

Washing solution 1: 2.5x SSC
1% SDS

Washing solution 2: 1x SSC
1% SDS

Washing solution 3: 0.5x SSC
1% SDS

Washing solution 4: 0.2x SSC
1% SDS

Washing solution 5: 0.1x SSC
0.5% SDS

Solutions and buffers which are not mentioned otherwise were prepared as described in Sambrook *et al*., (1989).

2.1.8 Antibodies

Table 3. Antibodies used for Western analysis

Protein or protein complex	Subunit	Source of an antibody
Photosystem I	PsaA/B	R. Nechushtai (Hebrew University, Jerusalem, Israel)
	PsaC	R. Herrmann
	PsaD	R. Herrmann
	PsaE	R. Herrmann
	PsaF	R. Herrmann
	PsaG	R. Herrmann
	PsaH	R. Herrmann

Table 3. Antibodies used for western analysis (continued)

LHCI	Lhca1	Agri Sera AB (Vännäs, Sweden)
	Lhca2	Agri Sera AB (Vännäs, Sweden)
	Lhca3	Agri Sera AB (Vännäs, Sweden)
	Lhca4	Agri Sera AB (Vännäs, Sweden)
Photosystem II	PsbB	R. Berzborn (Ruhr-University Bochum, Bochum, Germany)
	PsbC (CP43)	J. Mullet (Texas A&M University, College Station, Texas, USA)
	PsbD (D2)	J. Mullet
	PsbE	R. Herrmann
	PsbO (PSII-O)	R. Berzborn
	PsbZ	R. Herrmann
Cytochrome b_6f complex	Cytochrome *f* (PetA)	R. Herrmann
	Cytochrome b_6 (PetB)	R. Berzborn
	Rieske (PetC)	R. Herrmann
	Subunit IV (PetD)	R. Herrmann
ATP synthase	α subunit (CF_1 α, AtpA)	R. Berzborn
	β subunit (CF_1 β, AtpB)	R. Berzborn
	ε subunit (CF_1 ε, AtpE)	R. Berzborn
	Subunit II (CF_o II, AtpG)	R. Berzborn
Ribulose-1,5-bisphosphate carboxylase/oxygenase	Large subunit (RbcL)	R. Herrmann
Ferredoxin		R. Scheibe (Universität Osnabrück, Osnabrück, Germany)

Table 3. Antibodies used for western analysis (continued)

Ferredoxin-thioredoxin reductase	FtrA	P. Schürmann (Université de Neuchâtel, Neuchâtel, Switzerland)
	FtrB	P. Schürmann

2.2 Methods

2.2.1 Cultivation of bacteria

The *E.coli* strain was propagated in LB medium or on LB-agar plates at 37°C as described in Sambrook *et al*., 1989. For transformation with plasmids carrying ampicillin resistance, 70 μg/ml ampicillin were added into the medium. The *Agrobacterium* strain was propagated in YEB medium supplemented with 100 μg/ml rifampicin and 25 μg/ml kanamycin. For transformation with binary vector carrying ampicillin resistance, 100 μg/ml carbenicillin were used.

2.2.2 Seed sterilization, plant growth and mutant selection

Seed sterilization and growth conditions for wild-type and mutant plants were as described in Meurer *et al*. (1996b). For growth on MS-medium, seeds were sterilized with a solution containing 32% (v/v) ″bleach″ and 0.8% N-laurylsarcosinate for 8 min and afterwards washed three to five times with sterilized water. 12-15 seeds per Petri dish (94 x 16 mm) were put on solid MS-media and placed for 2 days at 4°C to synchronize germination. Seedlings were grown under continuous light at a photon flux density of 20 - 40 $\mu E\ m^{-2}\ sec^{-1}$ and at a constant temperature of 21°C. Selection of mutant plants was facilitated by a chlorophyll fluorescence video imaging system (FluorCam690M, Photon Systems Instruments, Brno, Czech Republic). The *hcf* mutants were readily distinguishable from wild-type plants because of their failure to quench chlorophyll fluorescence. Propagation of the lethal *hcf* mutants occurred via heterozygous offsprings grown on soil. In all experiments three-week-old plants were used if not differently indicated.

Light-dependent expression was performed on seedlings grown either in continuous light for 12 days and subsequently for 2, 8, or 24 h in darkness or in complete darkness for 12 days and subsequently for 2, 8, or 24 h in light. Three-week-old plants grown under greenhouse conditions were used for expression studies of roots and rosette leaves. Six-week-old plants grown under the same conditions were used for expression analyses of stems, green siliques, and young flowers.

2.2.3 General molecular biological methods

Phenol/chloroform extraction, precipitation, gel electrophoresis, staining and quantification of nucleic acids were performed according to standard protocols (Sambrook et al., 1989).

DNA fragments were purified from agarose gels using the QIAEX®-II Gel extraction kit and PCR products were purified with the QIAquick® PCR purification Kit (Qiagen, Hilden).

Restriction and ligation of DNA fragments were performed according to the manufacturers instructions.

Plasmid DNA for sequencing or cloning was isolated using QIAprep Spin Miniprep Kit (Qiagen, Hilden, Germany). The alkaline lysis protocol (Birnboim and Doly, 1979) was used to obtain plasmid DNA after ligation.

Preparation of competent cells and heat-shock transformation of *E. coli* occurred according to Hanahan (1985).

2.2.4 Hybridisation of nucleic acids

All hybridisations were performed overnight in hybridisation buffer (see Chapter 2.1.7) at 62°C (Church and Gilbert, 1984). Prehybridisations were carried out in the same buffer for at least two hours. After hybridisation filters were washed for 30 min in each of the washing solutions 1 to 5 (see Chapter 2.1.7). For exposure filtures were put in plastic foils and analysed by phosphorimaging (BASIII Fuji Bio Imaging plates and BAS2000 software package and the AIDA software package v3.25 beta; Raytest, Straubenhardt, Germany).

2.2.5 DNA analyses

2.2.5.1 Polymerase chain reaction (PCR)

For PCR amplifications of DNA templates 0.5 mM oligonucleotide primers, 0.2 mM dNTPs, 5 mM $MgCl_2$ and 2.5 U Taq polymerase were used in a 20 µl final reaction volume. An initial denaturation step was performed at 95°C for 3 min, and afterwards 32 cycles of denaturation (95°C for 15 sec), annealing (58 - 62°C for 15 sec) and extension (72°C for 1 min per 1 kb DNA) were performed followed by a final extension step at 72°C for 8 min.

2.2.5.2 Rapid DNA isolation for PCR

DNA was isolated from young *Arabidopsis* leaves (approx. 0.5 cm^2). Plant material was homogenised in 1.5 ml-Eppendorf tubes using a mechanical stirrer RW16 basic (Kika Labortechnik, Staufen, Germany) for approx. 5 sec, and immediately afterwards 400 µl extraction buffer (0.2 M Tris/HCl, pH 7.5; 0.25 M NaCl; 0.025 M EDTA and 0.5% (w/v) SDS) was added. After a short vortexing step, the extract was centrifuged for 3 min at 16,000 g at room temperature. 300 µl supernatant were transferred to a new Eppendorf tube and 300 µl isopropanol was added. The mixture was vortexed, incubated at room temperature for 2 min and centrifuged for 5 min at 16,000 g at room temperature or at 4°C. The supernatant was discarded, and the pellet was air-dried and resuspended in 50 µl TE buffer. For PCR amplification 2 µl DNA were used.

2.2.5.3 Dot-blot transfer of DNA onto nylon membrane

8 pmol of DNA probe were denatured in 0.4 M NaOH, diluted to 500 µl with 2 x SSC and immobilised onto a Biodyne A nylon membrane (0.2 µm; Pall, Dreieich, Germany) using a Minifold® I Dot-Blot device (Schleicher and Schüll, Dassel, Germany). DNA was fixed to the membrane by exposure to 12,000 to 120,000 µjoules of UV light (Khandijan 1986).

2.2.5.4 Radioactive labelling of DNA

DNA labelling was performed using the Random Primed DNA Labeling Kit (Roche Molecular Biochemicals, Mannheim, Germany) according to the method of Feinberg and Vogelstein (1983).

2.2.6 RNA analyses

2.2.6.1 Isolation of total RNA

Nucleic acids were isolated from 1 - 2 g of leaf material in 8 ml homogenisation solution (0.33 M sorbitol; 0.2 Tris-NaOH, pH 9.0; 0.3 M NaCl; 10 mM EDTA; 10 mM EGTA; 2% SDS) mixed with 4 ml phenol and 4 ml chloroform at 40°C. Total RNA was selectively precipitated with 2 M LiCl (Lizardi 1983; Westhoff *et al*., 1993).

2.2.6.2 Northern analyses

For Northern analysis 8 µg of total cellular RNA was used. RNA was denaturated through incubation with 30% glyoxal (McMaster and Carmichael, 1977), electrophoretically separated in 1.2% agarose gels in MOPS buffer and capillary transferred onto a Biodyne A nylon membrane (0.2 µm; Pall, Dreieich, Germany) in 20x SSC buffer (Grüne and Westhoff, 1988). RNA was fixed to the membrane by UV radiation (see Chapter 2.2.5.4). EcoRI/HindIII-digested and glyoxylized lambda DNA was used as a molecular weight standard.

2.2.6.3 Reverse transcription (RT)-PCR

Reverse transcription was performed with 1 µg total RNA using SuperScript II RNase H^- Reverse Transcriptase (Invitrogen, Karlsruhe, Germany) and either hexanucleotides (Roche Molecular Biochemicals, Mannheim, Germany) or gene-specific primers according to the manufacturers instructions. DNase I (RNase-free; Roche Molecular Biochemicals, Mannheim, Germany) was used for removal of DNA from RNA preparations prior to RT-

PCR reactions. For the case that some contaminating DNA remained in the RNA sample, primers were designed that anneal to sequences in exons at both sides of an intron to differentiate between amplification of cDNA and amplification of remaining, if any, DNA. With this approach PCR products derived from genomic DNA are longer compared to those derived from the intronless mRNA. If primers annealed to sequences in the same exon, the possibility of DNA contamination was controlled by using ycf3-f and ycf3-r primers (Table 2) annealing to the different exons of the *ycf3* gene and amplifying 202 and 990 bp fragments of cDNA and chloroplast DNA, respectively.

RT-PCR analysis of *atprfB* expression in the *hcf109* mutant was performed with the oligonucleotides atprfB-ex1-f and atprfB-ex3-r generated from exon regions.

2.2.6.4 Quantitative real-time RT-PCR

Quantitative two-step RT-PCR was carried out using the LightCycler Thermal Cycler System (Roche Molecular Biochemicals, Mannheim, Germany) applying the SYBR Green protocol (Wittwer *et al*., 1997b). Reverse transcription was performed as described in Chapter 2.2.6.3. For quantification of different intervals of the *psaA-psaB-rps14* transcripts, either hexanucleotides or gene-specific R14-3'-r primer located at the 3' end of the *psaA-psaB-rps14* transcript together with psbB-3'-r primer located at the 3' end of the *psbB* gene (Table2) were used.

Real-time PCR was performed using a commercially available master mix containing Taq DNA polymerase, SYBR-Green I dye and deoxyribonucleoside triphosphates (LightCycler - FastStart DNA master SYBR-Green I, Roche Molecular Biochemicals, Mannheim, Germany). Generation of PCR products was detected by measuring SYBR Green I fluorescence. SYBR Green I dye emits a fluorescence signal at 530 nm only when bound to double-stranded DNA. Therefore, during PCR the increase in SYBR Green I fluorescence is directly proportional to the amount of double-stranded DNA generated. For *hcf145*, primer combinations covering five different regions between the 5' and 3' ends of the *psaA-psaB-rps14* operon as well as for *psaC, psbB* and *18S rRNA* (Table 2) were chosen. Real-time PCR for *hcf101* and wild-type cDNA was performed with *HCF101* exon-specific primers hcf101-ex-f and hcf101-ex-r and as an internal control with *18S rRNA* primers 18S-rRNA-f and 18S-rRNA-r. After addition of primers (0.5 mM), $MgCl_2$ (4 mM) and template cDNA to the master mix, an initial denaturation step at 95°C for 10 min followed by 45 cycles of denaturation (95°C for 15 sec), annealing (58°C for 5 sec) and extension (72°C for 11 sec)

were performed. All ramp rates were set to 20°C per sec. Detection of the fluorescent product was performed at the end of the extension period.

To prove that only the desired PCR product had been amplified, a melting curve analysis was performed after completion of PCR. For this, PCR products were denatured at 95°C, annealed at 55°C, and gradually heated to 95°C, whereas SYBR-Green I fluorescence was detected stepwise every 0.1°C. During such slow heating of the reaction mixture, melting of double-stranded DNA and a corresponding decrease of SYBR Green I fluorescence occurred. When the temperature of the reaction mixture reached the characteristic melting temperature of a particular DNA product (where the DNA is 50% double-stranded and 50% single-stranded), this was represented by a peak in a melting curve. If PCR generates only one amplicon, melting curve analysis shows only one melting peak. If primer-dimers or other non-specific products are present, they cause additional melting peaks. To estimate primer-dimer formation, a control without template DNA was included in each experiment.

The template quantification was determined by the crossing point using the LightCycler analysis software, as described in Wittwer *et al*. (1997a). Serially diluted samples of *Arabidopsis* total DNA, ranging from 15 ng to 1.5 pg of DNA were used for calibration with the *hcf145* mutant. During estimation of the *HCF101* expression, serially diluted samples of *HCF101* cDNA, ranging from 50 ng to 0.5 pg of XbaI-digested *pbinhcf101* plasmid DNA were used for the calibration curve. Additionally, PCR products were analysed by 1% agarose gel electrophoresis and stained with ethidium bromide to obtain an independent validation check of the presence of a product.

2.2.6.5 Isolation of transcriptionally active chloroplasts from *Arabidopsis*

For studying transcription rates of plastid genes, intact chloroplasts were isolated according to the method of Somerville *et al* (1981). All working steps were performed at 4°C. 3 g leaf material were homogenised for 2 sec in 10 ml 0.3 M sorbitol, 5 mM $MgCl_2$, 5 mM EGTA, 20 mM HEPES/KOH (pH 8.0), 10 mM $NaHCO_3$ in a Warring blender. The homogenate was filtered through a 20 µm nylon mesh, and the remainder was homogenized 4 more times as described above. The suspensions were pooled and centrifuged (rotor JS 13.1, Beckman, Munich, Germany) for 8 min at 353 g. The supernatant was removed, and the pellet was resuspended in 0.5 ml of the same medium by careful shaking. The resulting suspension was layered onto a 42%/85% Percoll gradient prepared by loading 7 ml of 45% on 3 ml of

85% Percoll solution (see below) in Corex tubes. After centrifugation (12 min, 1411 g), intact chloroplasts were collected from the border of the two layers (Bartlett *et al.*, 1982). The chloroplasts were further washed in the same medium (8 min, 353 g), and finally resuspended in 300 mM sorbitol, 50 mM HEPES (pH 8.0) medium. Concentration of the intact chloroplasts was estimated under the phase-contrast microscope using a haemocytometer.

85% Percoll solution: 85% Percoll medium
- 95% (w/v) Percoll
- 3% (w/v) PEG6000
- 1% (w/v) Ficoll
- 1% (w/v) BSA

15% gradient mixture
- 25 mM HEPES/NaOH, pH 8.0
- 10 mM EDTA
- 5% (w/v) sorbitol

42% Percoll solution: 42% Percoll medium
58% gradient mixture

2.2.6.6 *Run-on* transcription analysis

Run-on transcription assays were performed with 9 x 10^6 chloroplasts in 50 µl of total reaction volume as described by Klein and Mullet (1990) with the modifications listed in Kubicki *et al*. (1994). The reaction was performed at 25°C for 20 min. Incorporation of [α-^{32}P]-UTP into transcripts was measured as described by Hallick *et al*. (1976). To avoid competitive binding of *run-on* transcripts to different segments of the same operon, probes for the *psaA, psaB* and *rps14* genes were spotted onto individual filters with individual internal controls, and were hybridized separately with one third of each of the *run-on* reaction (see Chapter 2.2.4). The signal intensities were quantified by phosphoimaging (BASIII Fuji Bio Imaging plates and BAS2000 software package and the AIDA software package v3.25 beta; Raytest, Straubenhardt, Germany).

2.2.7 Translation inhibition experiment

For application of plastid translation inhibitors, three-week-old plants of *hcf145* and *hcf109* were used. To avoid embolism, hypocotyls were clipped in a 1/2 MS solution containing 450 mg/l chloramphenicol or lincomycin. Leaves were not immersed to ensure increased uptake of the antibiotics by transpiration. At times 0 and 3, 9 or 27 hours after incubation in ambient light, leaves of the seedlings were harvested. Control plants were incubated for the same time in a solution containing 1/2 MS nutrients. Total RNA was isolated from the harvested material and used for Northern analysis. The *psaA*, *psaC*, *psbA*, *psbB*, *psbZ*, *atpA/trnR/trnG* and *rbcL* probes used for the hybridisations are listed in Table 1 and the primers for the *ndhC/K/J* probe are presented in Table 2.

2.2.8 Protein and pigment analyses

2.2.8.1 Measurement of protein and chlorophyll concentration

Protein concentrations were measured according to Bradford (1976). Protein amounts of mutants were equalised to amounts in wild-type (10 μg) according to silver-stained gels (Blum *et al*., 1987). Chlorophyll concentrations were measured according to Arnon (1949).

2.2.8.2 Sodium dodecyl sulfate polyacrylamide gel electrophoresis (SDS-PAGE)

Soluble and membrane proteins of three-week-old plants were isolated and separated by SDS-PAGE as described in Meurer *et al*., (1996b).

2.2.8.3 Western analyses

For immunodetection, proteins were transferred to polyvinylidene difluoride (PVDF) membranes (Amersham Buchler, Braunschweig, Germany) according to the manufacturer's instructions, incubated with specific antisera and visualized using the enhanced chemiluminescence technique (Amersham Buchler, Braunschweig, Germany).

2.2.8.4 *In vivo* labelling of chloroplast proteins

In vivo labelling of leaf proteins was performed for 15 min as described in Meurer *et al*. (1998). The hypocotyls were cut in 20 µg/ml cycloheximide solution to avoid embolism, incubated for 5 min in the solution containing the antibiotic and subsequently immersed into 1 mM KH_2PO_4 (pH 6.3), 0.1% (w/v) Tween 20 medium supplemented with 50 μCi [^{35}S]-methionine (>1000 Ci/mmol specific activity).

2.2.8.5 Polysome analysis

This experiment was performed by Katrin Amann. Polysomes were isolated from leaf tissue as described in Barkan (1998). Polysome aliquots (0.5 ml) were layered onto 4.4 ml 15 to 55% sucrose gradients and centrifuged for 65 min at 272,000 g at 4°C in a SW60Ti rotor (Beckman, Munich, Germany). Fractions of 0.4 ml were collected, and the RNA was purified, glyoxylized, and subjected to RNA gel blot analysis.

2.2.8.6 Separation of thylakoid membrane complexes

Approximately 1 g *Arabidopsis* seedlings were homogenized in 0.3 M sorbitol, 5 mM $MgCl_2$, 20 mM Tricine/KOH (pH 8.4), 20 mM EDTA, 0.1% (w/v) BSA. The homogenate was filtered through two Miracloth layeres (100 μm, Calbiochem, La Jolla, USA) and centrifuged for 3 min at 2,370 rpm in a table centrifuge at 4°C. The pellet containing the membrane fraction was resuspended in 1 ml TMK buffer (10 mM Tris-HCl, (pH 6.8), 10 mM $MgCl_2$ and 20 mM KCl). The suspension obtained was incubated for 10 min on ice and then centrifuged (3 min at 2,370 rpm). The pellet was washed twice with 500 μl TMK buffer to remove soluble proteins. Membrane fractions equivalent to 40 – 120 μg chlorophyll were resuspended in 40 μl TMK buffer, and 120 μl of 2% (w/v) β-dodecylmaltoside in TMK was added to obtain final concentration of β-dodecylmaltoside of 1.5% (w/v). The suspension was incubated for 10 min on ice to solubilize the major thylakoid membrane proteins and centrifuged (10 min, 21,000 rpm in a table centrifuge at 4°C). The supernatant containing the thylakoid lysate was loaded onto a linear 0.1 – 1.0 M sucrose gradient and centrifuged for 17 h at 125,000 g at 4°C in a SW60Ti rotor (Beckman, Munich, Germany). Fractions of 0.2 ml were collected bottom-to-top and used for SDS-PAGE and Western analysis.

2.2.8.7 Protein import

In organello import experiments were performed by Katrin Amann for HCF101 and by Dr. Staver Bezhani (Friedrich-Schiller-Universität, Jena, Germany) for AtprfB. *In vitro* transcripts of full-length cDNAs of *atprfB* and *HCF101* were generated by using T3 and T7 RNA polymerases, respectively, and translated in cell-free wheat germ extracts in the presence of [^{35}S]-methionine according to the manufacturer's instructions (Promega, Mannheim, Germany). For import of the AtprfB and HCF101 proteins, intact chloroplasts were isolated from young spinach and pea leaves, respectively. *In organello* protein import experiments were performed further as described by Michl *et al*. (1999). After reaction, chloroplasts were pelleted, resuspended in 500 μl of 50 mM HEPES and 0.33 M sorbitol, pH 8.0, and treated with thermolysin (100 μg/ml). Unbroken chloroplasts were reisolated by centrifugation through a 45% Percoll layer and divided into membrane and soluble proteins. The fractions were subjected to SDS-PAGE followed by fluorography essentially as described by Clausmeyer *et al*. (1993).

2.2.9 Spectroscopic and fluorimetric methods

2.2.9.1 Chlorophyll *a* fluorescence analyses

Chlorophyll *a* fluorescence analyses were performed using plants of the same age grown under identical conditions. A pulse amplitude–modulated fluorometer (PAM101; Walz, Effeltrich, Germany) equipped with a data acquisition system (PDA-100; Walz) and a personal computer using Wincontrol version 1.72 software (Walz, Effeltrich, Germany) for data collection were used to measure and analyze *in vivo* chlorophyll *a* fluorescence. The following settings were used for the PAM101 unit: light intensity, 4; gain, 6; damping, 9. After induction, saturating pulses of 4,000 μE m^{-2} sec^{-1} light intensity and 1 sec duration were applied in 30 sec intervals to estimate quenching parameters (Meurer *et al*., 1996b).

2.2.9.2 Light-induced change of the P700 redox state

Light-induced changes of the P700 redox state were recorded by absorbance changes at 830 nm, with the above described PAM system equipped with a dual wavelength emitter-

detector unit (Meurer *et al*., 1996b). Multiple turn-over flashes of 50 μsec were induced by a Xenon lamp (Walz, Effeltrich, Germany) and saturating light pulses of 1 sec were applied by halogene lamps.

2.2.9.3 Photochemical and non-photochemical chlorophyll *a* fluorescence quenching

Photochemical (qP) and non-photochemical (NPQ) chlorophyll *a* fluorescence quenching at room temperature were performed using the PAM system described in Chapter 2.2.9.1. The actinic light intensity was 20 μE m^{-2} sec^{-1}, and the intensity of the saturating light pulses (1 sec, 20-sec intervals) used for detection of the quenching parameters during induction was 4000 μE m^{-2} sec^{-1}.

2.2.9.4 Low temperature chlorophyll fluorescence spectra

Chlorophyll fluorescence emission spectra at 77 K were recorded with a Hitachi fluorometer (model F-3010; Hitachi, Tokyo, Japan), as described by Meurer *et al*. (1996a). Spectra were normalized with respect to equivalent long-wavelength emission bands.

2.2.10 Genetic methods

2.2.10.1 Mapping of the *hcf145* mutation

A mapping population was generated to identify the precise chromosomal location of the *HCF145* gene. The F_1 generation was produced by pollinating emasculated flowers of the accession Landsberg erecta with Wassilewskija plants heterozygous for the *hcf145* mutation. F_2 plants segregating the mutant offsprings were grown on soil and individual plants were taken for genetic mapping of the mutation with simple sequence length polymorphism (SSLP) markers covering the entire genome. The genotype of recombinants was identified by screening the progeny for mutant segregants. Segregating mutations were confirmed by fluorescence imaging of the F_3 offspring.

2.2.10.2 Complementation of the hcf101 mutant

The cDNA of *HCF101* was amplified from a cDNA library (see Chapter 2.1.6) with Pfu polymerase (Stratagene, Heidelberg, Germany) using the hcf101-f and hcf101-r primers, the latter includes a *Xba*I restriction site. The *Xba*I-digested and purified PCR product was ligated into the *Sma*I/*Xba*I sites of vector pSEX001-VS (see Chapter 2.1.3).

The construct obtained, *pbinhcf101*, was introduced into *Agrobacterium tumefaciens* GV3101(pMP90RK) (Koncz *et al*., 1994) and transformed into progenies of mutant segregants using the floral dip method (Clough and Bent, 1998). Homozygosity in resistant complemented lines was confirmed by sequencing the mutant allele amplified with intron-specific primers hcf101-int-f and hcf101-int-r. The presence of the cDNA was analysed by PCR using exon-specific primers hcf101-ex-f and hcf101-ex-r.

2.2.10.3 Complementation of the hcf109 mutant

The full-size *atprfB* cDNA was amplified by RT-PCR (see Chapter 2.2.6.3) using Pfu DNA polymerase (Stratagene, Heidelberg, Germany) and the oligonucleotide primers atprfB-f and atprfB-r. The resulting fragment was ligated into the SmaI site of vector pSEX001-VS (see Chapter 2.1.3).

The plasmid obtained, *pbinatprfB*, was introduced into *Agrobacterium tumefaciens* GV3101(pMP90RK) (Koncz *et al*., 1994) and transformed into progenies of mutant segregants by vacuum infiltration (Bechtold and Pelletier, 1998). The point mutation in *hcf109* induced a Tru9I restriction site. Therefore, *hcf109* homozygotes were identified among the progeny of complemented lines by amplifying genomic DNA with the intron 2 and exon 4 primers atprfB-int2-f and atprfB-ex4-r, respectively, and subsequent digestion of the PCR products with Tru9I. These lines were further tested for antibiotic resistance conferred by the T-DNA and for the presence of the cDNA using the exon 1 and exon 3 primers atprfB-ex1-f and atprfB-ex3-r, respectively, for PCR amplification.

2.2.11 Electron microscopy

Electron microscopy was performed by Prof. G. Wanner (LMU, München). Samples were prepared as described in Meurer *et al*. (1998).

2.2.12 Sequence analyses

Nucleotide sequences were determined using the ABI377 system (Applied Biosystems, Foster City, CA). Sequences were evaluated using Sequencher 3.0 software (Gene Codes Corp., Ann Arbor, MI).

Protein homologues were identified by BLAST analysis (Altschul *et al.*, 1997) of sequenced genomes at the NCBI website (http://www.ncbi.nlm.nih.gov/Blast). Sequence alignments were performed using the programme MacMolly tetra (SoftGene GmbH; Schöneberg *et al.*, 1994).

3 Results

3.1 High chlorophyll fluorescence (*hcf*) phenotypes of the *hcf145*, *hcf109* and *hcf101* mutants

Homozygous mutant seedlings developed pale green cotyledons when grown photoautotrophically, but were lethal at the stage of primary leaf formation. Cultivation under sterile heterotrophic conditions rescued mutant seedlings, although mutant plants still appeared pale and were smaller in size as compared to wild type. However, leaf morphology of the mutants was similar to that of the wild-type. Because of defects in photosynthetic electron transport, absorbed light energy could not be utilized properly and was, therefore, emitted as high fluorescence (Figure 4a; Meurer *et al.,* 1996b).

3.2 Characterisation of the *hcf145* mutant

3.2.1 Activity of PSI complexes is primarily abolished in *hcf145*

As the *hcf* phenotype indicated a defect in the photosynthetic electron transport, non-invasive fluorimetric and spectroscopic analyses were performed to assign the precise target of the *hcf145* mutation (Figure 4a-c; Meurer *et al*., 1996b). Application of light pulses showed that the ratio of variable to maximum fluorescence, indicative for the potential capacity of PSII, was reduced in the mutant (0.60±0.05 versus 0.81±0.01 in wild-type). During induction of even ambient actinic light of 20 μE m^{-2} sec^{-1}, chlorophyll fluorescence remained at its maximum level, indicating that almost no light-induced photochemical or non-photochemical quenching took place in the mutant (Figure 4b). This behaviour is typical for mutants affected either in the intersystemic electron transport or in PSI function (Meurer *et al*., 1996b). Absorbance changes of P700 at 830 nm after light/dark switches, during induction of far-red light or after application of strong white light pulses in far-red background, were almost below the limit of detection in the mutant, even when the PAM101 measuring unit was adjusted to its highest sensitivity (settings: light intensity, 12; gain, 12; damping, 0; Figure 4c). This indicated that PSI was either not functional or missing in the *hcf145* mutant.

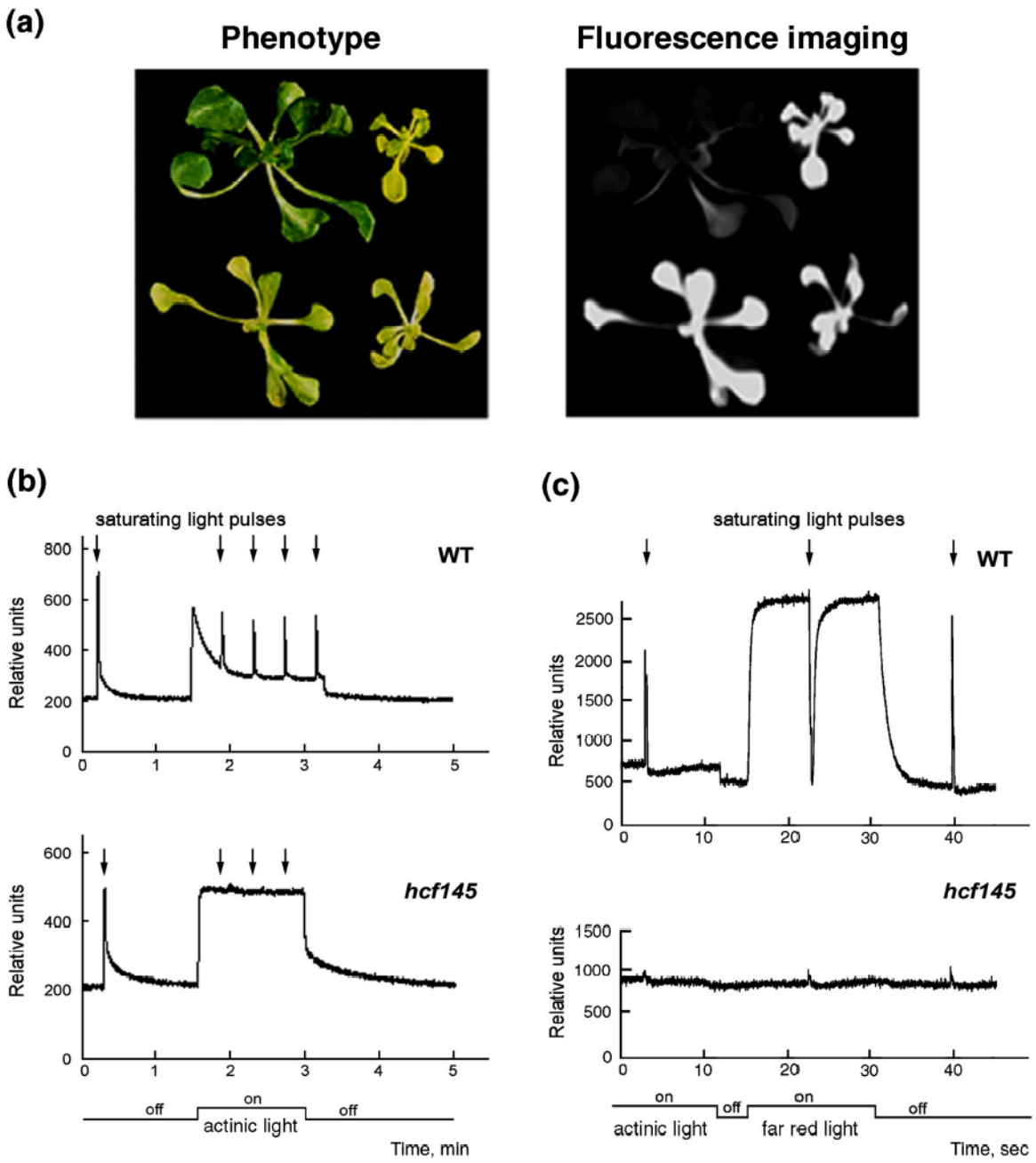

Figure 4. Phenotype and spectroscopic analysis of the *hcf145* mutant and wild-type (WT) *Arabidopsis* plants. **(a)** Phenotype (left) of three selected mutant plants as compared to the WT (upper left part) and chlorophyll fluorescence imaging (right) of the same plants which were all grown heterotrophically for three weeks. **(b)** Measurements of chlorophyll fluorescence induction were performed with three-week-old plants as described in Materials and methods. Arrows indicate application of 1 sec saturating light pulses of 4,000 μE m $^{-2}$ sec $^{-1}$ intensity. The actinic light intensity was 20 μE m $^{-2}$ sec $^{-1}$. **(c)** P700 redox kinetics of *hcf145* and WT plants. Under illumination, WT P700 was almost reduced, but could be completely oxidised by far-red light. Light-induced absorbance changes were indicative of PSI activity in the WT, but the low signal-to-noise ratio in the mutant did not allow quantification of P700 redox kinetics.

3.2.2 Accumulation of PSI subunits is dramatically affected whereas LHCI complexes are still present in *hcf145*

The spectroscopic data were complemented by immunoblot analyses using antibodies raised against subunits of photosynthetic thylakoid membrane complexes. Figure 5(a) shows that PSI is severely affected in the *hcf145* mutant. The levels of all nuclear- and plastid-encoded PSI subunits analysed (PsaA/B, PsaC, PsaD, PsaE, PsaF, PsaG and PsaH) amounted often less than 12.5% in *hcf145* as compared to those of the wild-type. In contrast, representative subunits of PSII (D2, CP43 and PSII-O), of the cytochrome b_6f complex (cytochrome b_6 and subunit IV) and the chloroplast ATP synthase (α-subunit and subunit II), were all present in levels comparable to those in the wild type (Figure 5b).

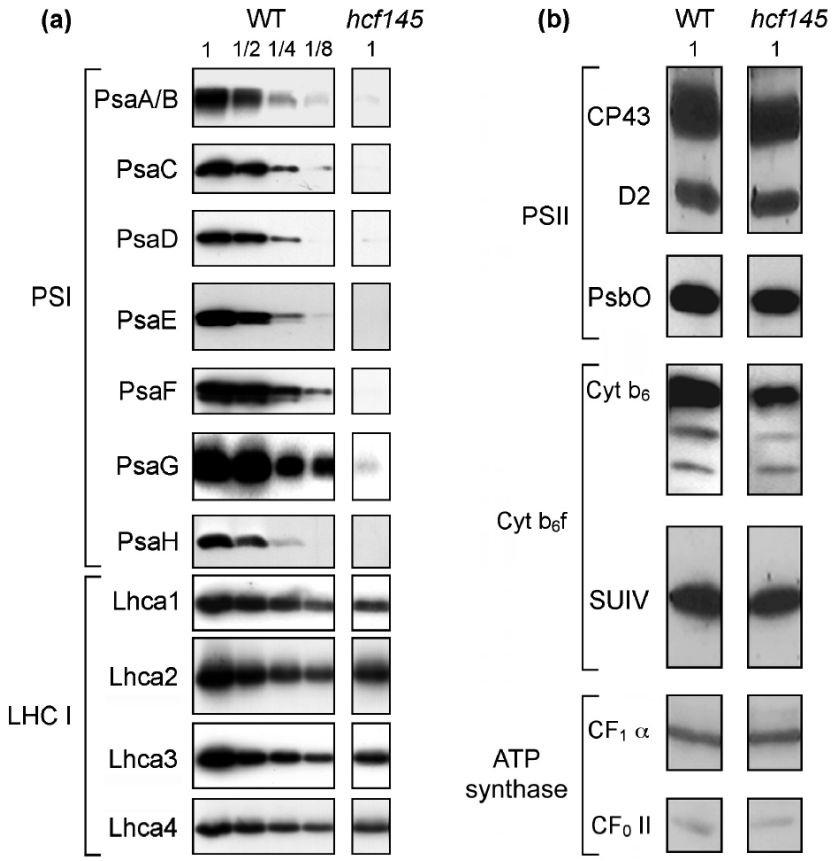

Figure 5. Immunoblot analysis of thylakoid-membrane proteins isolated from three-week-old *hcf145* and wild type (WT) plants. **(a)** Immunodetection of PSI subunits PsaA/B, PsaC, PsaD, PsaE, PsaF, PsaG and PsaH, and of Lhca1, Lcha2, Lhca3 and Lhca4 subunits of LHCI. **(b)** Immunoblot analysis of PSII subunits CP43, D2 and PsbO, of cytochrome b_6f complex subunits Cyt b_6 and SUIV, and of ATP synthase subunits CF_1 α and CF_0 II. Loading 1 corresponds to 10 μg membrane proteins of WT.

Despite the lack of a PSI core complex, subunits Lhca2 and Lhca3 of the chlorophyll-binding PSI light-harvesting complex (LHCI) accumulated to about 50%, whereas the quantities of the two other subunits, Lhca1 and Lhca4, were reduced to about 25% in *hcf145* (Figure 5a). Taken together, the results of the spectroscopic and immunoblot analyses suggested that the *hcf145* mutation specifically affects the PSI complex, leading to dramatic reduction of all core components and, to some extent, of LHCI.

3.2.3 *hcf145* has reduced rates of the *psaA* and *psaB* mRNA translation

To evaluate whether translational defects or instability of synthesised proteins lead to PSI deficiency, translation of chloroplast-encoded thylakoid-membrane proteins was studied by *in vivo* labelling. Leaf proteins were pulse-labelled in intact mutant seedlings with [^{35}S]-methionine. Synthesis of the nuclear-encoded chloroplast proteins was blocked with cycloheximide so that only plastome-encoded proteins appeared and were detected by phosphorimaging (Meurer *et al*., 1998). Incorporation rates were often lower in the mutant based on fresh weight (data not shown), therefore, equal amounts of incorporated radioactivity were loaded.

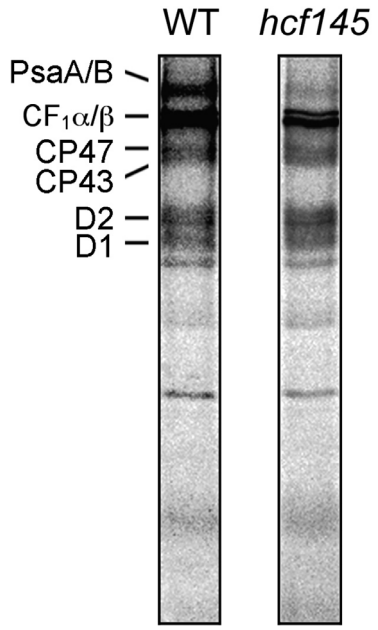

Figure 6. *In vivo* labelling of chloroplast-encoded membrane proteins from *hcf145* and wild-type (WT). Primary leaves of 12-day-old WT and *hcf145* seedlings were pulse-labelled with [^{35}S]-methionine for 15min in the presence of cycloheximide. WT and mutant membrane proteins with equal amounts of incorporated radioactivity (100 000 cpm) were separated by SDS-PAGE, blotted onto a PVDF membrane and analysed by phosphorimaging.

The labelling pattern of membrane proteins in *hcf145* was similar to that of wild-type (Figure 6). Abundance and known electrophoretic mobilities as well as mutant analysis,

allowed to identify the indicated bands as individual subunits of the thylakoid membrane, i.e. PsaA/B, AtpA/B, PsbB/C and PsbA/D (Meurer *et al*., 1998; Plücken *et al*., 2002; Dal Bosco *et al*., 2004). Labelling of the PSII subunits D1, D2, CP43 and CP47, and of the ATP synthase subunits α and β, remained largely unchanged in the mutant. Specifically, incorporation of radioactive label into PSI reaction centre subunits PsaA/B was dramatically reduced. Thus, the *hcf145* mutant appears to be impaired in the translation of the major PSI proteins PsaA and PsaB.

3.2.4 Amounts of the plastid *psaA-psaB-rps14* transcript unit are specifically decreased in *hcf145*

Northern analyses, using a set of probes for nuclear- and plastid-encoded subunits of PSI, as well as of several other chloroplast proteins, were performed to investigate whether the protein deficiencies of PSI were reflected at the mRNA level. Accumulation of the tricistronic *psaA-psaB-rps14* transcript of 5.3 kb, encoding the PSI subunits A and B, and the ribosomal protein S14, was drastically reduced, below 12.5% in the mutant (Figure 7a). However, processed intermediate mRNA species of 0.5 and 3.2 kb accumulated to nearly wild-type amounts. Levels of the larger transcripts of 7.1 and 6.3 kb, which also contain sequences of the intron-containing *ycf3* gene located further upstream, but do not contain sequences of the plastid tRNA gene, *trnfM* (Figure 7a,b), were slightly increased in *hcf145*.

In contrast, transcripts for two other PSI genes of plastid origin, *psaC* and *psaI,* for the nuclear-encoded PSI gene *psaE* and for the plastid PSII gene *psbA* were unchanged in *hcf145* (Figure 7c). These data are consistent with the deficiencies observed at the protein level, and demonstrate that the *hcf145* mutation primarily causes a decrease in the accumulation of the *psaA-psaB-rps14* tricistronic mRNA.

3.2.5 The *hcf145* mutation primarily affects the *psaA-psaB-rps14* mRNA stability

3.2.5.1 Comparison of the transcription rates of *hcf145* and wild-type

The deficiency in accumulating *psaA-psaB-rps14* transcripts could be caused by a reduction of transcriptional activities of the operon or by a decreased stability of the tricistronic message. To distinguish between these two possibilities, transcription rates were

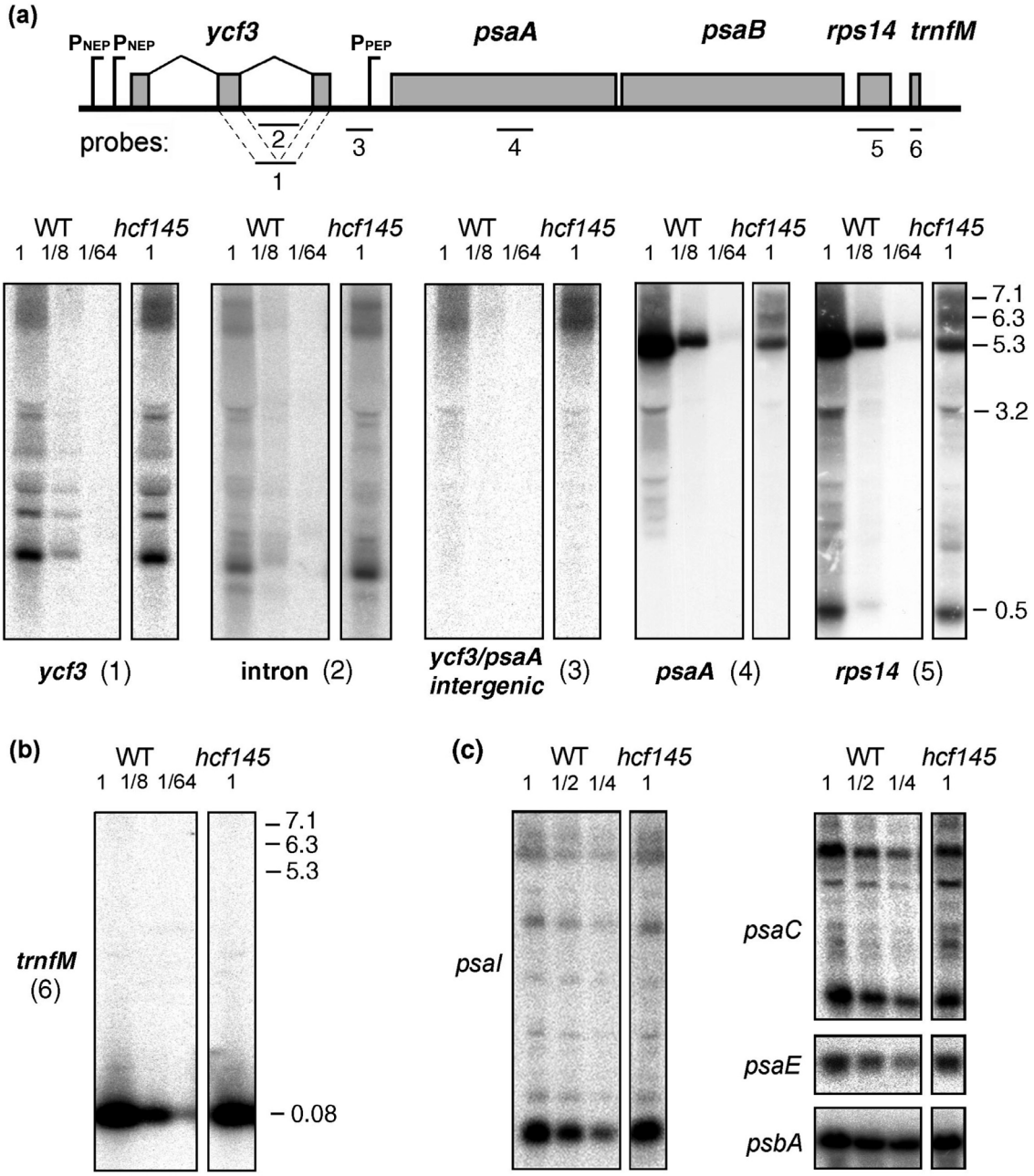

Figure 7. Northern analysis of transcripts in the *hcf 145* mutant and wild type (WT). **(a)** Levels and pattern of transcripts which contain sequences of *ycf3*, the intron of *ycf3*, the *ycf3-psaA* intergenic region, the *psaA* and *rps14* genes. The organisation of the genes analysed in (a) and (b) is shown above. Note that the intronless *ycf3* probe has been generated by RT-PCR. P_{NEP} and P_{PEP} are promoters for nuclear-encoded RNA polymerase and plastid-encoded RNA polymerase, respectively. **(b)** Levels of the plastid tRNA, *trnfM*, located downstream of the *psaA* operon. **(c)** Transcript levels of plastid *psaC, psaI* and *psbA* genes, and the nuclear *psaE* gene. For quantification, a dilution series of WT mRNA was compared to transcript quantities in *hcf145*. Loading 1 corresponds to 8 μg leaf RNA from three-week-old plants. Sizes are given in kb.

compared between mutant and wild-type seedlings. Radio-labelled chloroplast *run-on* transcripts were hybridised to filters with immobilised plastid *psaA, psaB* and *rps14* gene probes. Each filter contained, in addition, *rbcL, psbA, psbB* and *16S rRNA* gene probes, and a nuclear actin probe as internal control. The filters were used in separate hybridisations to avoid competition. Four independent experiments were performed, each with individual filters and chloroplast *run-on* assays. No reduction of signal intensity has been noted between wild-type and mutant chloroplasts hybridised with the *rps14* probe (Figure 8), establishing that the transcriptional activity of the *rps14* gene was not altered in the *hcf145* mutant. The intensity of *psaA* and *psaB* signals in the mutant constituted 52 ± 6 and 57 ± 5% of wild-type, respectively. Nonetheless, this decrease could not explain the low stationary *psaA-psaB* mRNA levels (below 12.5%). Therefore, reduced mRNA stability must account mostly for decreased *psaA-psaB-rps14* mRNA transcript levels.

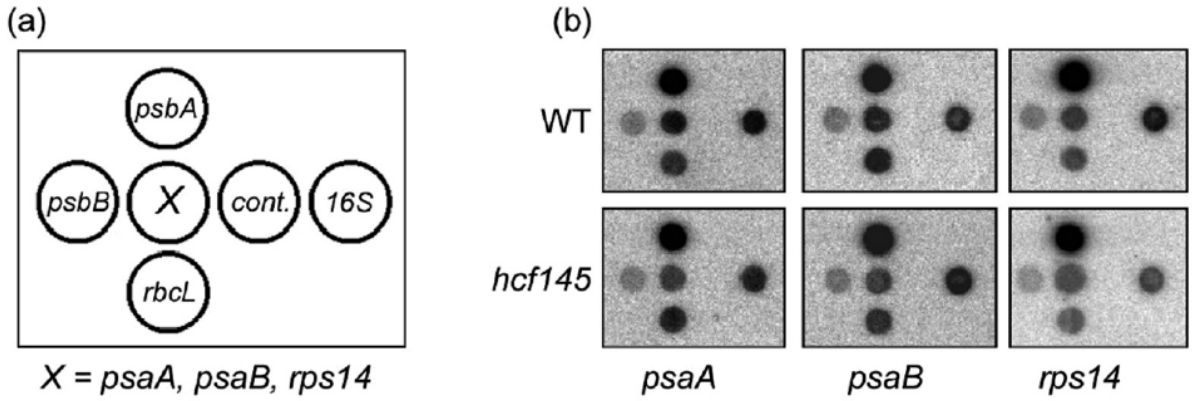

Figure 8. *Run-on* analysis of transcriptional activities of several plastid genes in *hcf145* and wild-type (WT). **(a)** Orientation of gene probes dotted onto nylon membranes used in (b). **(b)** *Run-on* reactions were performed with 9 x 10^6 chloroplasts from WT and *hcf145* seedlings. Afterwards, one-third of [α-^{32}P]-labelled transcripts was hybridised to each filter containing immobilised probes of the indicated genes. A nuclear actin probe was used as a negative control. The bound radioactivity was visualised and quantified by use of a phosphorimaging system (BASIII Fuji Bio Imaging plates and BAS2000 software package and the AIDA software package v3.25 beta; Raytest, Straubenhardt, Germany).

3.2.5.2 Translational events do not affect stability of the *psaA-psaB-rps14* operon

To answer the question, whether the *hcf145* mutation affects the *psaA-psaB-rps14* mRNA stability via translational alterations, primarily or indirectly, chloroplast protein synthesis was inhibited and steady-state levels of the *psaA-psaB-rps14* mRNA in *hcf145* were

followed. In case the stability of the polycistronic message is decreased due to defects in translation, accumulation of the *psaA-psaB-rps14* transcripts would be expected. Both inhibitors chosen, chloramphenicol and lincomycin, specifically affect translation at 70S ribosomes but the mechanism of their action is quite different (Nierhaus and Wittmann, 1980). The former inhibits the elongation of translation and interferes with ribosomal release, forcing transcripts into a polysome-bound state. The latter induces conformational changes of ribosomes inhibiting early peptide bond formation and, accordingly, liberation of transcripts from previously initiated ribosomes. After 15 min of incubation, both chemicals efficiently repressed plastid translation without any effect on translation in the cytosol in both wild-type and *hcf145* (data not shown).

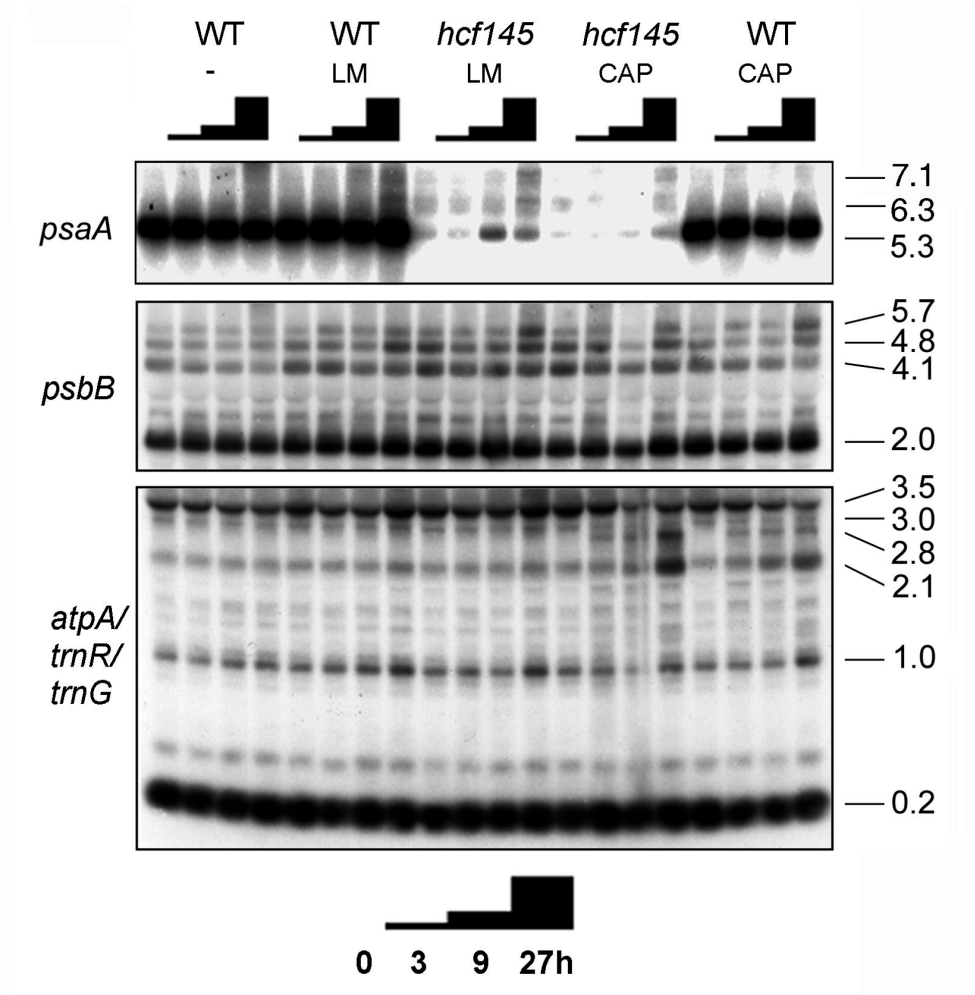

Figure 9. Effect of translation inhibitors on *psaA-psaB-rps14, psbB* and *atpA/trnR/trnG* transcript levels in *hcf145* and wild type (WT). Northern analysis of total RNA isolated from three-week-old *hcf145* and WT plants incubated for 0, 3, 9 and 27 h with chloramphenicol (CAP) or lincomycin (LM). Incubation for the same periods without antibiotics (-) served as a control. The *psaB, psbB* and *atpA/trnR/trnG* probes were used for hybridisation. Sizes are given in kb.

Interestingly, along with an inhibitory effect on translation, chloramphenicol affected mRNA accumulation in wild-type leaves (Figure 9). In the control without antibiotics, accumulation of all transcripts examined did not change significantly, but chloramphenicol specifically inhibited splicing of *petB* and *petD* introns (Westhoff and Herrmann, 1988; Meurer *et al*., 1996a), leading to increased accumulation of the primary 5.7 kb transcript and reduction of the spliced form of 4.1 kb after 27 h of incubation. Accumulation of the single spliced precursor of 4.8 kb did not change. In addition, chloramphenicol specifically affected endo- and/or exoribonucleolytic cleavage of the *atpA* operon in the wild type. Whereas the level of the primary 3.5 kb transcript was reduced, the level of the 2.1 kb message significantly increased within 27 h. A new band of 2.8 kb appeared in parallel with a reduction of the 3.0 kb mRNA.

During incubation of *hcf145* plants with both antibiotics, levels of the *psbB* and *atpA/trnR/trnG* transcripts, taken as a control, corresponded to those in wild type (Figure 9). Steady-state levels of the *psaA-psaB-rps14* mRNA were not significantly changed during 27 h of incubation in the presence of chloramphenicol in *hcf145* and wild-type. Lincomycin treatment caused a slight accumulation of the 5.3 kb *psaA-psaB-rps14* mRNA and of the two precursors of 7.1 and 6.3 kb within 27 h both in mutant and wild-type, indicating that this effect is independent of the mutation but specific for lincomycin.

Taken together, these data indicate that an impaired translation is not responsible for decreased *psaA-psaB-rps14* mRNA stability in the mutant, and that HCF145 primarily prevents rapid *psaA-psaB-rps14* mRNA degradation.

3.2.5.3 The 5′ ends of the *psaA-psaB-rps14* transcripts are less stable than the 3′ ends

The real-time RT-PCR technique was used to quantify different intervals of the *psaA-psaB-rps14* transcripts, and to estimate which part of the cistron is less stable and, probably, where the transcripts start to degrade progressively in *hcf145*. Reverse transcription reactions were performed with either the gene-specific R14-3'-r primer (Table 2) or random hexanucleotides (Figure 10). It is necessary to mention that the use of the gene-specific primer R14-3'-r, chosen from the very 3' end of the operon, allowed quantification of intervals until the 5' end of primary transcripts, whereas using random primers, it was possible to quantify defined intervals not only from the primary transcript, but also from processed intermediate mRNA species.

To equalise amounts of cDNA in *hcf145* and wild-type, the following internal controls were used: the *18S rRNA* and *psaC* primers were chosen for quantification of the cDNA generated with hexanucleotides, whereas the *psbB* primer (psbB-3'-r) was used in one reaction mix, together with R14-3'-r, for the gene-specific reverse transcription reaction, and the amount of *psbB* cDNA was quantified and used for normalisation thereafter (see Materials and Methods).

Primer combinations for the real-time RT-PCR were designed to quantify five representative and non-overlapping regions of the primary *psaA-psaB-rps14* transcript (Figure 10). When using primer R14-3'-r, the highest amount of template was determined for the *rps14* mRNA (25.2 ± 1.5% of the wild-type; transcript region R14) in the mutant. The quantities of the RNA segments further upstream decreased continuously, and constituted 20.5 ± 3.4% for *psaB* (transcript region B), 18.6 ± 2.8% for the intergenic *psaA-psaB* region (transcript region A/B), 15.9 ± 3.1% for *psaA* (transcript region A) and 14.1 ± 2.3% for the 5' end of *psaA* (transcript region A5') in *hcf145*.

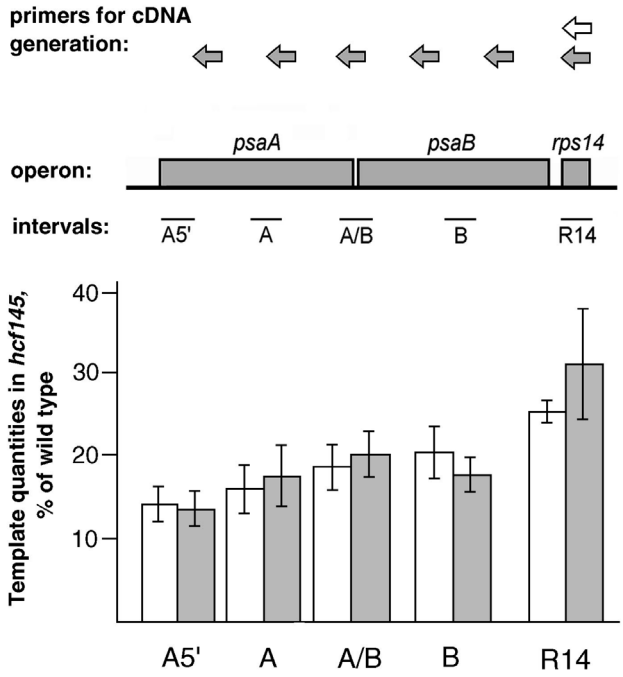

Figure 10. Quantities of individual segments of the *psaA-psaB-rps14* transcript in *hcf145* estimated by real-time two-step RT-PCR. The abundance of several regions, indicated as A5', A, A/B, B and R14, of the *psaA-psaB-rps14* polycistron was analysed in *hcf145* relative to wild-type controls using a *rps14*-gene-specific primer (white arrow and bars) and random primers (grey arrows and bars) for cDNA production. The RT-PCRs were performed with three RNAs isolated independently from three different batches of mutant and wild-type plants. Each sample has been used three times for RT-PCR and subsequent quantification. The tendency presented in this figure was observed in each experiment, and is not only evident by averaging several results.

A similar tendency was observed when random hexanucleotide primers were used for cDNA production with the exception that quantities of the *psaB* interval region (B) were reduced stronger, indicating endonucleolytic cleavage at the 3' region of the primary transcript further downstream of the region B, giving rise to the 0.5 kb *rps14*-containing fragment (Figure 7a). Accordingly, processed *rps14* transcripts of this size accumulated significantly as compared to the primary transcript in the mutant and caused higher estimates of *rps14* intervals obtained by real-time RT-PCR, using both R14-3'-r and random primers (25 and 31%, respectively), in comparison with the amounts of the primary tricistronic transcript of 5.3 kb as judged by Northern analyses (<12.5%). It should further be noted that segments of the tricistronic *psaA-psaB-rps14* transcript (Figure 10) are present not only in the main transcript of 5.3 kb, which is unstable (Figure 7), but also in the two larger transcripts of 7.1 and 6.3 kb, the levels of which are increased in the mutant. Therefore, quantities of the *psaA* transcript calculated with real time RT-PCR (about 15%, segments A and A5') cannot be linearly compared with the quantities of the 5.3 kb band (<12.5%), which appear in the Northern analysis. Taken together, the results of these experiments indicate that the *hcf145* mutation causes differential de-stabilisation of the analysed intervals, leading to less transcript quantities of the *psaA-psaB* region as compared to the *rps14* region.

3.2.6 Molecular mapping of the nuclear-encoded *hcf145* gene

The *hcf145* mutant was obtained from a T-DNA collection (Feldmann, 1991). The kanamycin-resistance marker carried by the T-DNA and the mutant phenotype did not co-segregate, thus indicating that the mutation was not caused by the insertion of the T-DNA. Uncoupling has also been confirmed by genomic Southern analyses using probes of the border regions (data not shown).

Therefore, in a first step, to isolate the affected *hcf145* gene, a mapping population was generated, which consisted of 288 F_2 individuals derived from back-crosses to the accession Landsberg. The mutant was first mapped on the upper part of chromosome 5 between the molecular SSLP markers nga158 and nga151 (with 13 and 17 recombinants, respectively), which are less than 3 Mb apart from each other and located on the bacterial artificial chromosomes MJJ3 (accession no. AB005237) and T15N1 (accession no. AL163792), respectively.

3.3 Characterisation of the *hcf109* mutation, identification and functional analyses of the affected AtprfB factor

3.3.1 Characterisation and complementation of the *hcf109* mutation

Initial studies of the *hcf109* mutant showed that the mutation is located on chromosome 5 and affects stability of distinct plastid-encoded transcripts of several protein complexes of thylakoid membrane, including *psaC* transcript of PSI (Meurer *et al*., 1996a). In the group of Dr. Jörg Meurer, the *hcf109* mutation has been mapped further with high resolution and shown to affect a gene with striking homology to eubacterial *prfB* genes which encode peptide chain release factor 2 (RF2). The mapped gene was named *atprfB* because it is generally accepted that genes in *Arabidopsis* are named according to the corresponding homologous genes. The *atprfB* gene contains six introns and the encoded protein consists of 456 amino acid residues. The ATG context consists of the nucleotides AACATGCCA, which are conserved among plant translational start sites (Lütcke *et al*., 1987).

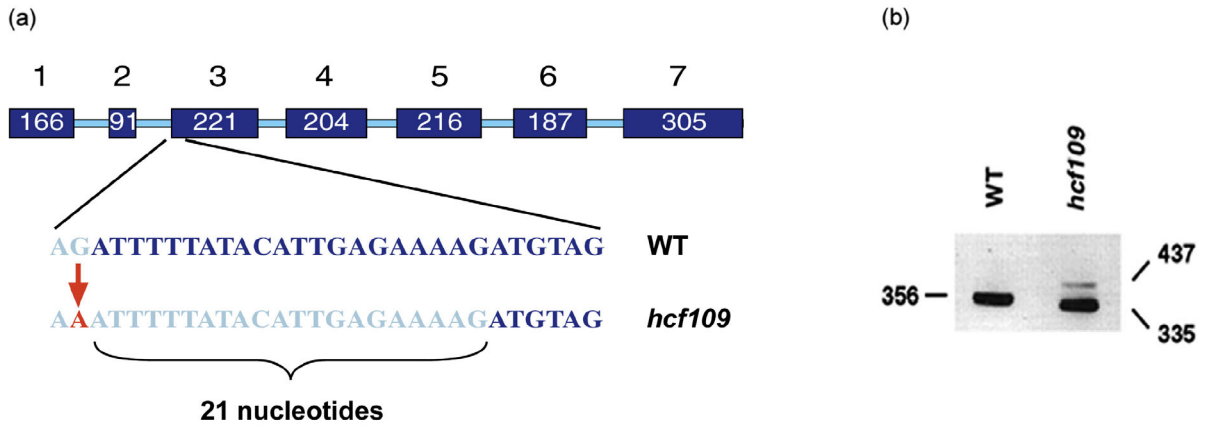

Figure 11. Gene structure and RT-PCR analysis of *atprfB*. **(a)** The seven exons are shown as black boxes, and introns are shown as gray lines. The *hcf109* mutation is based on a G-to-A transition of the last nucleotide of the second intron. The mutation results mainly in the splicing of 21 nucleotides further downstream. WT, wild type. **(b)** Specific primers of exon 1 and exon 3 (atprfB-ex1-f and atprfB-ex3-r, respectively) were used for RT-PCR of mutant and wild-type leaf mRNA. DNA fragments of the indicated sizes (bp) obtained were separated on an agarose gel and visualized with ethidium bromide staining. The top band in the mutant lane represents the unspliced form, the bottom band - the incorrectly spliced form of *atprfB*. WT, wild-type.

The *hcf109* mutation caused a single G-to-A transition at the last nucleotide of the second intron (Figure 11a) and led to the appearance of two mRNA species of different

abundance in the mutant as has been demonstrated by RT-PCR analysis of *atprfB* followed by cloning of the corresponding bands and sequencing of 29 clones (Figure 11b). The 437 bp band of very low abundance resulted from the failure of splicing intron 2. Consequently, the mutation generated a premature in-frame UGA stop codon present in this intron, resulting in a truncated protein of only 92 amino acids. The abundant fragment of 335 bp is characterized by a new 3' splice site of the second intron, which is 21 nucleotides downstream of the wild-type splice site (Figure 11b). As a consequence, seven amino acid residues are deleted in the N-terminal part of the mutated protein in *hcf109*. RT-PCR of wild-type tissue generated only one product of 356 bp, containing the complete and correctly spliced form.

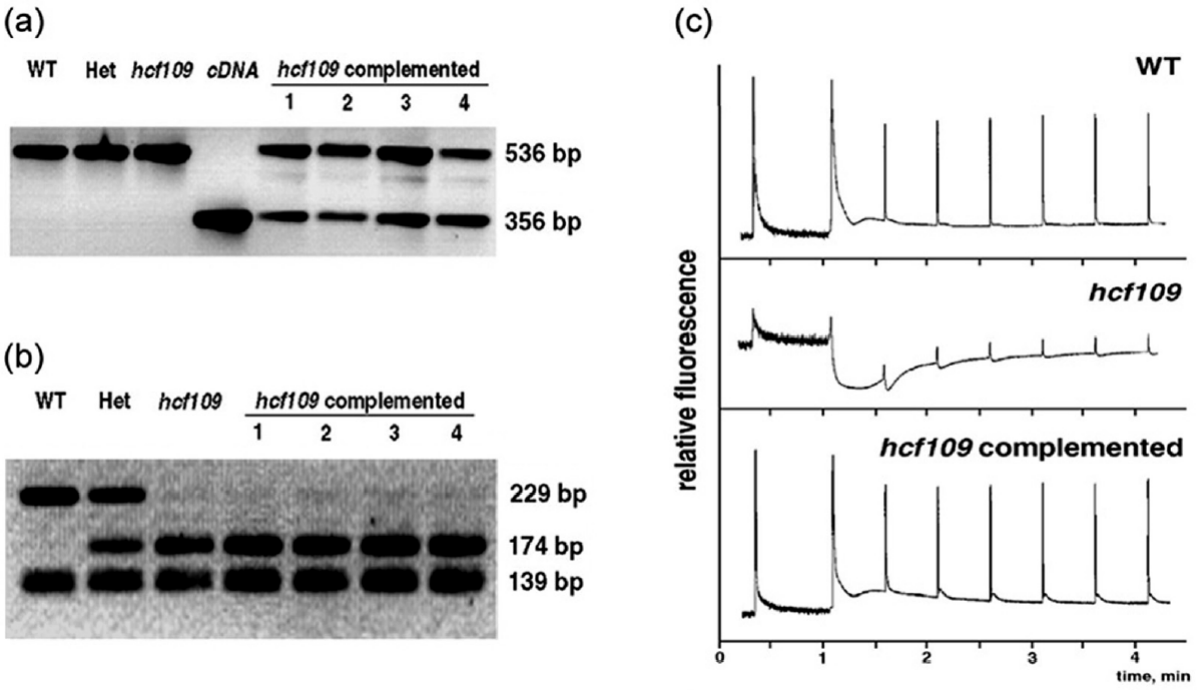

Figure 12. Functional complementation of *hcf109* with the *atprfB* cDNA. **(a)** PCR products generated with exon primers atprfB-ex1-f and atprfB-ex3-r for WT, heterozygous (Het) and mutant (*hcf109*) plants, sulfadiazine-resistant transformants 1 to 4 and the *atprfB* cDNA showing the presence of the cDNA in the genome of the transformant lines 1 to 4. **(b)** Tru9I-digested PCR products generated with intron and exon primers atprfB-int2-f and atprfB-ex4-r, respectively, amplifying exclusively endogenous genomic DNA of *atprfB* demonstrating that viable transformant lines 1 to 4 were homozygous for the *hcf109* mutation. Several restriction products of <50 bp are not shown. **(c)** Chlorophyll fluorescence induction kinetics of wild-type (WT), mutant and complemented lines.

Complementation of the mutant was performed by expressing the full-length cDNA of *atprfB* (accession no. AJ298098) in *hcf109* heterozygotes. Eleven independent transformants were obtained that could grow photoautotrophically and were fertile. The presence of the

wild-type cDNA was confirmed by PCR analysis (Figure 12a), and the homozygosity in the complemented lines was shown by restriction fragment length polymorphism that was induced by the mutation (Figure 12b). Whereas the mutant is characterized by a high initial level of chlorophyll fluorescence, reflecting disconnection between antenna and reaction center of photosystem II and disfunctions within PSII, and by decrease of fluorescence far below the initial level during induction, followed by an increase in fluorescence emission (Figure 12c), complemented mutant plants exhibited chlorophyll fluorescence parameters characteristic to those of wild-type plants. The ratio of variable to maximal fluorescence was 0.8 (compared with 0.19 in mutants), initial fluorescence was as low as in the wild-type based on leaf area, and the fluorescence quenching characteristics were identical to those of the wild-type (Figure 12c). Taken together, these data confirm that the deficiencies in *hcf109* are caused by the point mutation in *atprfB*.

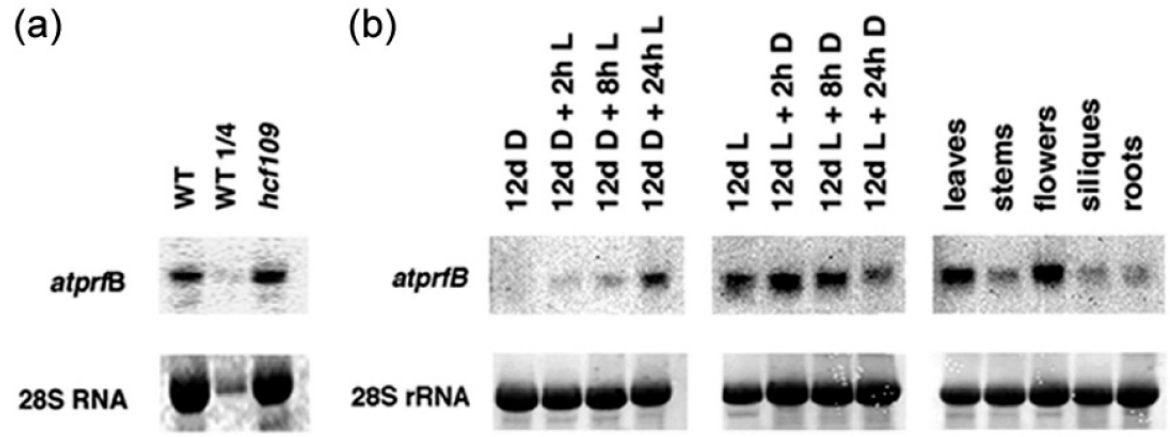

Figure 13. Expression analysis of *atprfB*. **(a)** Transcript levels of *atprfB* from three-week-old mutant and wild-type leaves of plants grown under the same conditions and analysed by RNA gel blot hybridisation. Filters were stained with methylene blue and levels of 28S rRNA are shown to demonstrate uniform loading. **(b)** The effect of light (L) and dark (D) incubation on the expression of *atprfB* in seedlings and the levels of the *atprfB* mRNA in different tissues were analysed from the wild-type using RNA gel blots, as described in Materials and methods.

3.3.2 Expression of *atprfB* correlates with chloroplast development

No differences in *atprfB* mRNA level were detected between wild-type and *hcf109* (Figure 13a). A transcript of 1.45 kb accumulated in light-grown seedlings but was barely detectable in dark-grown seedlings (Figure 13b). Illumination of dark-grown seedlings

induced a slow but continuous increase in the transcript level over 24 h. Subjecting seedlings to dark conditions after light growth significantly reduced the *atprfB* transcript levels after a dark period of 24 h. Surprisingly, high *atprfB* transcript levels were detected in flowers, and low transcript levels were detected in stem, silique and root tissues (Figure 13b).

3.3.3 AtprfB is a chloroplast stromal protein

Analysis of the N-terminal 57 amino acids of AtprfB revealed sequence similarities with chloroplast transit peptides (von Heijne, 1990). The presence of a putative cleavable transit peptide was predicted with high confidence using the algorithms ChloroP and TargetP (Emanuelsson *et al*., 2000), Predotar (http://www.inra.fr/Internet/Produits) and PSORT (http://psort.nibb.ac.jp/). Import experiments confirmed the localization of AtprfB in the soluble fraction of the chloroplast (Figure 14) .

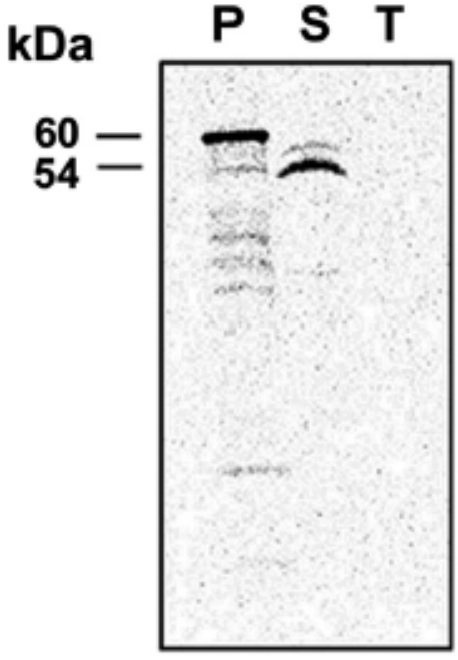

Figure 14. Import of AtprfB into isolated chloroplasts. The AtprfB protein was synthesized and labelled with [^{35}S]-methionine *in vitro*. The precursor protein (P) of 60 kDa was imported into isolated chloroplasts, and a mature protein of 54 kDa was detected in the stroma fraction (S). AtprfB was not present in the thylakoid membranes (T).

3.3.4 AtprfB and homologous eubacterial peptide chain release factors

3.3.4.1 *Synechocystis prfB* is a progenitor of *atprfB*

Sequence comparison of *prfB* genes from eubacteria revealed that at the time when the analyses were performed, the annotated sequence of *Synechocystis* sp PCC 6803 was incorrect

because a frameshift site was ignored, therefore, it was impossible to regard the *Synechocystis* protein as a close relative of the *Arabidopsis* one. Sequencing of the *prfB* gene of *Synechocystis* using hcf109-Syn-f and hcf109-Syn-r primers (Table 2) did not reveal any mistakes in the published sequence. The annotated RF2 protein was misleadingly predicted to start with an unusual GTG codon, located downstream of the real ATG start codon, and the protein had a length of 289 amino acid residues, which was at least 80 amino acid residues shorter than all other known eubacterial release factors.

For a large number of bacteria, a +1 frameshift had been described at a highly conserved distance relative to the start codon (Figure 15a; Craigen *et al*., 1985). If a +1 frameshift at an internal in-frame UGA termination codon was taken into consideration, the frameshifting site in *Synechocystis* turned out to be identical to that of genes in which frameshifting had been shown, and a number of conserved features characteristic of eubacterial RF2 proteins also could be detected in the *Synechocystis* protein (Figure 15).

The N-terminal part of the +1 frameshifted *prfB* from *Synechocystis* showed significant homology with *prfB* genes from other eubacteria, *atprfB* and *prfA* from *Synechocystis* (Figure 15b and data not shown). A characteristic purine-rich Shine-Dalgarno-like stretch directly upstream of the frameshift site was present in *Synechocystis* (Figure 15a). Interestingly, *prfB* from *Streptomyces coelicolor* does not perform frameshifting (Ogawara *et al*., 1995) and is missing the conserved motifs, although the homologies at the protein level are kept (Figure 15a). Thus, it appeared that *prfB* in *Synechocystis* contains the only known internal in-frame UGA stop codon and encodes a protein with 373 amino acid residues that is able to discriminate between UGA frameshifting sites and release signals. At present the sequence of the *Synechocystis prfB* gene in the database has been corrected.

3.3.4.2 Comparison of AtprfB and corresponding eubacterial proteins

The deduced protein of the frameshifted *prfB* in *Synechocystis* exhibits a striking homology of 71.8% with AtprfB and thus appears to be a putative progenitor of the plastid protein. The deduced size of 44.7 kDa for the mature AtprfB is similar to that calculated for the homologous eubacterial forms (e.g., 41.2 kDa for *E. coli*, 42.0 kDa for *Bacillus subtilis*, and 41.8 kDa for *Synechocystis*) taking the +1 frameshifting site into consideration.

In eubacteria, the N-terminal residues are less conserved than the remaining part of the protein. That also was observed in AtprfB. Hydropathy profiles indicate that the N terminus,

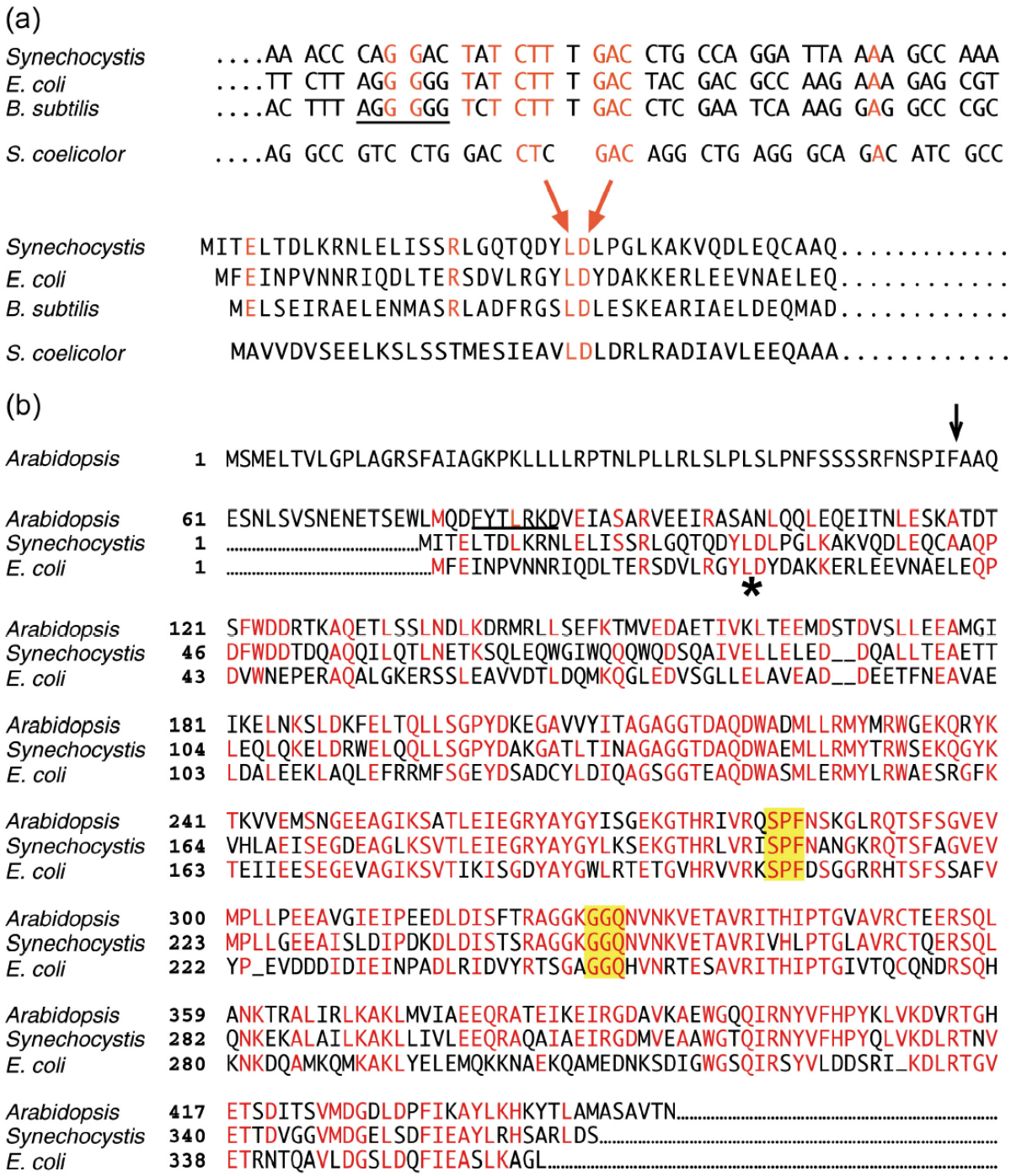

Figure 15. Frameshifting of *prfB* in *Synechocystis* and sequence alignments with AtprfB. **(a)** Conserved *prfB* frameshift sites in *E. coli* and *B. subtilis* were compared with that proposed in *Synechocystis* at the DNA (top) and protein (bottom) levels. The sequence of *S. coelicolor*, which does not perform frameshifting is included. Conserved sequences are highlighted in red. The purine-rich Shine-Dalgarno-like stretch upstream of the frameshift site is underlined. **(b)** Comparison of eubacterial release factors with AtprfB in *Arabidopsis*. The asterisk indicates the conserved eubacterial frameshifting site, and the arrow indicates the predicted cleavage site of the plastid target sequence of AtprfB. The deletion of seven amino acid residues in *hcf109* is underlined. Conserved motifs responsible for stop codon recognition (SPF) and the peptidyl-tRNA hydrolase reaction (GGQ) are highlighted in yellow.

which is modified in *hcf109*, is related more closely to the *Synechocystis* protein than to the *E. coli* protein (Figure 15b and data not shown). Highly conserved motifs in eubacterial RF2 also were identified in conserved positions of the plastid form (Figure 15b). The C-terminal part contains the tripeptide anticodon SPF, which determines RF2 specificity *in vivo* (Ito *et al.*, 2000; Nakamura *et al.*, 2000), and the universal GGQ motif, responsible for peptidyl-tRNA hydrolysis (Frolova *et al.*, 1999).

3.3.5 Translation of plastid mRNAs containing the UGA stop codon is impaired in *hcf109*

Protein gel blot analysis revealed that plastid proteins that are encoded by genes containing TAA or TAG stop codons (i.e., the large subunit of ribulose-1,5-bisphosphate carboxylase/oxygenase, RbcL, the subunits PetA, PetB, and PetD of the cytochrome b_6/f complex and the PSII subunit PsbE) accumulate at almost normal levels in the mutant (Figure 16a). Substantially lower levels were detected for proteins with termination signals triggered by a UGA stop codon: two subunits of the ATP synthase CF_1 subcomplex AtpB (20%) and AtpE (<<10%), the PSI protein PsaC (<<10%), the PSII subunits PsbB (<<10%) and PsbZ (formerly Ycf9) (10%) (Figure 16a) . An additional overlapping protein of higher molecular mass was detected in the mutant with an antibody raised against AtpB (Figure 16a). The amount of outer antenna proteins of photosystem II, which are encoded by nuclear genes appears to be unaffected in the mutant (Meurer *et al.*, 1996a).

Protein abundance in the mutant could be limited by translational efficiency. Therefore, plastid translation was estimated by pulse labelling with [^{35}S]-methionine in the presence of cycloheximide. In agreement with previous observations for *psbB* (Meurer *et al.*, 1996a), this study provides additional evidence for a decrease in translation of the UGA-containing *atpB* messages (20%) (Figure 16b). Translation of the AtpA subunit, which is terminated by a UAA stop codon, was unchanged in the mutant, nonetheless, only ~50% of the protein was detectable. This reflects decreased stability of AtpA, probably caused by the AtpB deficiency (Figure 16). However, the possibility cannot be excluded that some of the labelled AtpA band arises from the long form of the AtpB detected on the protein gel blot. The translation of a 4.4 kDa protein was repressed in *hcf109* (Figure 16b). Based on the molecular mass, this protein appears to be the photosystem II subunit PsbT containing a UGA stop codon in its transcript.

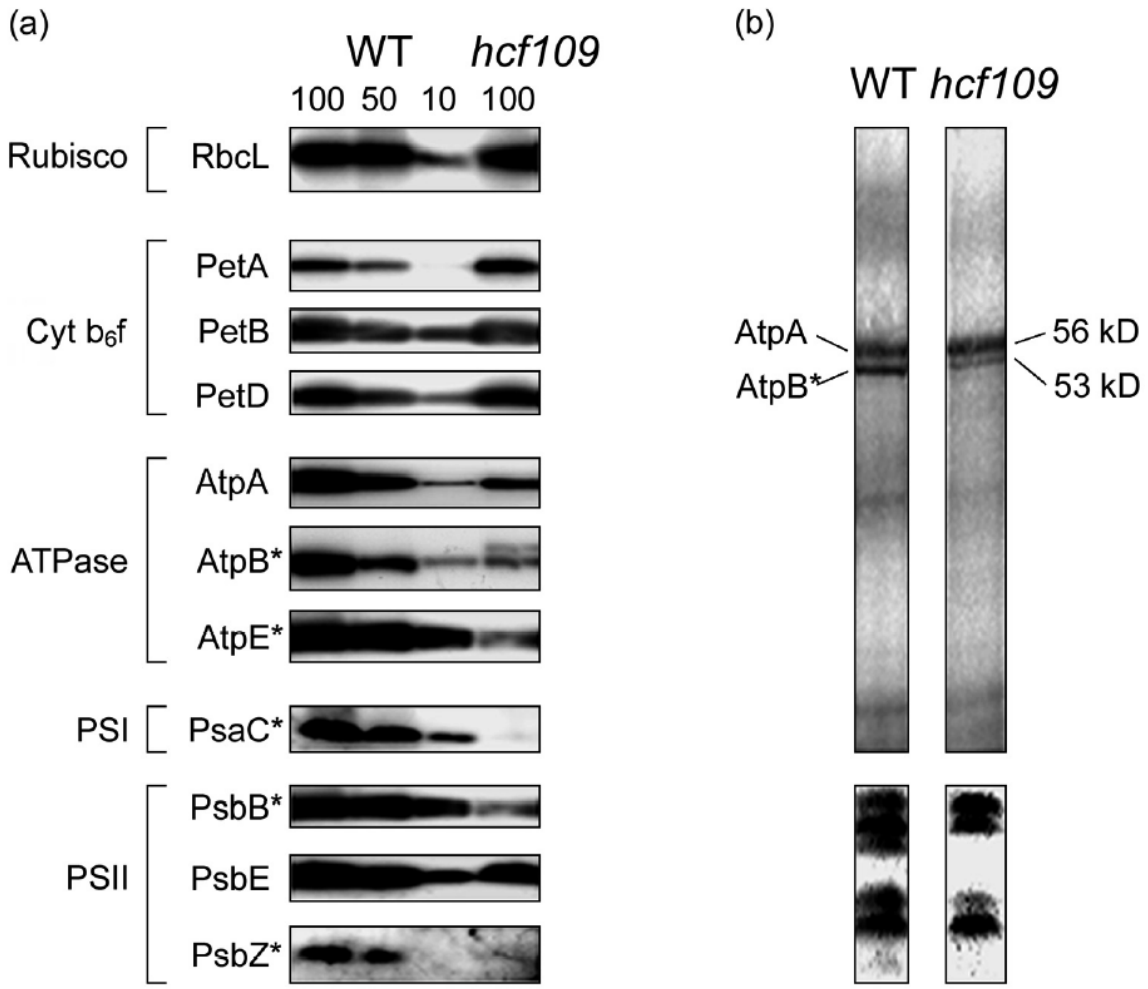

Figure 16. Accumulation and *in vivo* labelling of plastid proteins in *hcf109*. **(a)** Immunoblot analysis of thylakoid membrane proteins from three-week-old wild-type (WT) and *hcf109* seedlings. For quantification, 100, 50 and 10% of WT membranes were loaded. Asterisks indicate proteins encoded by genes containing a TGA stop codon. Cyt b_6f, cytochrome b_6/f; PSI and PSII, photosystems I and II; Rubisco, ribulose-1,5-bisphosphate carboxylase/oxygenase. **(b)** *In vivo* labelling of chloroplast membrane proteins separated on 10% (top) and 16% (bottom) polyacrylamide gels. Coseparation of molecular mass standards served to estimate the sizes (in kDa) of the labelled proteins.

3.3.6 Chloroplast mRNAs containing UGA stop codons are unstable in *hcf109*

In *hcf109*, plastid mRNAs containing the termination signals UAA (28 analyzed out of 47) and UAG (11 analyzed out of 18) and all tested rRNAs and tRNAs were unaffected in size and abundance (Figure 17a and data not shown) (Meurer *et al.*, 1996a). Specific deficiencies were observed for all 12 UGA stop codon–containing plastid transcripts, *i.e.* for the PSII genes *psbB*, *psbT* and *psbZ*, the PSI gene *psaC*, the *ndhC/K/J* (Meurer *et al.*, 1996a) and *ndhI*

genes encoding subunits of the NDH complex, the cytochrome b_6/f complex gene *petL*, the *atpB* and *atpE* genes of the ATP synthase, the *rps2* and *rps16* genes encoding ribosomal subunits and the *ycf4* gene (Figure 17b). Two transcripts of 2.1 and 1.7 kb that contain sequences of *ndhC/K/J* were almost absent, although only *ndhJ* is terminated by a UGA stop codon (Figure 18). Thus, messages from genes that are co-transcribed with TGA-containing genes were affected as well. The transcript levels were not reduced uniformly for the genes mentioned and ranged between 5 and 50% of wild-type levels. *Run-on* analysis demonstrated that transcription of these mRNAs in *hcf109* was unaltered (Meurer *et al.*, 1996a). Therefore, it appears that UGA stop codon-containing plastid transcripts had decreased stability in the mutant.

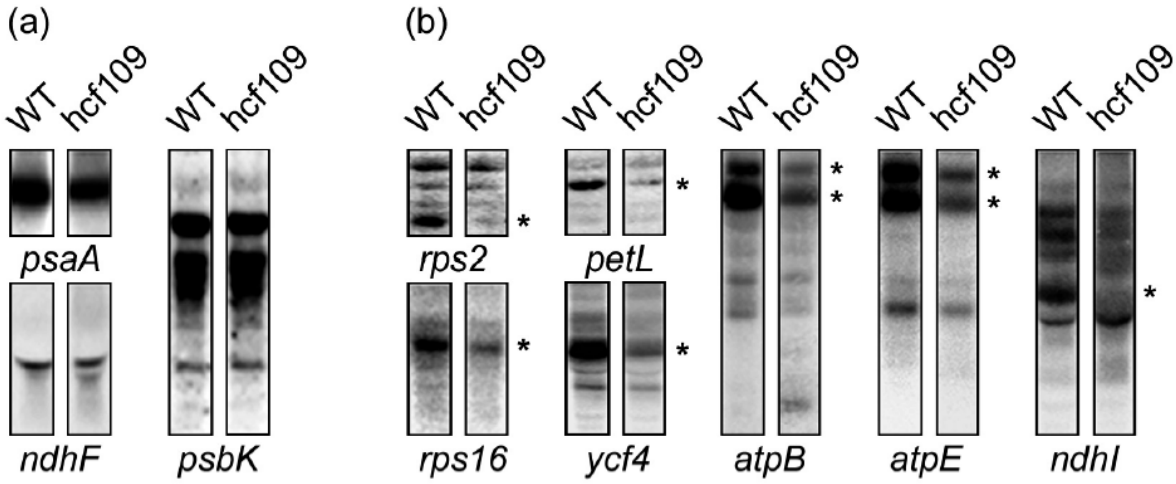

Figure 17. Northern analysis of plastid genes in mutant and wild-type leaves. **(a)** Transcript levels of plastid genes containing UAA and UAG stop codons. **(b)** Transcript levels of plastid genes containing UGA stop codons. Bands of reduced intensity in the mutant are indicated by asterisks.

3.3.7 The decreased stability of the UGA-containing transcripts is caused by translational events

Because AtprfB is involved in ribosomal release, translational or post-translational events at the UGA stop codon could be responsible for the decreased mRNA stability in *hcf109*. The translation inhibitors lincomycin and chloramphenicol, which could completely inhibit chloroplast translation in *hcf109* and wild-type after 15 min of incubation, without any effect on cytoplasmic translation (data not shown), were used to clarify whether translation

errors and/or increased polysome association were responsible for the decreased mRNA stability in the mutant (see also Chapter 3.2.5.2).

Whereas transcript levels of *psbA* and *rbcL*, which do not contain a UGA stop codon, remained constant, both inhibitors clearly gave rise to a substantial increase in the transcript levels of *psbB*, *psbZ*, *ndhC/K/J* and *psaC* in the mutant. Complete restoration of mRNA accumulation was finished after 27 h. In spite of the different target sites and effects, both inhibitors used in this study conferred the same stabilizing effect on otherwise highly unstable transcripts in *hcf109*, indicating that decreased mRNA stability in the mutant is independent of polysome loading but a consequence of translational events in UGA-containing transcripts.

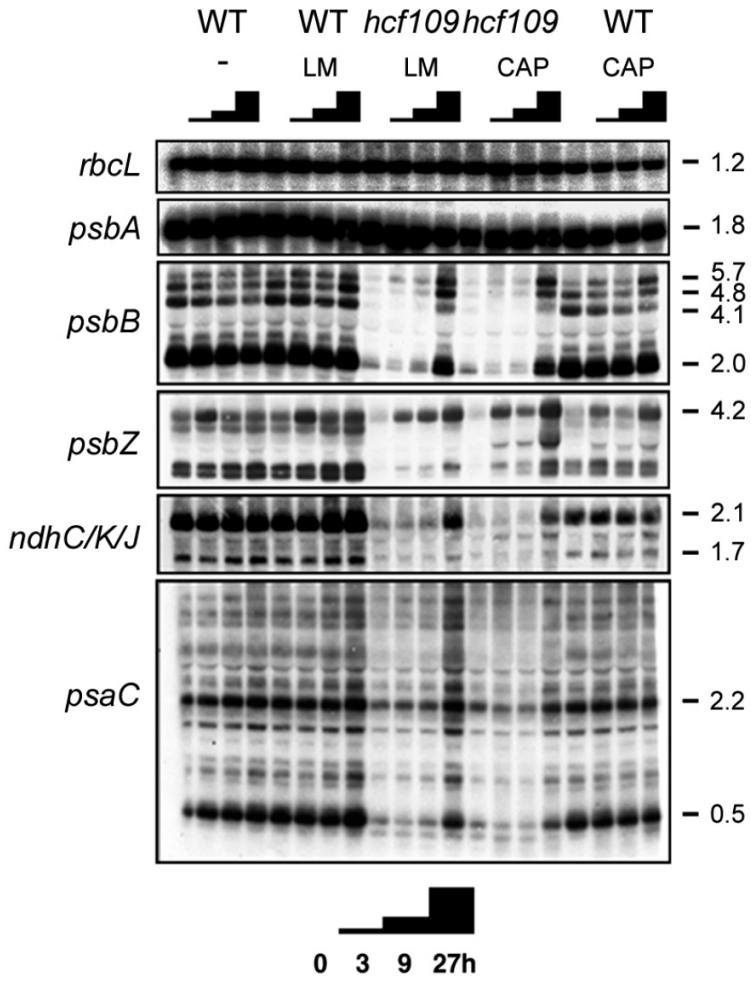

Figure 18. Effect of translation inhibitors on plastid transcript levels in *hcf109*. Three-week-old mutant and wild-type (WT) plants were incubated with the antibiotics chloramphenicol (CAP) and lincomycin (LM). At time 0 and after 3, 9 and 27 h of incubation, transcripts were isolated and analysed by RNA gel blot hybridisation. Incubation without antibiotics (-) served as a control. Probes of the TGA-containing genes *psbB*, *psbZ*, *ndhJ* and *psaC* were used in the analysis. The filters were re-hybridised with probes of the *rbcL* and *psbA* genes, which contain TAG and TAA stop codons, respectively. Within 27 h, UGA-containing transcripts accumulated in the mutant to wild-type levels. Sizes are given in kb.

Similarly to the results of the *hcf145* translation inhibition experiment (Chapter 3.2.5.2), antibiotics exerted different effects on mRNA accumulation in wild type. Generally, endonucleolytic processing of plastid transcripts remained unaffected with both inhibitors: processed forms were mostly unaltered in size and abundance. Chloramphenicol inhibited splicing of the *psbB* operon (Figure 18): the unspliced 5.7 kb form accumulated significantly, whereas the completely spliced 4.1 kb form was much weaker after 27 h of inhibition in the wild type. An unexpected transient increase of *psbZ*-containing transcripts was found in all wild-type samples after 3 h incubation.

3.4 Characterisation of the *hcf101* mutant

3.4.1 Activity of PSI is impaired in *hcf101*

Similarly to the *hcf145* mutant, spectroscopic analysis has shown that PSI is the primary target of the chemically-induced *hcf101* mutation. In line with findings from other PSI mutants (Meurer *et al.*, 1996a), the ratio of variable to maximal fluorescence was 0.5 ± 0.05, whereas qP and NPQ quenching was dramatically decreased in *hcf101* compared to wild-type plants, suggesting that photochemistry in PSII and reduction of the plastoquinone pool are not the prime defects in the mutant (see below). Failure to exhibit any light-induced absorbance changes of the PSI reaction centre molecule P700 at 820 nm revealed a significant deficiency of functional PSI complexes in *hcf101*.

3.4.2 Ultrastructure of the *hcf101* chloroplasts

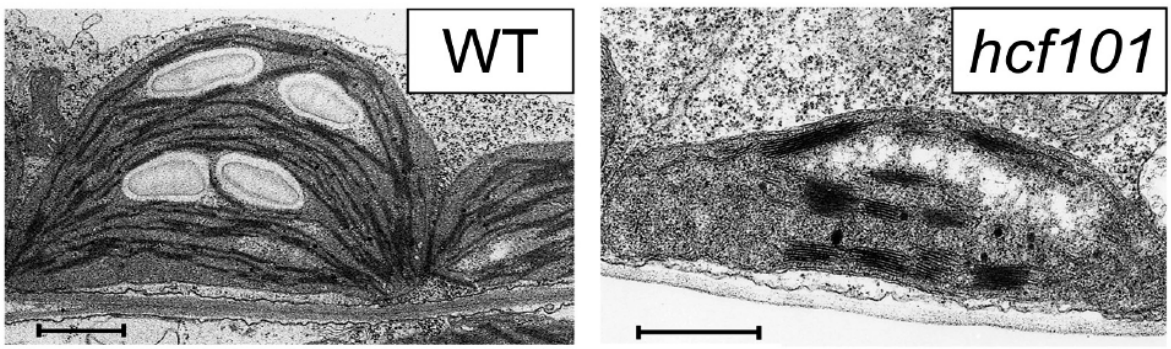

Figure 19. Chloroplast ultrastructure of wild-type and the *hcf101* mutant. The bars represent 1 μm.

At the ultrastructural level, the structure of the *hcf101* chloroplasts is typical for PSI-deficient mutants (Figure 19). Whereas wild-type chloroplasts possess a well-developed membrane system consisting of grana stacks interconnected by stroma thylakoids, *hcf101* mutant plastids are able to form grana stacks but contain fragmentary stroma lamellae (Figure 19), consistent with the location of the PSI complexes in the unstacked membranes.

3.4.3 *hcf101* fails to accumulate PSI core complexes

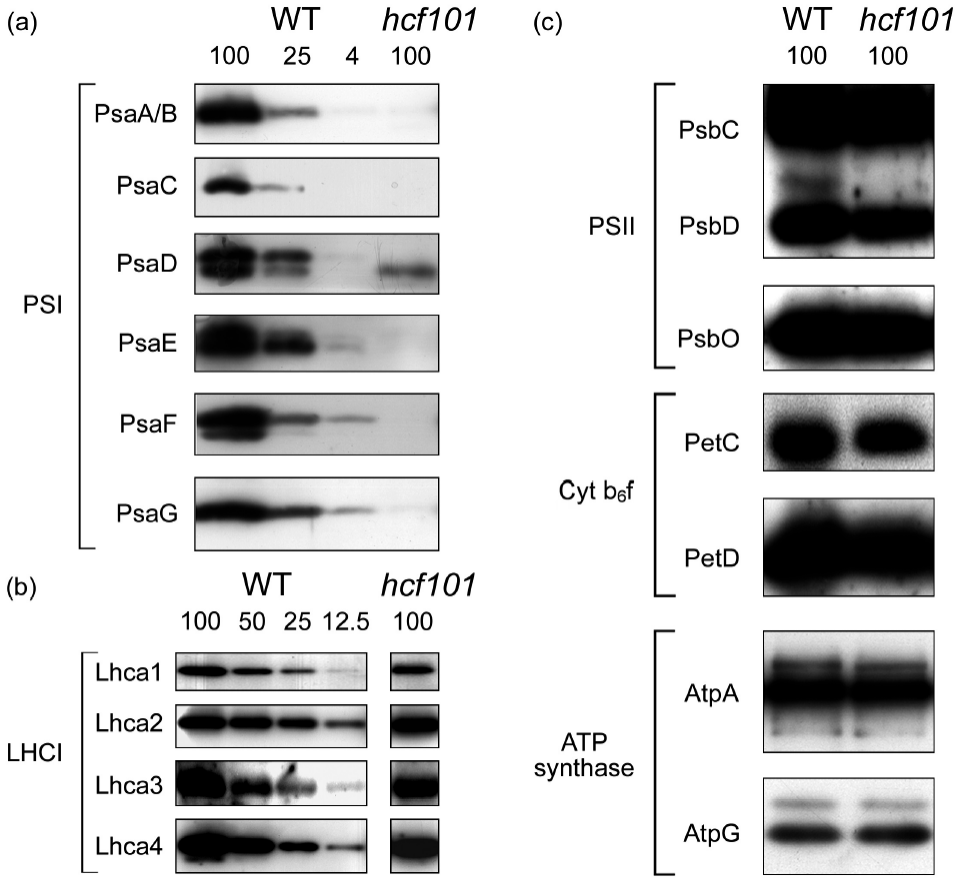

Figure 20. Western analysis of thylakoid membrane proteins isolated from three-week-old *hcf101* and wild-type (WT) plants. **(a)** Immunodetection of PSI subunits PsaA/B, PsaC, PsaD, PsaE, PsaF and PsaG. Loading 100 corresponds to 10 μg membrane proteins of WT. **(b)** Immunodetection of Lhca1, Lcha2, Lhca3 and Lhca4 subunits of LHCI. **(c)** Immunoblot analysis of ATP synthase subunits AtpA and AtpG, of cytochrome b_6f complex subunits PetC and PetD, and of PSII subunits PsbC, PsbD and PsbO.

Levels of representative subunits of the thylakoid membrane complexes ATP synthase, PSII and the cytochrome b_6/f did not show significant differences between mutant and the wild-type (Figure 20c). However, all nuclear- (PsaE, PsaF and PsaG) and plastid-

(PsaA/B and PsaC) encoded subunits of PSI analysed accumulated to levels much below 4% in *hcf101* (Figure 20a). Remarkably, two proteins were recognized by the anti-PsaD antibody. The form of higher molecular mass was also dramatically reduced to less than 4% whereas larger amounts of the lower molecular mass form accumulated in *hcf101*. Although it remains possible that the latter form has arisen because of a cross-reaction of the antibody with another protein, significantly reduced levels of both subunits are indicative that they represent PsaD isoforms encoded by the two genes, *PSAD1* and *PSAD2* (Legen *et al*., 2001). These findings supported the spectroscopic data and confirmed that accumulation of PSI core complexes is primarily impaired in *hcf101*.

3.4.4 Steady-state levels and translation events of photosynthetic transcripts are not altered in *hcf101*

No deficiencies in nuclear (*psaD, psaE, psaF, psaG, psaH* and *psaL*) and plastid (*psaA* and *psaB, psaC, psaI* and *psaJ*) transcripts encoding components of PSI could be observed in *hcf101* (data not shown), leading to the conclusion that *hcf101* is defective in post-transcriptional steps of PSI biogenesis.

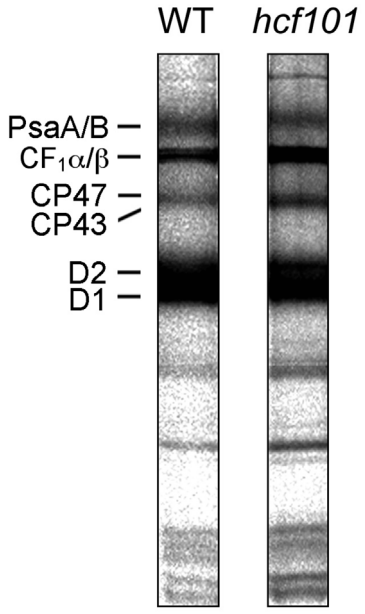

Figure 21. *In vivo* labelling of chloroplast-encoded membrane proteins from *hcf101* and wild type (WT). Primary leaves of 12-day-old WT and *hcf145* seedlings were pulse-labelled with [^{35}S]-methionine for 20 min in the presence of cycloheximide. WT and mutant membrane proteins with equal amounts of incorporated radioactivity (100 000 cpm) were separated by SDS-PAGE, blotted onto a PVDF membrane and analysed by phosphorimaging.

To figure out whether PSI protein abundance is limited by translational disturbances or complex assembly/degradation in the *hcf101* mutant, the rate of synthesis of the plastid PsaA and PsaB subunits was investigated in pulse-labelling experiments with [^{35}S]-methionine in the presence of cycloheximide (see also Chapter 3.2.3) (Figure 21). When proteins with equal

amounts of incorporated radioactivity were loaded, the protein-labelling patterns in mutant and wild-type were almost identical with respect to the size, the number of detectable polypeptides and their relative intensity of labelling.

To provide further evidence that the *hcf101* mutant is not affected at the translational level, polysomal loading of plastid transcripts was analysed. The sizes and distribution of polysomes loaded with the *psaA/B* and *psaC* mRNA did not differ in *hcf101* compared to wild type, as judged from RNA gel blot analysis of polysome fractions collected after a sucrose density gradient centrifugation (Figure 22). The fact that the two largest core subunits PsaA and PsaB are synthesized at normal levels as well as the unaltered polysome association of *psaA/B* and *psaC* mRNAs implies that HCF101 is crucial for (a) post-translational step(s) in PSI assembly.

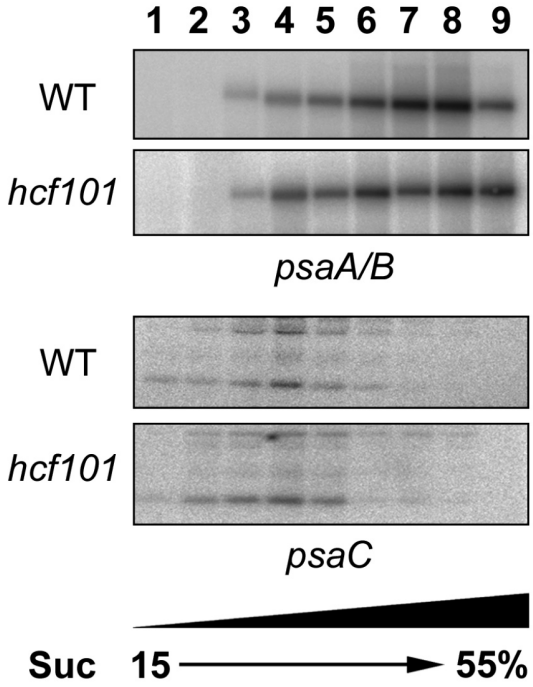

Figure 22. Polysome analysis in *hcf101* and wild-type (WT). Intact polysomes were ultracentrifuged in sucrose gradients. The gradients were fractionated, and the collected fractions were denatured and subjected to RNA gel blot analysis using probes of *psaA/B* and *psaC*. Before hybridisation, filters were stained with methylene blue to show equal distribution of the banding pattern of ribosomal RNA.

3.4.5 Assembly of the mature PSI core complexes is affected whereas the accumulation of the outer antenna of PSI is not changed in *hcf101*

At 77 K, the PSI-specific fluorescence band at 735 nm is shifted to 728 nm, indicating that exitons cannot be transferred efficiently to the PSI reaction centre (Figure 23). However, the signal of the high-wavelength band indicates a nearly normal accumulation of the outer antenna of PSI. This finding is in accordance with almost unchanged levels of all protein subunits of the outer chlorophyll-binding antenna, Lhca1-Lhca4 (Figure 20c).

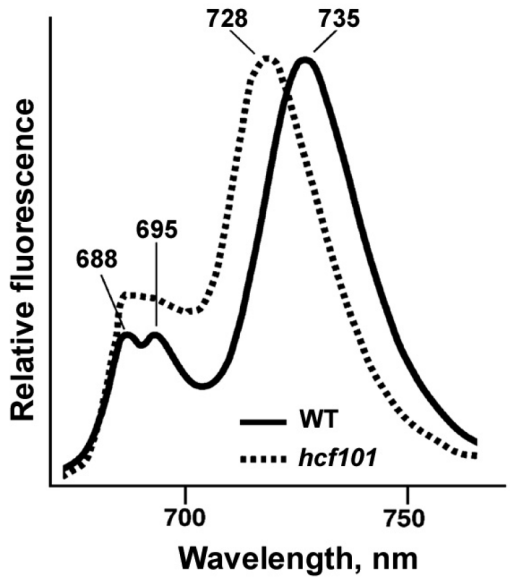

Figure 23. Chlorophyll fluorescence emission spectra at 77 K of *hcf101* and wild-type.

Sucrose gradient centrifugation has been used to separate thylakoid membrane complexes in mutant and wild-type (Figure 24a). Fractions of the gradient have been subjected to immunoblot analysis. PSI antenna proteins were detected as monomers at the top of the sucrose gradient (Figure 24b) whereas PSI supercomplexes were completely missing in *hcf101* (Figure 24a). This suggests that *hcf101* is not affected in the expression of the outer antenna but specifically fails to assemble mature PSI core complexes.

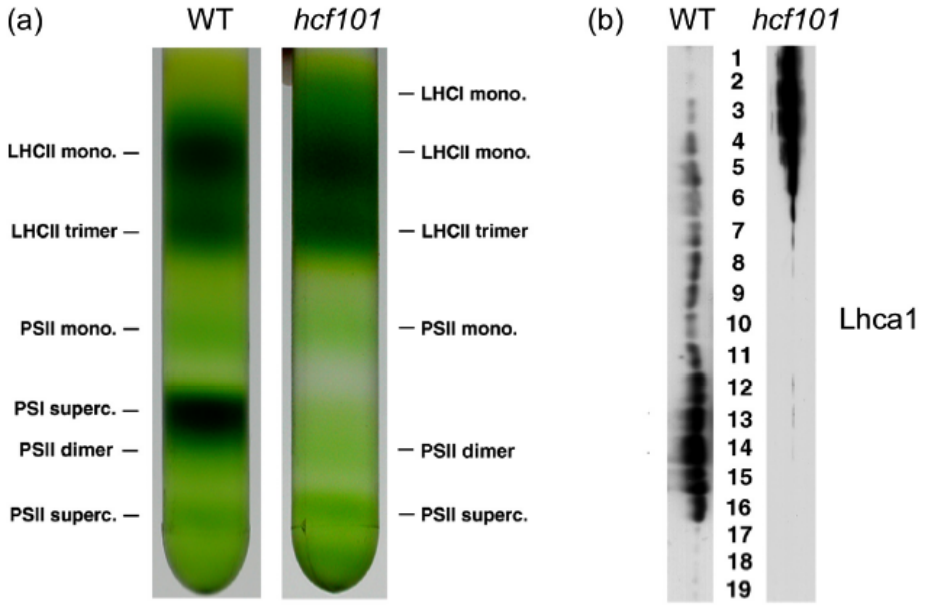

Figure 24. Analysis of function and assembly of the outer PSI antenna. **(a)** Separation of thylakoid membrane complexes on sucrose gradients. **(b)** Fractions 1 - 19 from top to bottom of the gradient have been subjected to SDS-PAGE and Western analysis using antibodies raised against Lhca1.

3.5 Characterisation of the *hcf101* mutation, identification and functional analyses of the HCF101 factor

3.5.1 Characterisation and complementation of the *hcf101* mutation

Mapping of the *hcf101* mutation was performed under the supervision of Dr. Jörg Meurer. The mutation affected a gene containing 13 introns and encoding a 532 amino acid residue protein of unknown function with a deduced molecular mass of 57.7 kDa. The *hcf101* mutation causes a single G-to-A transition of the last nucleotide of intron seven (Figure 25a, b). As a consequence, splicing takes place 30 bp upstream of the original splice site, leading to a premature in-frame stop codon and the production of a truncated protein, as revealed by sequencing RT-PCR products of the mutated *HCF101* gene (Figure 25a).

Homozygous *hcf101* mutants were functionally complemented by expressing the full-length *HCF101* cDNA (accession no. AY450358). Homozygosity of the *hcf101* mutation and the presence of the full-length *HCF101* cDNA in complemented lines were confirmed by sequencing PCR products generated with intron-specific primers and by PCR analyses using exon-specific priners, respectively (Figure 25b, c). Complemented *hcf101* homozygous lines were able to grow photoautotrophically and exhibited normal growth rates, PSI activity and chlorophyll fluorescence patterns (Figure 25d). These results confirmed that the G-to-A transition in the *hcf101* allele is responsible for the mutant phenotype.

3.5.2 Expression of *HCF101* is light-regulated and tissue-specific

Quantitative real-time RT-PCR analysis shows that expression of *HCF101* is low in 12-day dark-grown seedlings (about 3 - 4%) when compared to plants grown in continuous light (100%). Illumination of dark-adapted plants induced a slow but continuous increase in the transcript level up to 85% over 24 h. Subjecting illuminated seedlings to dark conditions significantly reduced the *HCF101* transcript levels after a period of 24 h to 6% of the light control. Expression was high in leaves and, surprisingly, in flowers (100 and 81%, respectively). Lower transcript levels were detected in stems (51%), silique (22%) and root (10%) tissues.

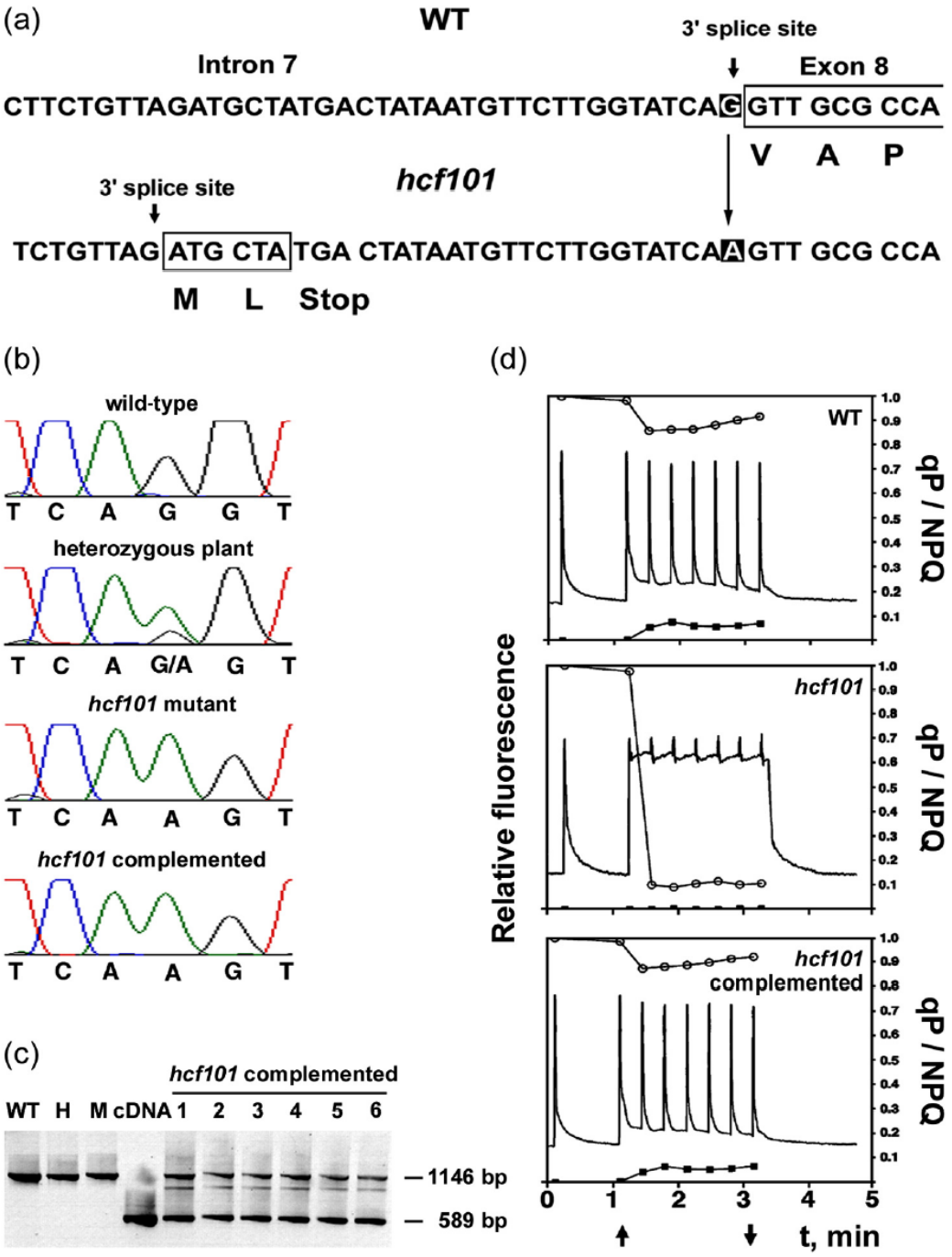

Figure 25. *hcf101* mutation and functional complementation. **(a)** The G-to-A transition of the last nucleotide in intron seven causes a new splice site 30 bp upstream, resulting in premature termination of translation in *hcf101*. **(b)** Sequence of the PCR products, generated with intron-specific primers hcf101-int-f and hcf101-int-r, which enclose the mutant locus and do not amplify the introduced cDNA in complemented lines. **(c)** Electrophoresis of PCR products generated with exon-specific primers hcf101-ex-f and hcf101-ex-r of wild type (WT), mutant and complemented homozygous *hcf101* lines. H, heterozygous line; M, mutant line. The products of 1146 and 589 bp represent the genomic and cDNA, respectively. The intermediate band is a hybrid product. **(d)** Chlorophyll fluorescence quenching analyses of WT, mutant and complemented lines. Open circles, qP; black squares, NPQ; light on, upward arrow; light off, downward arrow.

3.5.3 HCF101 is targeted to the chloroplasts

HCF101 contains a predicted N-terminal cleavable transit peptide of 64 amino acids. Import of *in vitro* synthesized HCF101 into purified chloroplasts confirmed that the predicted transit peptide targets the HCF101 precursor into the chloroplast and is cleaved thereafter giving rise to the mature protein of about 51 kDa (Figure 26). Two additional HCF101-like proteins (HCF101-L1 and -L2) present in *Arabidopsis* have no predicted target sequence for chloroplast import (see below).

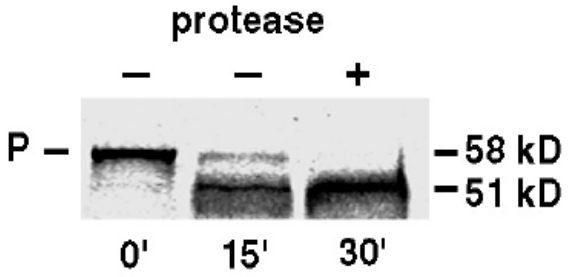

Figure 26. Import of the HCF101 protein into isolated chloroplasts. *In vitro* synthesized and radioactively labelled HCF101 precursors (P) of 58 kDa were added to isolated chloroplasts. After the indicated times, chloroplasts were washed twice, purified and treated with thermolysin (+) where indicated. Chloroplast extracts were gel-separated, and labelled proteins were detected by phosphorimaging. The precursor disappears, whereas the mature imported protein of 51 kDa is not degraded by thermolysin, indicating its localization inside the chloroplast.

3.5.4 HCF101 belongs to an ancient and universally conserved family of P-loop ATPases

The HCF101 protein exhibits striking similarities to P-loop ATPases of the MRP family, which is ubiquitous among sequenced genomes with the exception of those of a few highly reduced obligate parasites (Leipe *et al*., 2002). The designation of this family as 'MRP' is arbitrary, originating from the observation that the *E. coli* homologue is located next to the methionyl-tRNA synthetase gene, *metG*, and was hence named *metG*-related protein (*mrp*; Dardel *et al*., 1990), although there is no relationship between the MRP family of P-loop ATPases and *metG*. Furthermore, the designation 'MRP' for this family is confusing because multidrug resistance proteins are also termed MRPs, a designation which has priority.

Typically for many ATPases, a highly conserved domain is present in HCF101 and homologues, the Walker A motif (Walker *et al*., 1982), which contains a hydrophobic strand followed by the nucleotide-binding P-loop (Figure 27; Saraste *et al*., 1990). The P-loop has the highly conserved consensus sequence GKGGVGKS in 89 relatives of HCF101 with the exception of HCF101 in *Arabidopsis* and rice, where the first glycine at position 184 is replaced by a cysteine residue (Figure 27).

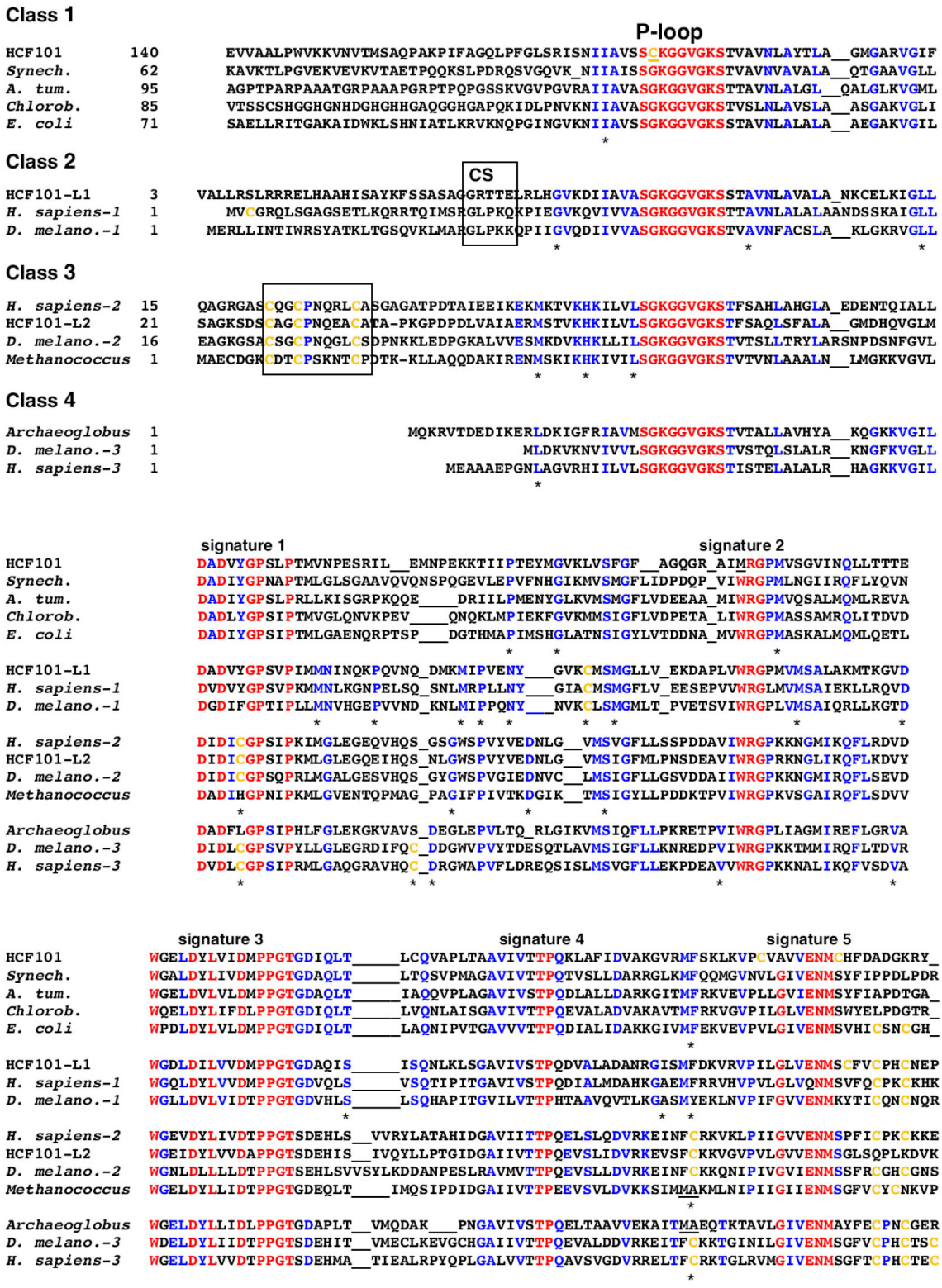

Figure 27. Sequence alignment of HCF101 representatives in all three superkingdoms. Class 1: HCF101 of *Arabidopsis*, *Synechocystis*, *A. tumefaciens, Chlorobium, E. coli*; Class 2: HCF101-L1, *Homo sapiens*-1, *Drosophila melanogaster*-1; Class 3: *H. sapiens*-2, HCF101-L2, *D. melanogaster*-1, *Methanococcus*; Class 4: *Archaeoglobus*, *D. melanogaster*-3, *H. sapiens*-3. CS, predicted mitochondrial cleavage site of class 2. The cysteine-rich region in class 3 is highlighted. Conserved amino acid residues of all 89 members of the HCF101 family are labelled in red (signatures), and those of a specific class are labelled in blue. Specific sites of the four classes are marked with asterisks.

According to N-terminal characteristics, the presence of sequence-specific domains and the proposed subcellular localization, four classes (1 - 4) can be distinguished within the MRP family. Class 1 is found in all lineages and possesses an N-terminal extension of variable length but often matching the DUF59 (domain of unknown function), which is present in HCF101 from *Arabidopsis* and rice (residues 71 - 172) and in MRP members from various eubacteria including *Synechocystis*, *Agrobacterium*, *Magnetococcus*, *Helicobacter* and *Deinococcus*. The DUF59 also occurs in other eubacterial proteins such as PhaH, which is thought to be involved in phenylacetic acid to 2-hydroxyphenylacetic acid conversion (Ferrández *et al*., 2000). Class 2, found only in eukaryotes so far, possesses an N-terminal extension that is predicted to represent a mitochondrial targeting sequence and might represent a mitochondrial MRP form (Figure 27). Class 3 is mostly present in non-photosynthetic organisms such as man, mice, *Caenorhabditis*, *Drosophila* and fungi but also in some eu- and archaebacteria and possesses members with a cysteine-rich N-terminal region with the signature CxxCxxxxC, which is indicative of a [4Fe-4S]-binding motif (Howard and Rees, 1991). The fact that the conserved cysteine-containing N-terminal extension of class 3 is found in members of all three superkingdoms (Figure 27) suggests that this motif was present in the ancestral form of HCF101, possibly having been removed in classes 2 and 4 or replaced by the DUF59 in class 1 during evolution. A class 3 protein has been localized to the nucleus in yeast (Vitale *et al*., 1996), but no data are available for the protein from other eukaryotes. Class 4 members are found in non-photosynthetic eukaryotes with the P-loop in the N-terminal region (Figure 27) and might represent the cytoplasmic MRP form.

In the central region of MRP proteins, there are five specific signatures (1 - 5) with stretches of conserved amino acid residues present in all 89 members of the MRP family. These signatures are not present in more distantly related members of the P-loop ATPase superfamily (Koonin, 1993) but are specific for HCF101 homologues (Figure 27). Signature 1 has the sequence [VITA]-[GA]-x2-D-x-D-xx-G-[PAH]. Signature 2 is characterized by [VLID]-W-R-G-[PLKS] whereby HCF101 contains a methionine instead of a tryptophan residue. Signature 3 has the consensus motif W-x3-D-[VFY]-x4-D-x-P-P-G-T-[GS]-[DE] (Nakashima *et al*., 1999). Signature 4, 16 amino acid residues downstream, can be defined as [VI]-[TSI]-P-[QHES]. Eukaryotic members of classes 3 and 4 possess an additional conserved cysteine residue further downstream whereas nearly all other members have a conserved methionine one position before (Figure 27). Signature 5 is defined as [VLIY]-[VLIA]-G-[VIL]-[VIL]-E-N-M-[SAKH] and is often followed by C-xx-C (Figure 27). Again, only HCF101 deviates from the last two consensus sequences, where glycine is changed to

alanine and the two conserved cysteines are missing, possibly having been shifted to the first and last position of signature 3. All MRP members contain a glycine-rich stretch followed by a conserved [IVLM]-P-[ILM] motif immediately downstream of the last consensus sequence in an otherwise less conserved C-terminal region.

Class 3 proteins contain at least two more cysteine residues at conserved positions in the C-terminal part, again resembling motifs with Fe-S cluster-binding capacity. HCF101 and its homologue from *Oryza sativa* contain a C-terminal extension with a conserved CVVQQC motif, which appears to be specific to the chloroplast form of the MRP protein family (data not shown).

3.5.5 Phylogeny and relatives of HCF101

The high conservation of HCF101 in archaea and eubacteria and all eukaryotic lineages clearly indicates that MRP represents an ancient and essential protein family (Leipe *et al*., 2002). Several well-known, highly conserved and distant relatives of HCF101 of quite diverse functions including the prokaryotic repressor of cell division MinD, the partition protein (ParA), the replicase component RepA, the arsenite transporter ArsA, the CooC protein with a functional role in the insertion of nickel into carbon monoxide dehydrogenase and the two [4Fe-4S]-containing proteins, NifH of the nitrogenase and ChlL/FrxC/BChlL of the light-independent protochlorophyllide reductase (Xiong *et al*., 2000), all derived from the MRP ancestor (Leipe *et al*., 2002). In two prokaryotic lineages, functionally uncharacterized proteins related to the MRP family contain an insertion of the [4Fe-4S]-containing ferredoxin domain (Leipe *et al*., 2002).

3.5.6 HCF101 is involved in accumulation of [4Fe-4S] cluster-containing chloroplast proteins

What could be the function of HCF101? From the present study, it follows that HCF101 is specifically involved in the biogenesis of PSI but not of the other thylakoid membrane complexes. Moreover, the HCF101 protein is highly conserved in the genomes of all - also non-photosynthetic - organisms and has an ancient evolutionary origin, therefore, the specific function of HCF101 must be connected to a process that is common in all lineages. The most plausible explanation seems to be that HCF101 has a role in biogenesis of [4Fe-4S] cluster-containing proteins. This suggestion is supported by the findings that (i) HCF101

homologues possess conserved [4Fe-4S]-binding motifs; (ii) the HCF101-related proteins NifH and CooC affect metal co-factor metabolism (Jeon *et al*., 2001; Rangaraj *et al*., 1997); (iii) in some prokaryotes, such as *Cytophaga hutchinsonii*, *Chlorobium tepidum* and *Nostoc*, *HCF101*-homologous genes are occasionally positionally clustered with thioredoxin-like *nfu* genes, known to be involved in Fe-S cluster metabolism (Garland *et al*., 1999; Nishio and Nakai, 2000; Schilke *et al*., 1999); and (iv) the HCF101 homologues ApbC in *Salmonella enterica* (Skovran and Downs, 2003) and CFD1 in *Saccharomyces cerevisiae* (Roy *et al*., 2003) appear to affect the accumulation of proteins containing [4Fe-4S] clusters.

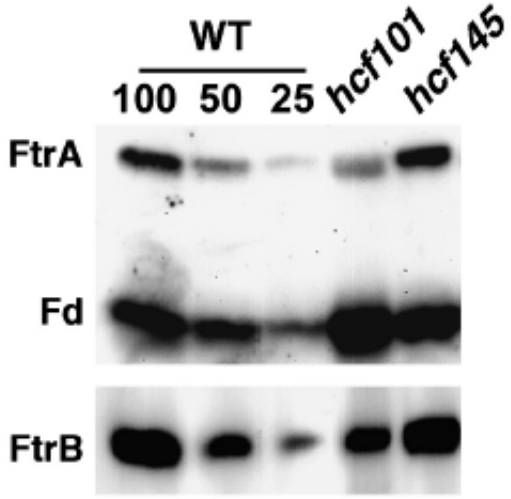

Figure 28. Accumulation of ferredoxin-thioredoxin reductase (FTR) complexes and ferredoxin (Fd) in *hcf101*. Immunoblot analysis of soluble proteins using antibodies raised against Fd and FTR subunits FtrA and FtrB.

Were this true, then not only PSI, but also additional [4Fe-4S]-containing proteins of the chloroplast should be affected in *hcf101* as well. Therefore, the accumulation of stromal ferredoxin-thioredoxin reductase (FTR), which consists of two subunits, α and β (FtrA and FtrB), was examined. The catalytic β subunit possesses a [4Fe-4S] cluster, which seems to be stabilized by the α subunit (Dai *et al*., 2000). Indeed, *hcf101* plants have reduced levels of mature FTR complexes (Figure 28). The deficiency in FTR accumulation is not characteristic of mutants lacking PSI, since *hcf145,* which is also missing the PSI core complex, shows normal levels of FTR subunits (Figure 28). Neither the Rieske protein of the cytochrome b_6/f complex (PetC) nor ferredoxin, both of which contain a [2Fe-2S] cluster, is affected in size or in abundance in *hcf101* (Figures 20c and 28). As FTR complexes that lack [4Fe-4S] clusters are known to be extremely unstable (Manieri *et al*., 2003), accumulated FTR complexes are assumed to contain [4Fe-4S] clusters, suggesting that HCF101 function is either redundant in case of FTR or partially dispensable for [4Fe-4S] cluster assembly into FTR. Thus, the available data suggest that HCF101 has a specific role of in the biogenesis of [4Fe-4S] clusters in chloroplasts of *Arabidopsis*.

4 Discussion

Plants have to tune photosynthesis to changing environmental conditions. For this purpose PSI/PSII ratios are balanced in response to exogenous and endogenous signals (Depège *et al*., 2003). Therefore, regulation of plastid gene expression and accumulation of the photosynthetic complexes is crucial for establishing photosynthetic efficiency. Expression of the chloroplast-encoded genes is modulated at the level of transcription (Allen and Pfannschmidt, 2000), transcript stability (Barkan and Goldschmidt-Clermont, 2000), translation (Zerges 2000) and assembly (Schwabe and Kruip, 2000).

4.1 PSI deficiencies in the *hcf145*, *hcf109* and *hcf101* mutants are not accompanied by entire loss of LHCI

Both spectroscopic and immunological analyses showed that the *hcf145* and *hcf101* mutations specifically affect the PSI complex (Figures 4, 5, 20a, c and 25), whereas the mutated HCF145 and HCF101 proteins are not constituent polypeptides of PSI. Lack of PSI activity was accompanied by a severe reduction of all polypeptide subunits of the PSI to less than 12.5 and 4% in *hcf145* and *hcf101*, respectively, whereas composition and activity of the other thylakoid membrane protein complexes (PSII, cytochrome b_6f and ATP synthase) remained mainly unaltered in both mutants (Figure 5, 20a and c). In contrast, the *hcf109* mutation caused pleiotropic deficiencies of several thylakoid membrane complexes. All analysed subunits of PSI amounted to about 25% in *hcf109*, consistent with the reduction of the overall PSI activity (Meurer *et al*., 1996a).

In spite of the loss of the entire PSI core in *hcf145* and *hcf101*, reduction of the LHCI proteins was not dramatic and uniform (Figure 5a and 20b). Generally, a shift of the PSI-derived 77 K fluorescence emission band from 735 nm toward shorter wavelengths is typically observed when the PSI core complex is impaired but the outer antenna is almost intact (Krause and Weis, 1991, Haldrup *et al*., 2000). Correspondingly, with the extent of the PSI core complex reduction, the 735-nm fluorescence band was shifted to 728 and 730 nm in *hcf101* and *hcf109*, respectively (Figure 23; Meurer *et al*., 1996a).

These data suggest that assembly of the core complex is not absolutely required for the accumulation of the antenna proteins, although they can be cross-linked to the PsaA/PsaB subunits (Jansson *et al*., 1996). The barley mutant *viridis-zb* ^{63} (Nielsen *et al*., 1996), the *ycf3*-

and *ycf4*-deficient mutants of *Chlamydomonas* (Boudreau *et al*., 1997), which possess strongly reduced amounts of PSI as well as *psaA* mutant of *Chlamydomonas* deficient in PSI (Girard-Bascou *et al*., 1987), all nonetheless retain LHCI proteins at almost normal levels. Therefore, it appears that membrane insertion of the PSI core and PSI antenna occurs independent also in *Arabidopsis*.

4.2 HCF145 encodes a factor involved in stabilisation of the plastid *psaA-psaB-rps14* mRNA

4.2.1 Deficiency of the PsaA/PsaB translation causes lack of PSI

In vivo labelling of chloroplast proteins uncovered that the synthesis of the core proteins PsaA/PsaB was specifically affected in *hcf145* (Figure 6). The formation of the heterodimer PsaA/PsaB initiates the assembly of PSI and appears to control the accumulation of other subunits (Schwabe and Kruip, 2000). The deficiency of *psaA-psaB* translation consequently leads to loss of the PSI core complex in *hcf145*. This is reminiscent of mutants with inactivated *psaA* or *psaB* genes in *Synechocystis* sp. PCC 6803 (Smart *et al*., 1991; Smart and McIntosh, 1993) and *Chlamydomonas* (Girard-Bascou *et al*., 1987), which are specifically deficient in PSI, without affecting PSII or other photosynthetic-membrane complexes.

4.2.2 *psaA-psaB-rps14* mRNA stability is primarily affected in *hcf145*

The reason for the defect in *psaA-psaB* translation in *hcf145* was apparent at the mRNA level. Steady-state levels of the *psaA-psaB-rps14* primary tricistronic message of 5.3 kb were specifically reduced to less than 12.5% (Figure 7a). *psaA-psaB-rps14* is cotranscribed with the *ycf3* gene, located upstream, but not with the downstream-located *trnfM* gene (Figure 7a,b). Larger transcripts, containing *ycf3*, were shown to be generated by the action of the nuclear-encoded RNA polymerase (Summer *et al*., 2000; Legen *et al*., 2002). Obviously, only the tricistronic mRNAs of 5.3 kb, which are supposed to be generated by the action of the plastid-encoded RNA polymerase and by processing of the larger precursor (Summer *et al*., 2000), represent a target for the *hcf145* mutation, but the unprocessed primary transcripts initiated upstream of *ycf3* remain stable.

Plastid *run-on* analyses demonstrated that the *rps14* transcription rate was unaltered, but the signal intensities of *psaA* and *psaB* constituted about half of those found in wild-type (Figure 8). Therefore, it appears that (i) HCF145 plays a crucial role in the stability of the tricistronic *psaA-psaB-rps14* transcript and, probably, (ii) it can also be involved in the regulation of the *psaA-psaB-rps14* transcription rate. On the other hand, the decrease of the *psaA-psaB* signal intensity in the *run-on* experiment could be caused by ribonucleolytic activity associated with the 5' end of the *psaA* transcript already during transcription and the time course of the experiment.

Translational events are known to interfere with mRNA accumulation (Barkan, 1993; Lee *et al*., 1996; Barkan and Goldschmidt-Clermont, 2000). For example, knockouts in the ribosomal subunits L11 and S17 affect the accumulation of several mRNAs and one mRNA, respectively (Schultes *et al*., 2000; Pesaresi *et al*., 2001). However, since *run-on* experiments have not been performed in these cases, it remains to be determined whether changes in mRNA stability are involved in the knock-outs reported. It is possible that in these cases defects in protein synthesis affect the plastid-encoded RNA polymerase and, therefore, result in decreased chloroplast mRNA accumulation. Generally, it is difficult to determine whether a mutation affects mRNA stability primarily or via changes in translation (Barkan and Goldschmidt-Clermont, 2000). One way to discriminate between the two processes is to cross the mutation into a mutant background with ribosome deficiencies (Fisk *et al*., 1999). However, RNA polymerase or ribosome-associated proteins involved in mRNA processing might not be active under those conditions (Klaff and Gruissem, 1991). Application of plastid translation inhibitors, turned out to be an useful approach to dissect translational events from effects on mRNA stability in the presence of ribosomes.

Inhibition of translation using lincomycin and chloramphenicol did not lead to recovery of accumulation of primary tricistronic transcripts to significant amounts in *hcf145* (Figure 9), indicating that the decreased *psaA-psaB-rps14* mRNA stability is independent of polysome loading in this mutant. Moreover, no effect of lincomycin treatment, inducing liberation of transcripts from ribosomes, indicates that the ribonuclease activity responsible for rapid degradation in *hcf145* is not associated with polysomes.

4.2.3 General translation rates are not altered in *hcf145*

All chloroplast genes for 30S ribosomal proteins are supposed to be functional (Yamaguchi and Subramanian, 2003). Deficiencies of *rps14* transcripts (25 - 31% of wild

type) may be expected to have consequences in translation rates (Figure 10). However, the *hcf145* mutant exhibited normal relative translation rates and protein accumulation (Figures 5 and 6). Precursor forms, which contain sequences of *rps14*, are probably not used for translation even in the wild-type. Exclusively, the monocistronic *rps14* transcript of 0.5 kb, which is processed in the 5' region of the coding sequence, seems to be translationally competent as it was supposed for the plastid *psbH* transcript (Figure 7a; Felder *et al*., 2001). Slightly reduced levels of the 0.5 kb *rps14* mRNA (Figure 7a) seem to be sufficient to guarantee accumulation of the *rps14* gene product to an extent which is necessary to fulfil its role in translation. The crystal structure (3 Å) of the *Thermus thermophilus* 30S ribosomal subunit demonstrates that the S14 protein, together with S3 and S10, belongs to the tertiary assembly class and helps to stabilise the structure of the 30S head (Wimberly *et al*., 2000; Culver 2003). The tertiary binders probably adjust the structure of the 30S subunit at a late assembly stage, and seem to be indirectly involved in the formation of the tRNA binding site(s), but are not likely to participate directly in 30S functioning (Culver 2003).

4.2.4 How could HCF145 be involved in stabilisation of the *psaA-psaB-rps14* transcript?

The questions of interest are (i) the *cis*-determinants conferring stability to the *psaA-psaB-rps14* transcript and (ii) the mode of action of the *hcf145* gene product. Although all sequence elements can potentially confer stability to mRNA, major determinants are often localised in 5' and 3' UTRs of plastid transcripts (Hayes *et al*., 1999; Monde *et al*., 2000). Chloroplast 5' UTRs have been shown to contain endonucleolytic sites and to be targets for 5'-3' exoribonucleolytic activities. In *Chlamydomonas*, nuclear factors and sequence elements responsible for the stability of a number of transcripts have been identified (Monde *et al*., 2000), and nuclear-encoded supressor mutants affecting *petD* (Esposito *et al*., 2001) and *psbD* (Nickelsen, 2000) mRNA stability via 5' UTRs have been isolated. Also, in vascular plants, 5' UTR regions have been suggested to confer stability to the *psbA* and *rbcL* mRNAs (Alexander *et al*., 1998; Shiina *et al*., 1998; Eibl *et al*., 1999; Zou *et al*., 2003). 3' UTRs can as well be involved in transcript stabilisation. Stable stem-loop structures in 3' UTRs seem to protect upstream sequences against 3'-5' exonucleolytic activity (Hayes *et al*., 1999). 3' UTR-binding proteins have been suggested to be involved in processing and stabilisation of 3' ends (Yang *et al*., 1996; Baginsky *et al*., 2001). Polyadenylation at the 3' end serves as a signal for

chloroplast mRNA degradation (Hayes *et al*., 1999; Schuster and Bock, 2001). Several reports point to a role for protein-coding sequences in mRNA stabilisation (Klaff, 1995; Singh *et al*., 2001; Drapier *et al*., 2002).

In order to determine the target of nuclear *trans*-factor action, generally *cis*-regions fused to a reporter gene are introduced into the chloroplast genome of *Chlamydomonas* mutants (Nickelsen *et al*., 1994; Drager *et al*., 1998; Vaistij *et al*., 2000b). As *Arabidopsis* is so far not accessible to chloroplast transformation, the real-time RT-PCR technique was applied to determine the *cis*-region of the *psaA-psaB-rps14* transcript responsible for mRNA degradation in *hcf145*. In case of a 3'-5' nucleolytic degradation, one would not expect changes of template quantities along the *psaA-psaB-rps14* transcript using gene-specific *rps14* primer for cDNA production. In case of a 5'-3' degradation, the template quantities should continuously decrease from the 3' to the 5' end, regardless of whether hexanucleotide or gene-specific primers are used for cDNA synthesis. Precise quantification of the expression level of distinct regions of the *psaA-psaB-rps14* mRNA (Figure 10) and stable accumulation of the monocistronic *rps14* mRNA in *hcf145* suggest that degradation of the primary transcript does not proceed in 3'-5' direction. Although the differences in the quantities of the intervals of the *psaA-psaB* region in *hcf145* might be too small to allow definitive conclusions about the direction of the degradation, it is evident that although the larger *psaA*-containing transcripts of 7.1 and 6.3 kb are slightly increased in the mutant, the *psaA* 5' region accumulates to significantly lower amounts compared to the *rps14* region, and constitutes 55.8 and 43.3% (SD < 3.8%) compared to the 3' region when gene-specific and random primers, respectively, are used for quantification. It is possible that either the transcripts which are generated by the plastid-encoded RNA polymerase or by processing of the larger precursor containing sequences of *ycf3* are subjected to the action of a 5'-3' exoribonuclease, or that progressive endonucleolytic pathway leads to rapid degradation in *hcf145*, as has been proposed to occur with chloroplast *atpB* transcripts in *Chlamydomonas* (Hicks *et al*., 2002). In the latter case, endonucleolytic cleavage should occur exclusively at the 5' end of the mature *psaA-psaB-rps14* transcripts and not on the larger 7.1 kb and 6.3 kb precursors, as these precursors are stable and their levels are even increased in *hcf145*. The plastid *ycf3* gene is known to be required for stabilisation of the PSI complex (Boudreau *et al*., 1997), and its slight overexpression might be explained by a compensatory effect as a result of loss of PSI function. Similarly, the dominant *mda1* mutation is proposed to de-stabilise *atpA*-containing transcripts by endonucleolytic cleavage (Drapier *et al*., 2002).

Because of the cyanobacterial origin of chloroplasts, the plastid mRNA degradation machinery possesses features of both eukaryotic host and prokaryotic endosymbiont. In eubacteria, crucial roles in mRNA decay are considered to belong to 3' UTRs and 3'-5' exoribonucleases because no 5'-3' exonuclease has been found up to date (Zuo and Deutscher, 2001; Kushner 2002; Dreyfus and Régnier, 2002). However, 5' UTRs are also supposed to operate as transcript stabilisers (Bechhofer 1993), and a number of studies indicate that RNase E starts the degradation process with endoribonucleolytic cleavage within the 5' UTR (Kushner 2002). It has been hypothesised that the endoribonuclease cleaves progressively successively in the 5'-3' direction, and the resulting fragments are subjected to 3'-5' exoribonucleolytic activity, which makes the overall direction of mRNA degradation from 5' to 3' end (Grunberg-Manago 1999; Régnier and Arraiano, 2000). In accordance with this, large-scale analysis of high-density oligonucleotide arrays, covering transcripts from *E. coli*, has shown that the stability of polycistronic transcripts increases towards the 3' end (Selinger *et al*., 2003). In contrast, in eukaryotes, 5'-3' exoribonucleolytic activities appear to play principal roles in regulation of mRNA stability (Gutiérrez *et al*., 1999). Chloroplasts possess 5'-3' exoribonucleolytic (Drager *et al*., 1998, 1999; Nickelsen *et al*., 1999; Vaistij *et al*., 2000b) as well as endoribonucleolytic activities (Hayes *et al*., 1999; Hicks *et al*., 2002). Protein homologues to the N-terminal catalytic part of RNase E are present in *Synechocystis* sp. PCC 6803 and plastids of *Arabidopsis* and *Porphyra purpurea* (Kaberdin *et al*., 1998; Baginsky *et al*., 2001). Moreover, the cyanobacterial enzyme binds to the same substrates *in vitro* and cleaves them at the same sites as known from RNase E in *E. coli* (Kaberdin *et al*., 1998). Therefore, degradation of *psaA-psaB-rps14* could involve both eubacterial and eukaryotic pathways.

As the *hcf145* mutation acts specifically on the *psaA* operon and not on other plastid transcripts, it appears that the *hcf145* locus encodes a nuclear *trans*-acting factor specifically involved in protecting the *psaA-psaB-rps14* mRNA from degradation, either directly or in a complex associated with other proteins. Most probably, HCF145 is imported into the chloroplast and interacts with *cis*-acting elements, conferring stability to the *psaA-psaB-rps14* mRNA, or it binds specifically exo- and/or endoribonucleases, preventing their activity. According to the roles of the plastid proteins NAC2 and MBB1, in both mRNA stabilisation and translation (Nickelsen *et al*., 1999; Vaistij *et al*., 2000b), it is conceivable that HCF145 exerts additional functions in translational or assembly processes. However, as the *HCF145* gene is still unknown, it cannot be excluded that HCF145 might function outside the chloroplast by regulating other gene products.

4.2.5 Possible role of HCF145 during chloroplast development

Whereas translational and/or post-translational processes are known to regulate accumulation of reaction-centre subunits PsaA/PsaB during greening (Hihara and Sonoike, 2001), transcriptional (Kim *et al*., 1993; Pfannschmidt *et al*., 1999) as well as post-transcriptional control (Glick *et al*., 1986; Deng *et al*., 1989) appears to prevail during acclimation to different light regimes. Light quality specifically affects transcription and turn-over rates of the *psaA* mRNA (Deng *et al*., 1989). Regulation of plastid transcripts simultaneously at the levels of transcription and RNA stability was also found in *Chlamydomonas* (Salvador *et al*., 1993), developing barley (Rapp *et al*., 1992), wheat (Kawaguchi *et al*., 1992), and in the mesophyll and bundle-sheath chloroplasts of maize and *Sorghum* (Kubicki *et al*., 1994). Therefore, HCF145 might be involved in the regulatory processes and could enable tissue-specific chloroplast development at an early stage and allow adaptation of photosynthesis to changing endogenous and environmental signals.

4.3 Dual role of AtprfB, a chloroplast peptide chain release factor of eubacterial origin, in protein synthesis and transcript stabilisation

4.3.1 Termination of translation in eukaryotes, prokaryotes and chloroplasts

The eukaryotic cytosolic system and archaebacteria require a single omnipotent release factor, eRF and aRF, respectively, for recognition of the three stop codons and peptidyl-tRNA hydrolysis. In contrast, eubacteria possess two peptide chain release factors: RF1 (*prfA*) which decodes UAA and UAG, and RF2 (*prfB*) decoding UAA and UGA (Scolnick *et al.,* 1968; Nakamura and Ito, 2003). The specificity of stop codon recognition is provided by the conserved tripeptides Pro-Ala-Thr (PAT) in RF1 and Ser-Pro-Phe (SPF) in RF2 (Ito *et al.,* 2000; Nakamura *et al.,* 2000). Essential for the catalysis of peptidyl-tRNA hydrolysis is a Gly-Gly-Gln (GGQ) motif which is conserved in all known release factors (Frolova *et al.,* 1999) and represents a structural counterpart to the CCA-3' acceptor stem of the tRNA-amino acyl group (Frolova *et al.,* 2000). The glutamine of the GGQ motif is N:(5)-methylated in *E. coli* (Dincbas-Renqvist *et al*., 2000). The crystal structures of the human eukaryotic release factor eRF1 and the bacterial RF2 (Song *et al*., 2000; Vestergaard *et al.,* 2001) and single particle cryo-electron microscopy of RF2 bound the bacterial ribosome (Klaholz *et al.,* 2003;

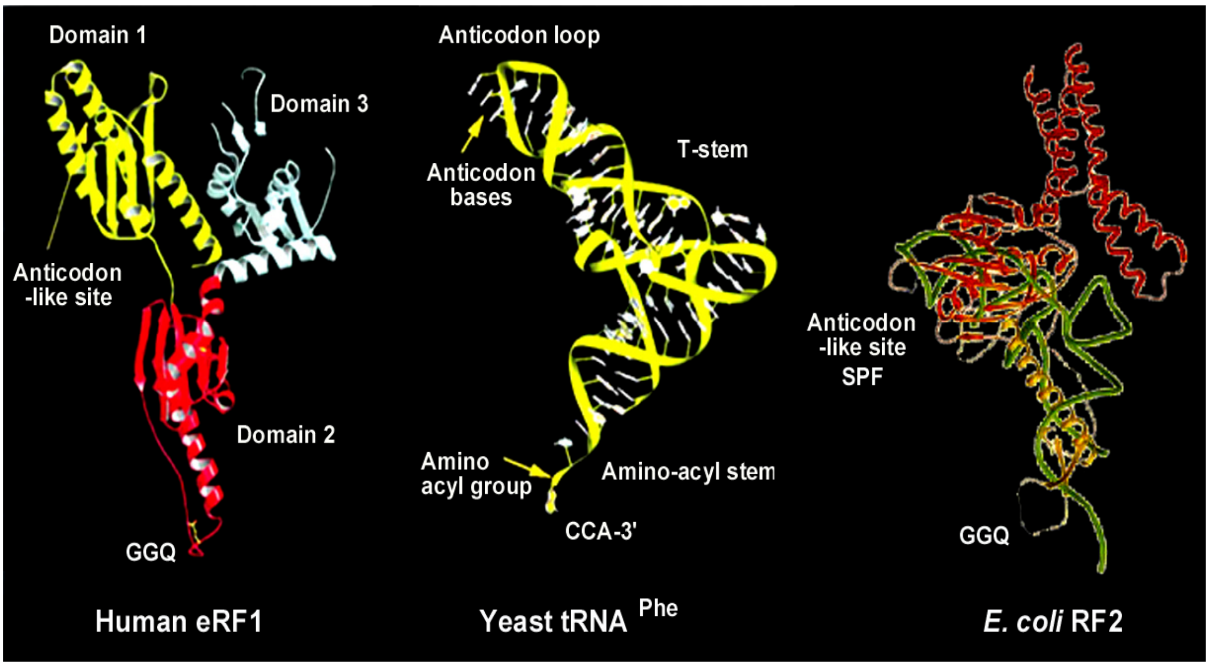

Figure 29. Molecular mimicry between RFs and tRNA molecules (Song *et al*., 2000; Klaholz *et al*., 2003 modified). Human eRF1 and yeast $tRNA^{Phe}$ have similar shapes. The position of domains 1, 2 and 3 of eRF1 matches that of the tRNA anticodon loop, aminoacyl stem and T stem, respectively. The GGQ motif of eRF1 is equivalent to the aminoacyl group attached to the CCA-3′ sequence of the aminoacyl stem of a tRNA molecule. A conserved groove on domain 1 of eRF1 is proposed to form the codon recognition site.

Rawat *et al*., 2003) supported the proposed tRNA–protein mimicry hypothesis, in which release factor anticodon determinants play a crucial role in stop codon recognition (Figure 29; Ito *et al*., 1996; Nakamura and Ito, 2003).

In chloroplasts, little is known about the role of stop codons in the processes of termination and regulation of translation (Zerges, 2000). Comparison of AtprfB with eubacterial RF2 revealed that the SPF anticodon recognition motif and the hydrolytic GGQ center (Frolova *et al*., 1999; Ito *et al*., 2000) are conserved in AtprfB, indicating similarities in the mechanism of ribosomal release at UGA and UAA stop codons between chloroplasts and eubacteria. On the other hand, the N-terminal part of the protein, which is thought to interact with ribosomal proteins (Ito *et al*., 1996) and is mutated in *hcf109*, is much less conserved (Figure 15b). Therefore, the N-terminus could possess features making chloroplast and eubacterial translation systems different. The differences in the interaction of release factors with ribosomes and in termination processes could also be caused by the evolutionary acquisition of novel nucleus-encoded subunits of chloroplast ribosomes that are not homologous with any known protein in eubacteria (Yamaguchi and Subramanian, 2000, 2003).

4.3.2 Autoregulation of *prfB* expression in eubacteria by +1 frameshifting

An in-frame UGA codon inside the *prfB* gene allows many eubacteria to autoregulate exquisitely the synthesis of their own release factors by a +1 frameshift in the recoding site (Craigen and Caskey, 1986). The finding of a frameshifting site of a nonsense in-frame UGA codon of *prfB* in *Synechocystis,* the putative progenitor of *atprfB* (Figure 15), suggests that this organism also autoregulates synthesis of RF2. In chloroplasts, +1 frameshifting has not been found so far. In addition, the conserved amino acids leucine and aspartic acid of the eubacterial frameshift site were changed completely in AtprfB (Figure 15b). None of the plastid chromosomes sequenced to date contains release factor-encoding genes, therefore, it appears that a transfer of the gene to the nucleus occurred very early during evolution and that the internal in-frame UGA stop codon of the progenitor gene must have been eliminated to express a functional protein. Therefore, the questions remain: (i) why the apparently simple and efficient mechanism of regulation of RF2 concentration by frameshifting in the cell is not used in all eubacteria (Figure 15a; Adamski *et al.,* 1993; Baranov *et al.,* 2002) and (ii) which mechanisms, if any, were adopted by the eukaryotic expression system for this function.

4.3.3 Light- and tissue-regulated expression of *AtprfB*

atprfB is predominantly expressed in photosynthetic tissues, moreover light strongly enhances the levels of the *atprfB* transcripts (Figure 13b). Therefore, the *atprfB* expression is tightly coupled to chloroplast development and function indicating a specific role of AtprfB in plants. In the dark, the stability and translation of many plastid transcripts are generally reduced (Mullet 1993), and their expression increases during chloroplast development (Klein *et al.,* 1988; Bruick and Mayfield, 1999). The low level of *atprfB* transcripts in the dark might have an impact on the translation and stability of the UGA-containing mRNAs and, accordingly, on the levels of the protein subunits of PSII, PSI, NDH complexes, ATP synthase and ribosomes. Otherwise, low *atprfB* expression levels were observed in stems, siliques and roots but, surprisingly, high *atprfB* amounts accumulated in flowers suggesting a specific role of polypeptides from messages containing UGA stop codons in this tissue (Figure 13b). Consequently, when constitutive or organ-independent expression of foreign genes in transplastomic approaches is desired, one should avoid equipping the transgene with a TGA stop codon.

4.3.4 Effect of *AtprfB* modification on protein and transcript accumulation in chloroplasts

In prokaryotes, mutations in *prfB* lead to nonsense suppression, most often causing misreading of UGA stop signals by incorporating non-encoded amino acids or increased frameshifting. As a result, *prfB* mutants have temperature-sensitive or lethal phenotypes (Mikuni *et al.,* 1991; Adamski *et al.,* 1993). The *hcf109* mutation results in a deletion of seven amino acids in the N-terminal part of AtprfB. Modification of AtprfB causes significant decrease in the accumulation of all 12 UGA-containing plastid transcripts and corresponding proteins (Figures 16a and 17b). In addition, it appears that the mutation has also affected translational efficiencies because the AtpE protein level was reduced to <10%, whereas *atpE* transcripts accumulated to ~50% in *hcf109*. Since low amounts of proteins encoded by UGA-containing transcripts still accumulate, it follows that translation of the corresponding transcripts must be terminated correctly in *hcf109*. Probably, this is possible because the C-terminal domain, which is highly conserved among prokaryotes and possesses the two essential SPF and GGQ motifs (Frolova *et al.,* 1999; Ito *et al.,* 2000), is not mutated in *hcf109*. Therefore, the mutated AtprfB protein could contain some residual activities.

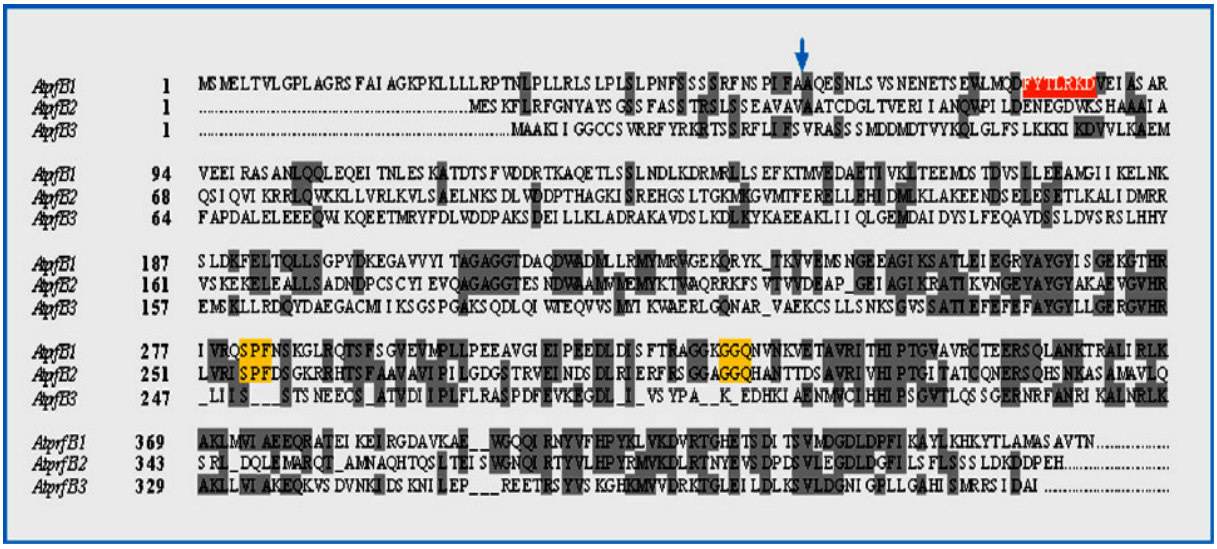

Figure 30. Comparison of *prfB*-like genes in *Arabidopsis*.

Two additional genes, *atprfB2* and *atprfB3*, located on chromosomes 1 and 3, respectively, encode proteins homologous to AtprfB1 (Figure 30). However, these gene products do not complement *hcf109*. *AtprfB2* is predicted to represent the mitochondrial form,

whereas *AtprfB3* is lacking the SPF and GGQ motifs and therefore appears to lose the release factor function and to possess other functions related to ribosomal release.

It has been shown previously that decreased accumulation of plastid transcripts in *hcf109* was caused by impaired stability (Meurer *et al*., 1996b). Application of translation inhibitors lincomycin, liberating transcripts from ribosomes, and chloramphenicol, transferring mRNA into a highly polysome-bound state, stabilized the UGA-containing *psbB*, *psbZ*, *ndhC/K/J* and *psaC* mRNAs, which normally fail to accumulate in the mutant (Figure 18). Thus, translational events but not the polysome loading appear to affect the transcript stability. Chloramphenicol is supposed to affect release factor function as well, supporting involvement of the termination machinery in the stabilization of plastid mRNAs.

4.3.5 How could the termination machinery be involved in the stabilisation of plastid mRNAs

Several molecular scenarios are conceivable to illustrate how release factor could be involved in the transcript stabilisation. First, ribosomes could traverse into the 3' UTRs of the messages and perturb stabilising elements which are often housed within this regions (Monde *et al*., 2000). Two processes may be responsible for this: read-through by incorporation of an non-encoded amino acid or frameshifting. For instance, introduction of genes with an extended reading frame into the genome of *Chlamydomonas* resulted in a destabilization of transcripts (Lee *et al*., 1996). Each kind of read-through or frameshift at UGA stop codons produces larger proteins. Although frameshifting has not been reported previously for chloroplasts, in the case of AtpB, an additional larger protein that might result from +1 frameshifting could be detected (Figure 16a).

Often, stabilizing elements are represented by secondary structures (Stern and Gruissem, 1987). However, a pronounced stable 3' UTR structure that might have been perturbed could be predicted only for *psbT* (data not shown; Zuker *et al*., 1999). Numerous stop codons in all reading frames downstream of the UGAs in the *Arabidopsis* plastid chromosome would prevent an extensive movement of ribosomes into the 3' UTRs in nearly all affected genes (data not shown). Hence, the instability of UGA-containing transcripts in *hcf109* cannot always be explained by traversing ribosomes.

Second, decreased mRNA stability might be caused by translational processes at the UGA stop codon that involve both AtprfB and ribosomes. Also, recycling of ribosomes

between a still unidentified connection between the 3' and 5' ends of plastid mRNAs might be impaired, provoking decreased mRNA stability (Zerges, 2000). A plastid ribosomal recycling factor identified in *Arabidopsis* (Rolland *et al.,* 1999) could be involved in this process.

Third, a eukaryote-like surveillance mechanism (Culbertson 1999; Hilleren and Parker, 1999a, 1999b) responsible for the nonsense-mediated degradation of RNA in chloroplasts could be proposed. In eukaryotes, related mechanisms regulate the stability and expression of mRNAs that fail to signal translational termination (Frischmeyer *et al.,* 2002). The protein Ski7p, which is involved in the exosome-mediated degradation of mRNAs lacking a termination signal, shows homology with the GTPase domain of the translation termination factor eRF3 (van Hoof *et al.,* 2002). Similar surveillance might have been acquired for the regulation of chloroplast transcript stability or for the accuracy of the gene expression machinery. Once acquired, such a cleaning system recognizing and disposing dysfunctional transcripts might have been established for individual transcripts during co-evolution of the plastome and the nuclear genome. Therefore, individual differences in the sequences posing as targets of degradation might explain the discrepancies of the mutational effect on the stability of individual UGA-containing transcripts.

Fourth, in eubacteria, stalled ribosomes on mRNAs that lack a stop codon are released for recycling by a transfer mRNA (Keiler *et al.,* 1996; Watanabe e*t al.,* 1998; Karzai *et al.,* 2000). This mechanism targets the protein and probably also the displaced mRNA for degradation (Karzai and Sauer, 2001; Flynn *et al.,* 2001). Interestingly, in eubacteria, transfer mRNA tagging is inversely correlated with RF2 activity (Collier *et al.,* 2002). In chloroplasts of vascular plants, such a cleaning system might be expected, but has yet to be demonstrated (Watanabe *et al.,* 1998).

4.3.6 The additional regulatory function of AtprfB might cause evolutionary constraints keeping the number of plastid TGA stop codons high in vascular plant organelles

To understand the evolutionary role of the nuclear-encoded AtprfB in chloroplasts of higher plants, the distribution of stop codons and the GC content in 41 plastid chromosomes was analyzed (Figure 31).

4.3.6.1 TGA distribution in genes and open reading frames of plastid chromosomes

Annotation of plastid genomes gives rise to three classes of reading frames, those with known functions (genes) or homologues in any other organism (*ycf*, hypothetical chloroplast reading frame) or open reading frames (ORFs) of unknown function and without any obvious homology with other known genes. To be sure that annotated ORFs really represent genes, the distribution of TGA stop codons was compared in ORFs and genes (*ycf*s and known genes). Surprisingly, the number of TGA-containing ORFs in most algae and higher plants is several fold higher than that among conserved genes (e.g., 17.0-, 7.4- and 6.7-fold higher in *Nephroselmis olivacea*, *Odontella sinensis* and *Guillardia theta*, respectively, and up to 3.3-fold higher in *Oenothera elata*, spinach and maize) (data not shown). The organisms, which exhibit an almost identical distribution of TGA elements in both gene classes, are the algae *Porphyra purpurea* and *Cyanidium caldarium*. Lateral gene transfer into the plastome, which was proposed in the case of *N. olivacea* (Turmel *et al.,* 1999), resulted in the acquisition of ORFs with a high bias of TGA stop codons. Thus, statistical considerations lead to the general conclusion that many annotated TGA-containing ORFs do not seem to represent genes, or, at least, are not always representative of cyanobacteria-derived genes in plastid chromosomes. Therefore, the ORFs were excluded from the analyses of the stop codon distribution.

The two annotated TGA stop codons in the *Chlamydomonas* plastome are present in ORFs (Maul *et al.*, 2002; http://www.biology.duke.edu/chlamy_genome/chloro.html). Therefore, it is reasonable to assume that *Chlamydomonas* has completely lost the RF2 function. This is consistent with the absence of the *prfB* gene in the almost completely sequenced nuclear genome of *Chlamydomonas*. Taking this into consideration, caution is advised when performing transplastomic experiments using this alga: reporter genes containing TGA stop codons might not work because of the failure of translation termination. Although two reports have shown that UGA stop codons can be functional in *Chlamydomonas* chloroplasts (Lee *et al.,* 1996; Sizova *et al.,* 1996), the possibility of frameshifting and read-through was not investigated in these cases.

4.3.6.2 The distribution of stop codons compared with GC content in organelles

Generally, the distribution of TAG codons in algae and higher plants often directly correlates with GC content (Figure 31), whereas changes in the number of TAA-containing

genes are mostly accompanied by inverse changes in the use of TAG and in GC content. TGA-containing genes in plastid chromosomes are not represented by gene groups that are connected functionally, structurally or biochemically to each other. They are distributed randomly along the chromosomes and embedded into different nucleotide surroundings (data not shown). TGA stop codon use is independent of the distribution of TAG, another guanidine-containing stop codon, and of GC content. Plastids of *Toxoplasma gondii* have

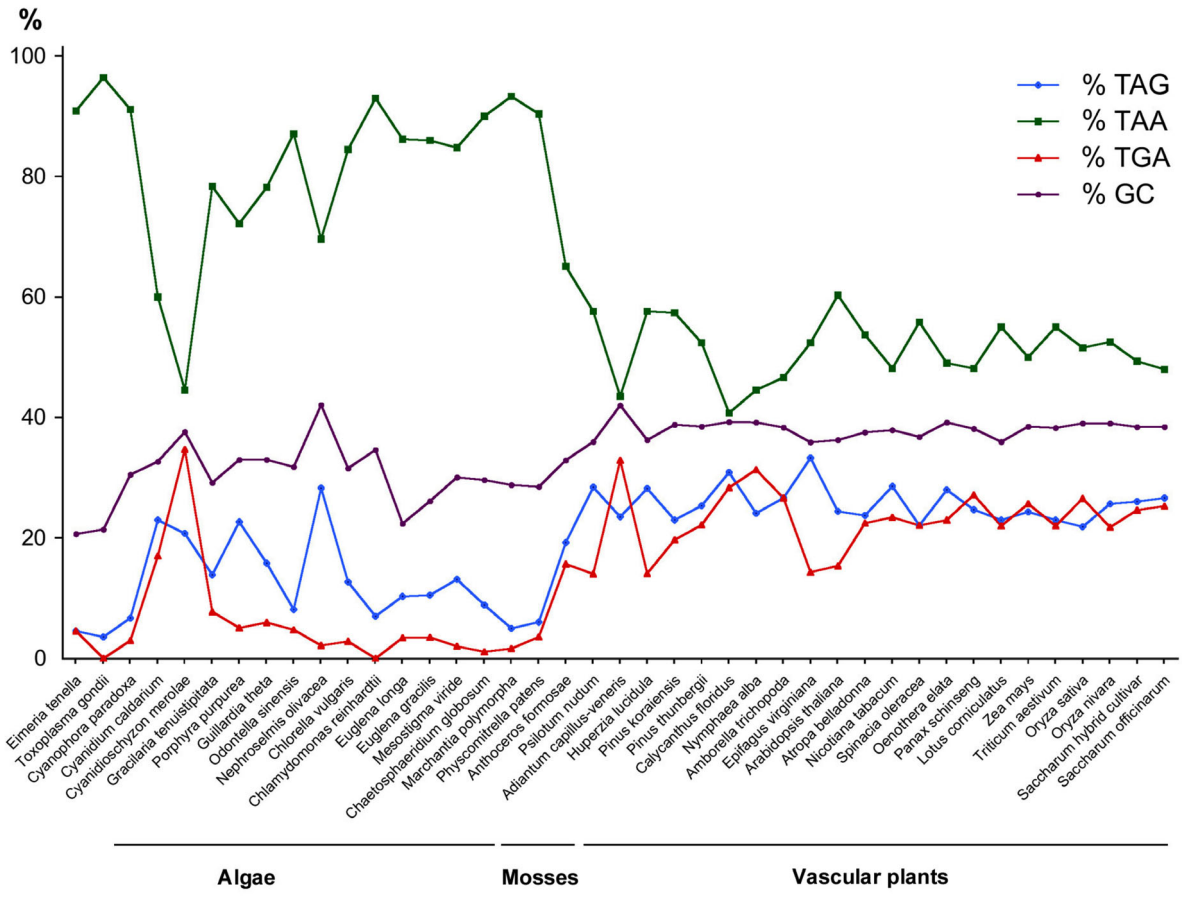

Figure 31. Distribution of stop codons and GC content in plastid chromosomes. Completely sequenced plastid chromosomes of the algae *Eimeria tenella*, *Toxoplasma gondii*, *Cyanophora paradoxa*, *Cyanidium caldarium*, *Cyanidioschyzon merolae*, *Gracilaria tenuistipitata*, *Porphyra purpurea*, *Guillardia theta*, *Odontella sinensis*, *Nephroselmis olivacea*, *Chlorella vulgaris*, *Chlamydomonas reinhardtii*, *Euglena longa*, *Euglena gracilis*, *Mesostigma viride* and *Chaetosphaeridium globosum*, the mosses *Marchantia polymorpha* and *Physcomitrella patens*, the hornwort *Anthoceros formosae*, the ferns *Psilotum nudum*, *Adiantum capillus-veneris* and *Huperzia lucidula*, gymnospermae *Pinus koraiensis* and *Pinus thunbergii*, the Magnoliopsida species *Calycanthus floridus*, *Nymphaea alba* and *Amborella trichopoda*, the Rosopsida plants *Epifagus virginiana*, *Arabidopsis thaliana*, *Atropa belladonna*, *Nicotiana tabacum Spinacia oleracea*, *Oenothera elata*, *Panax schinseng* and *Lotus japonicus* and the Liliopsida species *Zea mays*, *Triticum aestivum, Oryza sativa*, *Oryza nivara*, *Saccharum hybrid cultivar* and *Saccharum officinarum* (http://www.ncbi.nlm.nih.gov/PMGifs/Genomes/plastids_tax.html) were included in the analysis. ORFs were excluded from the analysis (see Discussion).

completely lost the TGA as a stop codon but are assumed to use this codon to decode tryptophan (Denny *et al.*, 1998). The plastid genomes of algae also tend to lose TGA stop codons: the amount of TGA in these organisms most often is far below 5% (Figure 31). The only exceptions known to date are represented by *C. caldarium* and *Cyanidioschyzon merolae* which have GC contents comparable to those of other algae but show a significant increase in TGA use of 18% and 35%, respectively. Despite a higher GC content of 42.1% in *N. olivacea* compared with land plants (<40%), UGA stop codon use is not increased in this species. The mosses *Marchantia polymorpha* and *Physcomitrella patens* at the border to land plants, contain as few TGA stop codons as algae. Compared with algae, the TGA content is increased ~10- to 15-fold in land plant plastomes and ranges from 15.4% in *Arabidopsis* to 31.3% in *Liliopsida*. This increase is not reflected by a comparable increase in GC content. Therefore, important functions other than solely ribosomal release might be associated with the plastid AtprfB explaining the significant bias for keeping the number of TGA stop codons high in land plants.

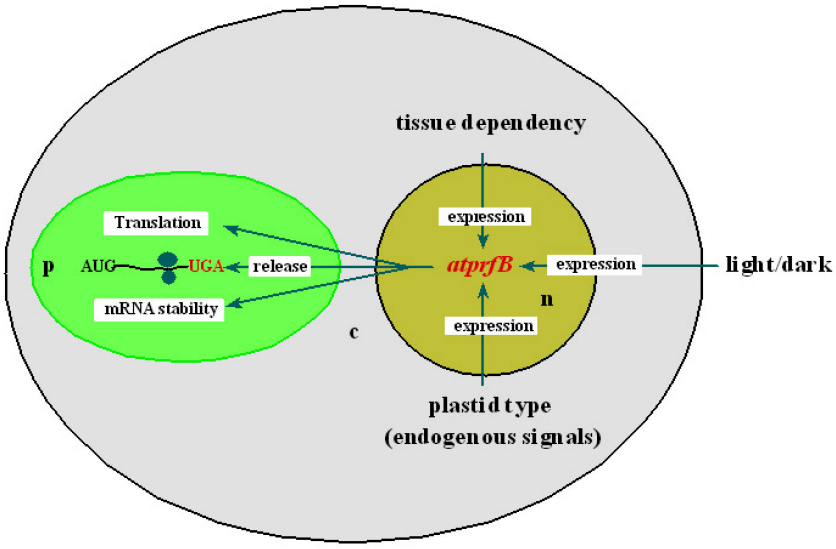

Figure 32. Model for *AtprfB* expression. **c**, **n**, and **p** represent cytosol, nucleus and plastid, respectively.

Similar to plastid genomes of algae and *Toxoplasma* (Denny *et al.*, 1998), all non-plant and several algal mitochondria tend to lose TGA stop codons (Inagaki *et al.*, 1998; Kück *et al.*, 2000). In human, yeast, *Drosophila* and *Caenorhabditis elegans*, this reduction was accompanied by a loss of eubacterial *prfB*-like genes in the entire genomes (http://www.ncbi.nlm.nih.gov). On the other hand, there is significant accumulation of TGA stop codons in land plant mitochondria (e.g., 38.6% in the *Arabidopsis* mitochondria genome; data not shown) (Unseld *et al.*, 1997). Thus, it appears that evolutionary constraints for the

bias to accumulate TGA stop codons and corresponding release factors might become operative almost exclusively in organelles of land plants. It could be connected with acquisition of tissues and necessity to adapt to adverse and changing environmental conditions after change to sessile life on land that would require additional regulatory mechanisms acting at the molecular level.

The observed role of AtprfB not only in ribosomal release but also in the regulation of the stability and translation of the UGA-containing transcripts has never been demonstrated in its prokaryotic counterparts. Therefore, it could be that these additional regulatory functions acquired by AtprfB keep the number of TGA stop codons high in land plants and have abolished the need to autoregulate the *AtprfB* gene expression in chloroplasts (Figure 32).

4.4 HCF101 is involved in the biogenesis of Fe-S clusters in *Arabidopsis* chloroplasts

4.4.1 New designation FSC ([4Fe-4S] cluster) is suggested for the 'MRP' family according to the proposed function of HCF101

Although orthologs of *HCF101* from different organisms have been characterized (Table 4), in most cases the function of the protein remained unknown. Since the designation ′MRP′ is misleading (see Chapter 3.5.4), the function proposed for HCF101 suggests a new designation 'FSC' for this family, including *Arabidopsis* HCF101, *Salmonella* ApbC (Skovran and Downs, 2003) and *S. cerevisiae* CFD1 (Roy *et al*., 2003).

4.4.2 Members of the FSC classes

The *hcf101* mutant of *Arabidopsis* accumulates reduced levels of the plastid FSC-containing complexes PSI and FTR. This phenotype of *hcf101* and the inability of two mutant homologues of HCF101, ApbC in *Salmonella enterica* and CFD1 in *Saccharomyces cerevisiae*, to accumulate FSC-containing proteins (Skovran and Downs, 2003; Roy *et al*., 2003) suggest a role for HCF101 in [4Fe-4S] biogenesis. Furthermore, the fact that *hcf101* plants accumulate normal levels of the [2Fe-2S] cluster-containing proteins ferredoxin and Rieske (PetC) suggests that HCF101 is involved in a step of FSC metabolism, i.e. synthesis, stability or incorporation of the cofactor into proteins, that is not required for [2Fe-2S] cluster

assembly. Conserved cysteines resembling FSC-binding motifs in most HCF101 homologous proteins and the ubiquitous distribution of highly conserved FSC homologues in all lineages support the functional role proposed. The plastid translational activity based on fresh weight was generally reduced in *hcf101*, indicative of reduced redox regulation of the protein synthesis machinery in mutants deficient in photosynthesis and FTR (Balmer *et al*., 2003).

Table 4. *HCF101* orthologous genes

Designation	Name	Organism	Proposed function	Reference
mrp	*metG* (methionyl-tRNA synthetase gene) related protein	*E. coli*	chromosome partitioning ?	Dardel *et al*., 1990
NBP	nucleotide binding protein	human	relationship to the bacterial *MinD*	Shahrestanifar *et al*., 1994
NBP35	„ „	yeast	essential function (division ?)	Vitale *et al*., 1996
YIA3w	„ „	„ „	unknown function (similarity to *E. coli* MinD)	Voss *et at*., 1995
NUBP1	„ „	mouse	unknown function (ATP/GTP binding motif)	Nakashima *et al*., 1999
NUBP2	„ „	„ „	„ „	„ „
NUBP2	„ „	human	„ „	„ „
F10G8.6		*C.elegans*	„ „	Wilson *et al*., 1994
ApbC	alternative pyrimidine biosynthetic pathway	*Salmonella*	Thiamine synthesis	Petersen and Downs, 1996; Skovran and Downs, 2003
CFD1	cytosolic Fe-S cluster deficient	yeast	Fe-S cluster assembly	Roy *et al*., 2003

Mutations of N-terminal cysteines and knock-outs of the class 2 FSC form in yeast were lethal (Vitale *et al*., 1996), pointing out an essential role of this protein in eukaryotes. *S. enterica* knock-outs in FSC (ApbC) are conditionally lethal, suggesting that the proposed function of FSC in Fe-S cluster assembly is redundant to some extent in this organism and

HCF101 homologues have partially been replaced by the Isc and Suf (see below) proteins in the mutant (Skovran and Downs, 2003). HCF101 in *Arabidopsis* and rice are unique among FSC family members in that they possess a cleavable transit peptide for chloroplast import. Deviations in HCF101 from the signatures defined for the FSC class of proteins concern in particular cysteines (Figure 27) and the C-terminal extension, pointing to a specialized role of HCF101 in FSC metabolism in chloroplasts. HCF101 does not appear to be redundant in chloroplasts with regard to PSI assembly, but may have a less efficient redundant partner for FTR assembly. That circumstance, in addition to the conditional lethality of *Arabidopsis hcf101* homozygotic recessives (that can be grown on solid media at low light) makes them an attractive system for studying FSC biogenesis.

4.4.3 Three pathways for iron-sulphur cofactor assembly

The biogenesis of Fe-S clusters in the chloroplast is much less understood in comparison to that of eubacteria and mitochondria (Lill and Mühlenhoff, 2005; Beinert *et al*., 2000; Frazzon and Dean, 2003). In general, three phylogenetically related pathways for iron sulphur cofactor assembly have been described to date: the ISC system, the NIFS/NIFU system and the newly characterized SUF system (Takahashi and Tokumoto, 2002; Frazzon and Dean, 2003).

In eukaryotes, ISC homologues play an essential role in Fe-S cluster synthesis and have been identified in mitochondria (Lill and Mühlenhoff, 2005), in hydrogenosomes (Tachezy *et al*., 2001; Sutak *et al*., 2004) and in eukaryotes that possess mitochondrial remnant organelles, so-called mitosomes (Tachezy *et al*., 2001; Tovar *et al*., 2003). A mitochondrial export pathway and cytosolic assembly machinery have been identified in yeast, which provides other cellular compartments with Fe-S co-factors outside of the mitochondrion (Lill and Mühlenhoff, 2005).

NIFS- and NIFU-like proteins (NFU), which may be involved in the activation of sulphur from L-cysteines and in the assembly of a [2Fe-2S] cluster, respectively, have been found recently in the chloroplast (Pilon-Smits *et al*., 2002; Léon *et al*., 2003; Touraine *et al*. 2004; Yabe *et al*., 2004). NIFU contains three defined domains with conserved cysteines and serves as the acceptor site for iron and sulphur for transient Fe-S cluster assembly (Yuvaniyama *et al*., 2000; Ollagnier-de Choudens *et al*., 2003;). The C-terminal NIFU domain of unknown function contains a CxxC signature and has been named 'thioredoxin-like' or NFU module because it is similar to those of thioredoxins. Several low-molecular mass

proteins present in all lineages consist only of the NFU domain and are involved in the transfer of [2Fe-2S] cluster into the apoferredoxin in *Synechocystis* PCC 8603 (Garland *et al*., 1999; Schilke *et al*., 1999; Nishio and Nakai, 2000). NFU-like proteins have been found to be localized in mitochondria and chloroplasts and to bind a labile [2Fe-2S] cluster *in vitro* (Léon *et al*., 2003).

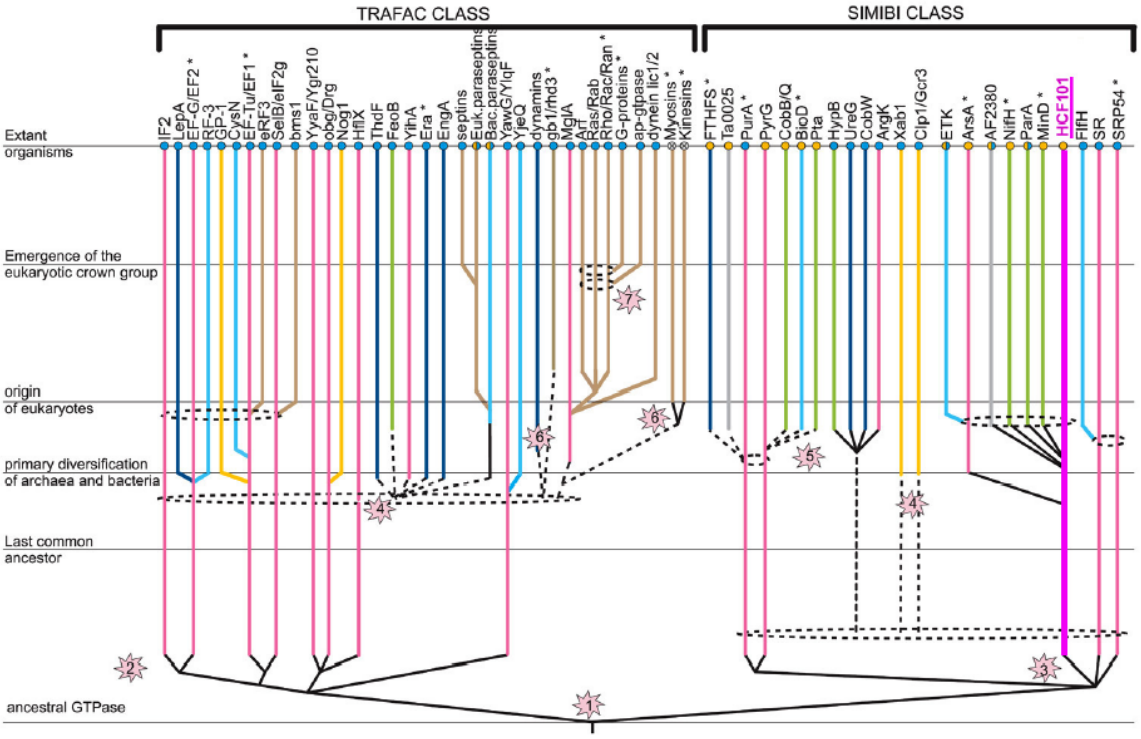

Figure 33. Evolutionary history of GTPase families (Leipe *et al*., 2002 modified). The GTPase superclass can be divided into two large classes: TRAFAC (after translation factors) and SIMIBI (after signal recognition particle, MinD, and BioD). The FSC family belongs to the SIMIBI class (represented by HCF101). 1 - separation of GTPases from the rest of the P-loop fold; 2 -origin and diversification of the most ancient TRAFAC GTPases; 3 - origin of the cell membrane and diversification of the SIMIBI class proteins; 4 - bacterial or archaeo-eukaryotic lineage-specific diversification of GTPases into functional niches; 5 - diversification of metabolic enzymes in the SIMIBI class; 6 - origin of the eukaryotic cytoskeleton and intracellular transport apparatus; 7 - diversification of the eukaryotic signal transduction apparatus. Color key: red/pink, universal; dark blue, Bacteria and Eukaryota; light blue, Bacteria; brown, Eukaryota; grey, Archaea and Thermotoga; green, Archaea and Bacteria; orange, Eukaryota and Archaea. HCF101 is highlighted in violet.

The SUF pathway for [Fe-S] cluster assembly is present in a wide range of eubacteria, archaebacteria and plastids (Takahashi and Tokumoto, 2002; Nachin *et al*., 2003). Some prokaryotes possess either the ISC or SUF systems; many contain both pathways. ICS and SUF homologues are also encoded in plastomes of algae and in the nuclear genome of *Arabidopsis*.

Inspection of bacterial genomes revealed that *HCF101* homologous genes are very rarely embedded in operons, but are occasionally positionally clustered with the thioredoxin-like *nfu* genes in several bacterial genomes, including *Cytophaga hutchinsonii*, *Chlorobium tepidum* and *Nostoc* (data not shown), hinting that HCF101 might be functionally related to NFU in catalysing steps of FSC biogenesis.

4.4.4 An essential role of FSC during the very earliest phases of cell evolution

Models for the origin of autotrophic life suggest an essential role of Fe-S in early biochemistry (Russell *et al*., 1990; Wächtershäuser 1992; Martin and Russel, 2003; Baymann *et al*., 2003). Naturally forming Fe-S compartments may have fulfilled the function of cell membranes prior to the origin of lipid synthesis, and the incorporation of Fe-S clusters into proteins was one of the earliest problems that had to be solved *en route* to genetically encoded biochemistry (Martin and Russel, 2003). The antiquity of the FSC family (Figure 33) points clearly to the importance of Fe-S cluster biogenesis during the earliest phases of cell evolution. The ubiquity of FSC genes indicates that they are essential for all free-living cells.

5 Summary

During evolution of photoautotrophic eukaryotes, the nucleus has gained a dominant role in the coordination of the integrated genetic system of the cell consisting of three specifically coevolved genetic compartments. The photosynthetic machinery is encoded by the chloroplast and nuclear genomes. Therefore, biosynthesis and assembly of stochiometric amounts of subunits as well as association of the proteins with corresponding cofactors need to be managed and precisely regulated. To identify novel nuclear-encoded factors involved in the regulation of chloroplast gene expression at different levels, 12 nuclear mutants with *high chlorophyll fluorescence* (*hcf*) phenotypes denoting quite diverse defects in the photosynthetic apparatus were selected. Three of them, *hcf145*, *hcf109* and *hcf101*, were analysed and the affected genes were characterized in more detail. Spectroscopic, fluorimetric and immunological studies have revealed that *hcf145* and *hcf101* were predominantly affected in photosystem I (PSI), while *hcf109* had pleiotropic deficiencies.

Remarkably, the dramatic reduction of PSI core complex accumulation in *hcf145* was not accompanied by corresponding deficiencies of the outer light-harvesting antenna complex. A comparison of stationary transcript levels with rates of transcription, as estimated by Northern and chloroplast *run-on* transcription analysis, revealed that the *hcf145* mutant is primarily and specifically characterised by a reduced stability of tricistronic chloroplast *psaA-psaB-rps14* transcripts. The corresponding operon encodes the two large PSI polypeptides PsaA and PsaB, which form the heterodimeric PSI reaction centre, and the ribosomal protein S14. Chloroplast translation inhibition experiments excluded translational defects as the primary cause of impaired mRNA stability. Defined intervals of the tricistronic transcript were quantified by real-time RT-PCR which established that the *psaA* region is less stable than the *rps14* region in *hcf145*. Therefore, although up to date, no 5′-3′ exoribonucleases have been found in eubacteria (including the ancestors of plants), factor HCF145 appears to be required for the protection of the *psaA-psaB-rps14* mRNA against progressive ribonucleolytic degradation starting at the 5′ end.

In the *hcf109* mutant, exclusively plastid transcripts containing UGA stop codons are unstable. The affected gene encodes the first described chloroplast peptide chain release factor AtprfB. Its full-length cDNA, introduced into *hcf109* via *Agrobacterium*-mediated transformation, could functionally complement the mutant. Homology of AtprfB to eubacterial release factors indicates that processes of translational termination in chloroplasts

resemble those in eubacteria. The mutant phenotype revealed that translation of all plastid mRNAs containing UGA stop codons is exclusively terminated by AtprfB. However, besides its peptide chain release function, AtprfB appears to acquire yet unknown roles in regulating the stability and translation of the chloroplast mRNAs containing UGA stop codons. These additional regulatory functions could reflect evolutionary constraints which keep the number of plastid TGA stop codons high in vascular plant organelles in contrast to those of algae, mosses and ferns.

In contrast to *hcf145*, steady-state levels and translation of photosynthetic transcripts are not altered in the PSI mutant *hcf101*. Separation of thylakoid membrane complexes by sucrose gradient centrifugation has uncovered that, similar to *hcf145*, accumulation of the outer antenna of PSI is not changed in *hcf101*. Therefore, *hcf101* is affected in the assembly of the PSI core complexes. Expression of the *HCF101* full-length cDNA in the *hcf101* genetic background functionally complemented the mutant. The HCF101 protein encodes a very ancient and universally conserved protein of P-loop ATPases. HCF101 is plastid-localised and represents the first described factor essentially required for the assembly of PSI and other [4Fe-4S]-containing protein complexes in the chloroplast. Relatives of HCF101 are divided into four classes present in all organisms and in all cellular compartments. The antiquity of HCF101 points to the importance of Fe-S cluster biogenesis during the earliest phases of cell evolution. The ubiquity of HCF101 indicates that it is essential for all free-living cells.

6 Literature

Adamski, F.M., Donly, B.C. and Tate, W.P. (1993) Competition between frameshifting, termination and suppression at the frameshift site in the *Escherichia coli* release factor-2 mRNA. Nucl. Acids Res. 21, 5074–5078.

Alexander, C., Faber, N. and Klaff, P. (1998) Characterization of protein-binding to the spinach chloroplast *psbA* mRNA 5' untranslated region. Nucl. Acids Res. 26, 2265-2272.

Allen, J.F. and Pfannschmidt, T. (2000) Balancing the two photosystems: photosynthetic electron transfer governs transcription of reaction centre genes in chloroplasts. Philos. Trans. R. Soc. Lond. B Biol. Sci. 355, 1351-1359.

Allison, L.A. (2000) The role of sigma factors in plastid transcription. Biochimie 82, 537-548.

Alonso, J.M., Stepanova, A.N., Leisse, T.J., Kim, C.J., Chen, H., Shinn, P., Stevenson, D.K., Zimmerman, J., Barajas, P., Cheuk, R., Gadrinab, C., Heller, C., Jeske, A., Koesema, E., Meyers, C.C., Parker, H., Prednis, L., Ansari, Y., Choy, N., Deen, H., Geralt, M., Hazari, N., Hom, E., Karnes, M., Mulholland, C., Ndubaku, R., Schmidt, I., Guzman, P., Aguilar-Henonin, L., Schmid, M., Weigel, D., Carter, D.E., Marchand, T., Risseeuw, E., Brogden, D., Zeko, A., Crosby, W.L., Berry, C.C. and Ecker, J.R. (2003) Genome-wide insertional mutagenesis of *Arabidopsis thaliana*. Science 301, 653-657.

Altschul, S. F., Madden, T. L., Schaffer, A.A., Zhang, J., Zhang, Z., Miller, W. and Lipman, D. J. (1997) Gapped BLAST and PSI-BLAST: a new generation of protein database search programs. Nucl. Acids Res. 25, 3389-3402.

Alvarado, M.C., Zsigmond, L.M., Kovacs, I., Cseplo, A., Koncz, C. and Szabados, L.M. (2004) Gene trapping with firefly luciferase in *Arabidopsis*. Tagging of stress-responsive genes. Plant Physiol. 134, 18-27.

Arabidopsis Genome Initiative (2000) Analysis of the genome sequence of the flowering plant *Arabidopsis thaliana*. Nature 408, 796-815.

Arnon, D.I. (1949) Copper enzymes in isolated chloroplasts. Polyphenoloxidase in *Beta vulgaris*. Plant Physiol. 24, 1-13.

Baginsky, S., Shteiman-Kotler, A., Liveanu, V., Yehudai-Resheff, S., Bellaoui, M., Settlage, R.E., Shabanowitz, J., Hunt, D.F., Schuster, G. and Gruissem, W. (2001) Chloroplast PNPase exists as a homo-multimer enzyme complex that is distinct from the *Escherichia coli* degradosome. RNA 7, 1464-1475.

Baker, K.E. and Parker, R. (2004) Nonsense-mediated mRNA decay: terminating erroneous gene expression. Curr. Opin. Cell Biol. 16, 293-299.

Balmer, Y., Koller, A., del Val, G., Manieri, W., Schürmann, P. and Buchanan, B.B. (2003) Proteomics gives insight into the regulatory function of chloroplast thioredoxins. Proc. Natl. Acad. Sci. USA 100, 370-375.

Baranov, P.V., Gesteland, R.F. and Atkins, J.F. (2002) Recoding: translational bifurcations in gene expression. Gene 286, 187-201.

Barber, J. and Nield, J. (2002) Organization of transmembrane helices in photosystem II: comparison of plants and cyanobacteria. Philos. Trans. R. Soc. Lond. B Biol. Sci. 357, 1329-1335.

Barkan, A. (1993) Nuclear mutants of maize with defects in chloroplast polysome assembly have altered chloroplast RNA metabolism. Plant Cell 5, 389-402.

Barkan, A. (1998) Approaches to investigating nuclear genes that function in chloroplast biogenesis in land plants. Methods Enzymol. 297, 38–57.

Barkan, A. and Goldschmidt-Clermont, M. (2000) Participation of nuclear genes in chloroplast gene expression. Biochimie 82, 559-572.

Bartlett, S.G., Grossman, A.R. and Chua, N.H. (1982) *In vitro* synthesis and uptake of cytoplasmically synthesized chloroplast proteins. In: Methods in Chloroplast Molecular Biology (Edelman, M., Hallick, R. and Chua, N.H., eds). Amsterdam: Elsevier Biomedical Press, pp. 1081-1091.

Baumgartner, B.J., Rapp, J.C. and Mullet, J.E. (1993) Plastid genes encoding the transcription/translation apparatus are differentially transcribed early in barley (*Hordeum vulgare*) chloroplast development. Evidence for selective stabilization of *psbA* mRNA. Plant Physiol. 101, 781-791.

Baymann, F., Brugna, M., Mühlenhoff, U. and Nitschke, W. (2001) Daddy, where did (PS) I come from? Biochim. Biophys. Acta 1507, 291-310.

Baymann, F., Lebrun, E., Brugna, M., Schoepp-Cothenet, B., Giudici-Orticoni, M.T. and Nitschke, W. (2003) The redox protein construction kit: pre-last universal common ancestor evolution of energy-conserving enzymes. Philos. Trans. R. Soc. Lond. B Biol. Sci. 358, 267-274.

Bechhofer, D.H. (1993) 5' mRNA stabilizers. In: Control of Messenger RNA Stability (Belasco, J. and Brawerman, G., eds). New York: Academic Press, pp. 31-52.

Bechtold, N. and Pelletier, G. (1998) In planta *Agrobacterium*-mediated transformation of adult *Arabidopsis thaliana* plants by vacuum infiltration. Methods Mol. Biol. 82, 259–266.

Beinert, H., Holm, R.H. and Munck, E. (2000) Iron-sulfur clusters: nature's modular, multipurpose structures. Science 277, 653-659.

Ben-Shem, A., Frolow, F. and Nelson, N. (2003) Crystal structure of plant photosystem I. Nature 426, 630-635.

Birky, C.W. Jr. (2001) The inheritance of genes in mitochondria and chloroplasts: Laws, mechanisms, and models. Annu. Rev. Genet. 35, 125-148.

Birnboim, H.C. and Doly, J. (1979) A rapid alkaline extraction procedure for screening recombinant plasmid DNA. Nucl. Acids Res. 7, 1513-1523.

Blum, H., Beier, H. and Gross, H.J. (1987) Improved silver staining of plant proteins, RNA and DNA in polyacrylamide gels. Electrophoresis 8, 93-99.

Boudreau, E., Nickelsen, J., Lemaire, S.D., Ossenbühl, F. and Rochaix, J.D. (2000) The Nac2 gene of *Chlamydomonas* encodes a chloroplast TPR-like protein involved in *psbD* mRNA stability. EMBO J. 19, 3366-3376.

Boudreau, E., Takahashi, Y., Lemieux, C., Turmel, M. and Rochaix, J.D. (1997) The chloroplast *ycf3* and *ycf4* open reading frames of *Chlamydomonas reinhardtii* are required for the accumulation of the photosystem I complex. EMBO J. 16, 6095-6104.

Bradford, M.M. (1976) A rapid and sensitive method for the quantification of microgram quantities of protein utilizing the principle of protein-dye binding. Anal. Biochem. 72**,** 248-254.

Bruick, R.K. and Mayfield, S.P. (1999). Light-activated translation of chloroplast mRNAs. Trends Plant Sci. 4, 190–195.

Buckhout, T.J. and Thimm, O. (2003) Insights into metabolism obtained from microarray analysis. Curr. Opin. Plant Biol. 6, 288-296.

Butterfass, T. (1980) The continuity of plastids and the differentiation of plastid populations. In: Results and problems in cell differentiation. Vol. 10. Chloroplasts (Reinert, J., ed.). Berlin: Springer, pp. 29-44.

Choquet, Y. and Wollman, F.A. (2002). Translational regulations as specific traits of chloroplast gene expression. FEBS Lett. 529, 39–42.

Church, G.M. and Gilbert, W. (1984) Genomic sequencing. Proc. Natl. Acad. Sci. USA 81, 1991-1995.

Clausmeyer, S., Klösgen, R.B. and Herrmann, R.G. (1993) Protein import into chloroplasts: The hydrophilic lumenal proteins exhibit unexpected import and sorting specificities in spite of structurally conserved transit peptides. J. Biol. Chem. 268, 13869–13876.

Clough, S.J. and Bent, A.F. (1998) Floral dip: a simplified method for *Agrobacterium*-mediated transformation of *Arabidopsis thaliana*. Plant J. 16, 735-743.

Cohen, A., Yohn, C.B. and Mayfield, S. (2001) Translation of the chloroplast-encoded *psbD* is arrested post-initiation in a nuclear mutant of *Chlamydomonas reinhardtii*. J. Plant. Physiol. 158, 1069–1075.

Collier, J., Binet, E. and Bouloc, P. (2002) Competition between SsrA tagging and translational termination at weak stop codons in *Escherichia coli*. Mol. Microbiol. 45, 745–754.

Craigen, W.J. and Caskey, C.T. (1986) Expression of peptide chain release factor 2 requires high-efficiency frameshift. Nature 322, 273–275.

Craigen, W.J., Cook, R.G., Tate, W.P. and Caskey, C.T. (1985) Bacterial peptide chain release factors: Conserved primary structure and possible frameshift regulation of release factor 2. Proc. Natl. Acad. Sci. USA 82, 3616–3620.

Culbertson, M.R. (1999) RNA surveillance: Unforeseen consequences for gene expression, inherited genetic disorders and cancer. Trends Genet. 15, 74–80.

Culver, G.M. (2003) Assembly of the 30S ribosomal subunit. Biopolymers 68, 234-249.

Czechowski, T., Bari, R.P., Stitt, M., Scheible, W.R. and Udvardi, M.K. (2004) Real-time RT-PCR profiling of over 1400 *Arabidopsis* transcription factors: unprecedented sensitivity reveals novel root- and shoot-specific genes. Plant J. 38, 366-379.

Dai, S., Schwendtmayer, C., Schürmann, P., Ramaswamy, S. and Eklund, H. (2000) Redox signaling in chloroplasts: cleavage of disulfides by an iron-sulfur cluster. Science 287, 655-658.

Dal Bosco, C., Lezhneva, L., Biehl, A., Leister, D., Strotmann, H., Wanner, G. and Meurer, J. (2004) Inactivation of the chloroplast ATP synthase γ subunit results in high non-photochemical fluorescence quenching and altered nuclear gene expression in *Arabidopsis thaliana*. J. Biol. Chem. 279, 1060-1069.

Dardel, F., Panvert, M. and Fayat, G. (1990) Transcription and regulation of expression of the *Escherichia coli* methionyl-tRNA synthetase gene. Mol. Gen. Genet. 223, 121-133.

Dauvillée, D., Stampacchia, O., Girard-Bascou, J. and Rochaix, J.D. (2003). Tab2 is a novel conserved RNA binding protein required for translation of the chloroplast *psaB* mRNA. EMBO J. 22, 6378-6388.

Deng, X.W., Tonkyn, J.C., Peter, G.F., Thornber, J.P. and Gruissem, W. (1989) Post-transcriptional control of plastid mRNA accumulation during adaptation of chloroplasts to different light quality environments. Plant Cell 1, 645-654.

Denny, P., Preiser, P., Williamson, D. and Wilson, I. (1998) Evidence for a single origin of the 35 kb plastid DNA in Apicomplexans. Protist. 149, 51–59.

Depège, N., Bellafiore, S. and Rochaix, J.D. (2003) Role of chloroplast protein kinase Stt7 in LHCII phosphorylation and state transition in *Chlamydomonas*. Science 299, 1572-1575.

Dincbas-Renqvist, V., Engstrom, A., Mora, L., Heurgue-Hamard, V., Buckingham, R. and Ehrenberg, M. (2000) A post-translational modification in the GGQ motif of RF2 from *Escherichia coli* stimulates termination of translation. EMBO J. 19, 6900–6907.

Douglas, S.E. (1998) Plastid evolution: origins, diversity, trends. Curr. Opin. Genet. Dev. 8, 655-661.

Drager, R.G., Girard-Bascou, J., Choquet, Y., Kindle, K.L. and Stern, D.B. (1998) *In vivo* evidence for 5'→3' exoribonuclease degradation of an unstable chloroplast mRNA. Plant J. 13, 85-96.

Drager, R.G., Higgs, D.C., Kindle, K.L. and Stern, D.B. (1999) 5' to 3' exoribonucleolytic activity is a normal component of chloroplast mRNA decay pathways. Plant J. 19, 521-531.

Drapier, D., Girard-Bascou, J., Stern, D.B. and Wollman, F.A. (2002) A dominant nuclear mutation in *Chlamydomonas* identifies a factor controlling chloroplast mRNA stability by acting on the coding region of the *atpA* transcript. Plant J. 31, 687-697.

Dreyfus, M. and Régnier, P. (2002) The poly(A) tail of mRNAs: bodyguard in eukaryotes, scavenger in bacteria. Cell 111, 611-613.

Eibl, C., Zou, Z., Beck, A., Kim, M., Mullet, J. and Koop, H.U. (1999) *In vivo* analysis of plastid *psbA, rbcL* and *rpl32* UTR elements by chloroplast transformation: tobacco plastid gene expression is controlled by modulation of transcript levels and translation efficiency. Plant J. 19, 333-345.

Eichacker, L.A., Soll, J., Lauterbach, P., Rüdiger, W., Klein, R.R. and Mullet, J.E. (1990). *In vitro* synthesis of chlorophyll *a* in the dark triggers accumulation of chlorophyll *a* apoproteins in barley etioplasts. J. Biol. Chem. 265, 13566-13571.

Emanuelsson, O., Nielsen, H., Brunak, S. and von Heijne, G. (2000) Predicting subcellular localization of proteins based on their N-terminal amino acid sequence. J. Mol. Biol. 300, 1005–1016.

Esposito, D., Higgs, D.C., Drager, R.G., Stern, D.B. and Girard-Bascou, J. (2001) A nucleus-encoded supressor defines a new factor which can promote *petD* mRNA stability in the chloroplast of *Chlamydomonas reinhardtii*. Curr. Genet. 39, 40-48.

Fedoroff, N.V. (2002) RNA-binding proteins in plants: the tip of an iceberg? Curr. Opin. Plant Biol. 5, 452-459.

Feinberg, A.P. and Vogelstein, B. (1983) A technique for radiolabeling DNA restriction endonuclease fragments to high specific activity. Anal. Biochem. 132, 6-13.

Felder, S., Meierhoff, K., Sane, A.P., Meurer, J., Driemel, C., Plücken, H., Klaff, P., Stein, B., Bechtold, N. and Westhoff, P. (2001) The nucleus-encoded HCF107 gene of *Arabidopsis* provides a link between intercistronic RNA processing and the accumulation of translation-competent *psbH* transcripts in chloroplasts. Plant Cell 13, 2127-2141.

Feldmann, K.A. (1991) T-DNA insertion mutagenesis in *Arabidopsis*: mutational spectrum. Plant J. 1, 71-82.

Ferrández, A., Garcia, J.L. and Diaz, E. (2000) Transcriptional regulation of the divergent *paa* catabolic operons for phenylacetic acid degradation in *Escherichia coli*. J. Biol. Chem. 275, 12214-12222.

Fisk, D.G., Walker, M.B. and Barkan, A. (1999) Molecular cloning of the maize gene *crp1* reveals similarity between regulators of mitochondrial and chloroplast gene expression. EMBO J. 18, 2621-2630.

Flynn, J.M., Levchenko, I., Seidel, M., Wickner, S.H., Sauer, R.T. and Baker, T.A. (2001). Overlapping recognition determinants within the ssrA degradation tag allow modulation of proteolysis. Proc. Natl. Acad. Sci. USA. 98, 10584–10589.

Foth, B.J. and McFadden, G.I. (2003) The apicoplast: A plastid in *Plasmodium falciparum* and other Apicomplexan parasites. Int. Rev. Cytol. 224, 57-110.

Frazzon, J. and Dean, D.R. (2003) Formation of iron-sulfur clusters in bacteria: an emerging field in bioinorganic chemistry. Curr. Opin. Chem. Biol. 7, 166-173.

Frischmeyer, P.A., van Hoof, A., O'Donnell, K., Guerrerio, A.L., Parker, R. and Dietz, H.C. (2002) An mRNA surveillance mechanism that eliminates transcripts lacking termination codons. Science 295, 2258–2261.

Frolova, L.Y., Merkulova, T.I. and Kisselev, L.L. (2000) Translation termination in eukaryotes: Polypeptide release factor eRF1 is composed of functionally and structurally distinct domains. RNA 6, 381–390.

Frolova, L.Y., Tsivkovskii, R.Y., Sivolobova, G.F., Oparina, N.Y., Serpinsky, O.I., Blinov, V.M., Tatkov, S.I. and Kisselev, L.L. (1999) Mutations in the highly conserved GGQ motif of class 1 polypeptide release factors abolish ability of human eRF1 to trigger peptidyl-tRNA hydrolysis. RNA 5, 1014–1020.

Ganeteg, U., Klimmek, F. and Jansson, S. (2004) Lhca5--an LHC-type protein associated with photosystem I. Plant Mol. Biol. 54, 641-651.

Garland, S.A., Hoff, K., Vickery, L.E. and Culotta, V.C. (1999) *Saccharomyces cerevisiae* ISU1 and ISU2: members of a well-conserved gene family for iron-sulfur cluster assembly. J. Mol. Biol. 294, 897-907.

Germano, M., Yakushevska, A.E., Keegstra, W., van Gorkom, H.J., Dekker, J.P. and Boekema, E.J. (2002) Supramolecular organization of photosystem I and light-harvesting complex I in *Chlamydomonas reinhardtii*. FEBS Lett. 525, 121-125.

Girard-Bascou, J., Choquet, Y., Schneider, M., Delosme, M. and Dron, M. (1987) Characterization of a chloroplast mutation in the *psaA2* gene of *Chlamydomonas reinhardtii*. Curr. Genet. 12, 489-495.

Glick, R.E., McCauley, S.W., Gruissem, W. and Melis, A. (1986) Light quality regulates expression of chloroplast genes and assembly of photosynthetic membrane complexes. Proc. Natl. Acad. Sci. USA 83, 4287-4291.

Golbeck, J.H. (2003) The binding of cofactors to photosystem I analyzed by spectroscopic and mutagenic methods. Annu. Rev. Biophys. Biomol. Struct. 32, 237-256.

Gray, J.C., Sullivan, J.A., Wang, J.H., Jerome, C.A. and MacLean, D. (2003) Coordination of plastid and nuclear gene expression. Philos. Trans. R. Soc. Lond. B Biol. Sci. 358, 135-144.

Groth, G. and Pohl, E. (2001) The structure of the chloroplast F_1-ATPase at 3.2 Å resolution. J. Biol. Chem. 276, 1345–1352.

Groth, G. and Strotmann, H. (1999) New results about structure, function and regulation of the chloroplast ATP synthase (CF_0CF_1). Physiol. Plant. 106, 142-148.

Gruissem, W. (1989) Chloroplast gene expression: how plants turn their plastids on. Cell, 56, 161-170.

Grunberg-Manago, M. (1999) Messenger RNA stability and its role in control of gene expression in bacteria and phages. Annu. Rev. Genet. 33, 193-227.

Grüne, H. and Westhoff, P. (1988) Transfer von RNA auf Pall Biodyne A Nylonmembranen und Immobilisierung mittels UV-crosslinking. Pall BioSupport SD 1217 G.

Guo, H.S., Fei, J.F., Xie, Q. and Chua, N.H. (2003) A chemical-regulated inducible RNAi system in plants. Plant J. 34, 383-392.

Gutiérrez, R.A., MacIntosh, G.C. and Green, P.J. (1999) Current perspectives on mRNA stability in plants: multiple levels and mechanisms of control. Trends Plant Sci. 4, 429-438.

Hadi, M.Z., Kemper, E., Wendeler, E. and Reiss, B. (2002) Simple and versatile selection of *Arabidopsis* transformants. Plant Cell Rep. 21, 130–135.

Hagemann, R. (1992) Plastid genetics in higher plants. In: Plant gene research. Vol. 6 (Herrmann, R.G., ed.). Wien, New York: Springer, pp. 65-96.

Haldrup, A., Simpson, D.J. and Scheller, H.V. (2000) Down-regulation of the PSI-F subunit of photosystem I (PSI) in *Arabidopsis thaliana*. The PSI-F subunit is essential for photoautotrophic growth and contributes to antenna function. J. Biol. Chem. 275, 31211-31218.

Hallick, R.B., Lipper, C., Richards, O.C. and Rutter, W.J. (1976) Isolation of a transcriptionally active chromosome from chloroplasts of *Euglena gradis*. Biochemistry 15, 3039-3045.

Hanahan, D., Jessee, J. and Bloom, F.R. (1991) Plasmid transformation of *Escherichia coli* and other bacteria. Meth. Enzymol. 204, 63-113.

Hankamer, B., Barber, J. and Boekema, E.J. (1997) Structure and membrane organisation of photosystem II in green plants. Annu. Rev. Plant Physiol. Plant Mol. Biol. 48, 641-671.

Hankamer, B., Morris, E., Nield, J., Carne, A. and Barber, J. (2001) Subunit positioning and transmembrane helix organization in the core dimer of photosystem II. FEBS Lett. 504, 142-151.

Hayes, R., Kudla, J. and Gruissem, W. (1999) Degrading chloroplast mRNA: the role of polyadenylation. Trends Biochem. Sci. 24, 199-202.

Hedtke, B., Legen, J., Weihe, A., Herrmann, R.G. and Börner, T. (2002) Six active phage-type RNA polymerase genes in *Nicotiana tabacum*. Plant J. 30, 625-637.

Hedtke, B., Wagner, I., Börner, T. and Hess, W.R. (1999) Inter-organellar crosstalk in higher plants: impaired chloroplast development affects mitochondrial gene and transcript levels. Plant J. 19, 635-643.

Henikoff, S., Till, B.J. and Comai, L. (2004) TILLING. Traditional mutagenesis meets functional genomics. Plant Physiol. 135, 630-636.

Herrmann, R.G. (1997) Eukaryotism, towards a new interpretation. In: Eukaryotism and symbiosis (Schenk, H.E.A., Herrmann, R.G., Jeon, K.W., Müller, N.E. and Schwemmler, W., eds). Heidelberg, New York: Springer, pp. 73-118.

Herrmann, R.G. and Westhoff, P. (2001) Thylakoid biogenesis and dynamics: The result of a complex phylogenetic puzzle. In: Regulation of photosynthesis (Aro, E.-M. and Andersson, B., eds). Dordrecht: Kluwer Academic Publishers, pp. 1-28.

Herrmann, R.G., Maier, R.M. and Schmitz-Linneweber, C. (2003) Eukaryotic genome evolution: rearrangement and coevolution of compartmentalized genetic information. Philos. Trans. R. Soc. Lond. B Biol. Sci. 358, 87-97.

Hicks, A., Drager, R.G., Higgs, D.C. and Stern, D.B. (2002) An mRNA 3' processing site targets downstream sequences for rapid degradation in *Chlamydomonas* chloroplasts. J. Biol. Chem. 277, 3325-3333.

Hihara, Y. and Sonoike, K. (2001) Regulation, inhibition and protection of photosystem I. In: Regulation of Photosynthesis (Aro, E.-M. and Andersson, B., eds). Dordrecht: Kluwer Academic Publishers, pp. 507-531.

Horiguchi, G. (2004) RNA silencing in plants: a shortcut to functional analysis. Differentiation 72, 65-73.

Horlitz, M. and Klaff, P. (2000) Gene-specific *trans*-regulatory functions of magnesium for chloroplast mRNA stability in higher plants. J. Biol. Chem. 275, 35638-35645.

Howard, J.B. and Rees, D.C. (1991) Perspectives on non-heme iron protein chemistry. Adv. Protein Chem. 42, 199-280.

Ichikawa, T., Nakazawa, M., Kawashima, M., Muto, S., Gohda, K., Suzuki, K., Ishikawa, A., Kobayashi, H., Yoshizumi, T., Tsumoto, Y., Tsuhara, Y., Iizumi, H., Goto, Y. and Matsui, M. (2003) Sequence database of 1172 T-DNA insertion sites in *Arabidopsis* activation-tagging lines that showed phenotypes in T1 generation. Plant J. 36, 421-429.

Inagaki, Y., Ehara, M., Watanabe, K.I., Hayashi-Ishimaru, Y. and Ohama, T. (1998) Directionally evolving genetic code: The UGA codon from stop to tryptophan in mitochondria. J. Mol. Evol. 47, 378–384.

Ito, K., Ebihara, K., Uno, M. and Nakamura, Y. (1996) Conserved motifs in prokaryotic and eukaryotic polypeptide release factors: tRNA-protein mimicry hypothesis. Proc. Natl. Acad. Sci. USA 93, 5443–5448.

Ito, K., Uno, M. and Nakamura, Y. (2000) A tripeptide 'anticodon' deciphers stop codons in messenger RNA. Nature 403, 680–684.

Jansson, S., Andersen, B. and Scheller, H.V. (1996) Nearest-neighbor analysis of higher-plant photosystem I holocomplex. Plant Physiol. 112, 409-420.

Jeon, W., Cheng, J. and Ludden, P. (2001) Purification and characterisation of membrane-associated CooC protein and its functional role in the insertion of nickel into carbon monoxide deydrogenase from *Rhodospirillum rubrum*. J. Biol. Chem. 276, 38602-38609.

Jordan, P., Fromme, P., Witt, H.T., Klukas, O., Saenger, W. and Krauss, N. (2001) Three-dimensional structure of cyanobacterial photosystem I at 2.5 Å resolution. Nature 411, 909-917.

Jung, Y.S., Vassiliev, I.R., Yu, J., McIntosh, L. and Golbeck, J.H. (1997) Strains of *Synechocystis* sp. PCC 6803 with altered PsaC. Part II. EPR and optical spectroscopic properties of F_A and F_B in aspartate, serine and alanine replacements of cysteines 14 and 51. J. Biol. Chem. 272, 8040-8049.

Kaberdin, V.R., Miczak, A., Jakobsen, J.S., Lin-Chao, S., McDowall, K.J. and von Gabain, A. (1998) The endoribonucleolytic N-terminal half of *Escherichia coli* RNase E is evolutionarily conserved in *Synechocystis* sp. and other bacteria but not the C-terminal half, which is sufficient for degradosome assembly. Proc. Natl. Acad. Sci. USA 29, 11637-11642.

Kamiya, N. and Shen, J.R. (2003) Crystal structure of oxygenevolving photosystem II from *Thermosynechococcus vulcanus* at 3.7 Å resolution. Proc. Natl. Acad. Sci. USA 100, 98-103.

Karzai, A.W. and Sauer, R.T. (2001) Protein factors associated with the SsrA-SmpB tagging and ribosome rescue complex. Proc. Natl. Acad. Sci. USA 98, 3040–3044.

Karzai, A.W., Roche, E.D. and Sauer, R.T. (2000). The SsrA-SmpB system for protein tagging, directed degradation and ribosome rescue. Nat. Struct. Biol. 7, 449–455.

Kashino, Y., Lauber, W.M., Carroll, J.A., Wang, Q., Whitmarsh, J., Satoh, K. and Pakrasi, H.B. (2002) Proteomic analysis of a highly active photosystem II preparation from the cyanobacterium *Synechocystis* sp. PCC 6803 reveals the presence of novel polypeptides. Biochemistry 41, 8004-8012.

Kawaguchi, H., Fukuda, I., Shiina, T. and Toyoshima, Y. (1992) Dynamical behavior of *psb* gene transcripts in greening wheat seedlings. Part I. Time course of accumulation of the *psbA* through *psbN* gene transcripts during light-induced greening. Plant Mol. Biol. 20, 695-704.

Keiler, K.C., Waller, P.R. and Sauer, R.T. (1996). Role of a peptide tagging system in degradation of proteins synthesized from damaged messenger RNA. Science 271, 990–993.

Khandijan, E.W. (1986) UV crosslinking of RNA to nylon membranes enhances hybridization signals. Molec. Biol. Rep. 11, 107-115.

Kim, J., Eichacker, L.A. Rüdiger, W. and Mullet. J.E. (1994) Chlorophyll regulates accumulation of the plastid-encoded chlorophyll proteins P700 and D1 by increasing apoprotein stability. Plant Physiol. 104, 907-916.

Kim, M., Christopher, D.A. and Mullet, J.E. (1993). Direct evidence for selective modulation of *psbA*, *rpoA*, *rbcL* and *16S* RNA stability during barley chloroplast development. Plant Mol. Biol. 22, 447–463.

Klaff, P. (1995) mRNA decay in spinach chloroplasts: *psbA* mRNA degradation is initiated by endonucleolytic cleavages within the coding region. Nucl. Acids Res. 23, 4885-4892.

Klaff, P. and Gruissem, W. (1991) Changes in chloroplast mRNA stability during leaf development. Plant Cell 3, 517–529.

Klaholz, B.P., Pape, T., Zavialov, A.V., Myasnikov, A.G., Orlova, E.V., Vestergaard, B., Ehrenberg, M. and van Heel, M. (2003) Structure of the *Escherichia coli* ribosomal termination complex with release factor 2. Nature 421, 90-94.

Kleffmann, T., Russenberger, D., von Zychlinski, A., Christopher, W., Sjolander, K., Gruissem, W. and Baginsky, S. (2004) The *Arabidopsis thaliana* chloroplast proteome reveals pathway abundance and novel protein functions. Curr. Biol. 14, 354-362.

Klein, R.R. and Mullet, J.E. (1990). Light-induced transcription of chloroplast genes: *psbA* transcription is differentially enhanced in illuminated barley. J. Biol. Chem. 265, 1895-1902.

Klein, R.R., Mason, H.S. and Mullet, J.E. (1988). Light-regulated translation of chloroplast proteins. I. Transcripts of *psaA-psaB*, *psbA*, and *rbcL* are associated with polysomes in dark-grown and illuminated barley seedlings. J. Cell Biol. 106, 289–301.

Koncz, C., Martini, N., Szabados, L., Hrouda, M., Bachmair, A. and Schell, J. (1994) Specialized vectors for gene tagging and expression studies. In: Plant Molecular Biology Manual. Vol. B2 (Gelvin, S.B. and Schilperoort, R.A., eds). Dordrecht: Kluwer Academic Publishers, pp. 1-22.

Konieczny, A. and Ausubel, F.M. (1993) A procedure for mapping *Arabidopsis* mutations using co-dominant ecotype-specific PCR-based markers. Plant J. 4, 403-410.

Koonin, E.V. (1993) A superfamily of ATPases with diverse functions containing either classical or deviant ATP-binding motif. J. Mol. Biol. 229, 1165-1174.

Krause, G.H. and Weis, E. (1991) Chlorophyll fluorescence and photosynthesis: the basics. Annu. Rev. Plant. Physio. Mol. Biol. 42, 313-349.

Krysan, P.J., Young, J.C. and Sussman, M.R. (1999) T-DNA as an insertional mutagen in *Arabidopsis*. Plant Cell 11, 2283-2290.

Kubicki, A., Funk, E., Westhoff, P. and Steinmüller, K. (1996) Differential expression of plastome-encoded *ndh*-genes in mesophyll and bundle sheath chloroplasts of the C4-plant *Sorghum bicolor* indicates that the complex I-homologous NAD(P)H-plastoquinone-oxidoreductase is involved in cyclic electron transport. Planta 199, 276-281.

Kubicki, A., Steinmüller, K. and Westhoff, P. (1994) Differential transcription of plastome-encoded genes in the mesophyll and bundle-sheath chloroplasts of the monocotyledonous NADP-malic enzyme-type C4 plants maize and *Sorghum*. Plant Mol. Biol. 25, 669-679.

Kück, U., Jekosch, K. and Holzamer, P. (2000) DNA sequence analysis of the complete mitochondrial genome of the green alga *Scenedesmus obliquus*: Evidence for UAG being a leucine and UCA being a non-sense codon. Gene 253, 13–18.

Kurisu, G., Zhang, H., Smith, J.L. and Cramer, W.A. (2003) Structure of the cytochrome b_6f complex of oxygenic photosynthesis: tuning the cavity. Science 302, 1009-1014.

Kuromori, T., Hirayama, T., Kiyosue, Y., Takabe, H., Mizukado, S., Sakurai, T., Akiyama, K., Kamiya, A., Ito, T. and Shinozaki, K. (2004) A collection of 11800 single-copy Ds transposon insertion lines in *Arabidopsis*. Plant J. 37, 897-905.

Kushner, S.R. (2002) mRNA decay in *Escherichia coli* comes of age. J. Bacteriol. 184, 4658-4665.

Kushnir, S., Babiychuk, E., Bannikova, M., Momot, V., Komarnitsky, I., Cherep, N. and Gleba, Y. (1991) Nucleo-cytoplasmic incompatibility in cybrid plants possessing an *Atropa* genome and a *Nicotiana* plastome. Mol. Gen. Genet. 225, 225-230.

Lee, H., Bingham, S.E. and Webber, A.N. (1996) Function of 3' non-coding sequences and stop codon usage in expression of the chloroplast *psaB* gene in *Chlamydomonas reinhardtii*. Plant Mol. Biol. 31, 337–354.

Legen, J., Kemp, S., Krause, K., Profanter, B., Herrmann, R.G. and Maier, R.M. (2002) Comparative analysis of plastid transcription profiles of entire plastid chromosomes from tobacco attributed to wild-type and PEP-deficient transcription machineries. Plant J. 31, 171-188.

Legen, J., Misera, S., Herrmann, R.G. and Meurer, J. (2001) Map positions of 69 *Arabidopsis thaliana* genes of all known nuclear encoded constituent polypeptides and various regulatory factors of the photosynthetic membrane: a case study. DNA Res. 27, 53-60.

Leipe, D.D., Wolf, Y.I., Koonin, E.V. and Aravind, L. (2002) Classification and evolution of P-loop GTPases and related ATPases. J. Mol. Biol. 317, 41-72.

Léon, S., Touraine, B., Ribot, C., Briat, J.F. and Lobreaux, S. (2003) Iron-sulphur cluster assembly in plants: distinct NFU proteins in mitochondria and plastids from *Arabidopsis thaliana*. Biochem. J. 371, 823-830.

Lill, R. and Kispal, G. (2000) Maturation of cellular Fe-S proteins: an essential function of mitochondria. Trends Biochem. Sci. 25, 352-356.

Lill, R. and Mühlenhoff, U. (2005) Iron-sulfur-protein biogenesis in eukaryotes. Trends Biochem. Sci. 30, in press.

Lindsey, K., Wei, W., Clarke, M.C., McArdle, H.F., Rooke, L.M. and Topping, J.F. (1993) Tagging genomic sequences that direct transgene expression by activation of a promoter trap in plants. Transgenic Res. 2, 33-47.

Liu, Z., Yan, H., Wang, K., Kuang, T., Zhang, J., Gui, L., An, X. and Chang, W. (2004) Crystal structure of spinach major light-harvesting complex at 2.72 Å resolution. Nature 428, 287-292.

Lizardi, P.M. (1983) Methods for the preparation of messenger RNA. Meth. Enzymol. 96, 24-38.

Lukowitz, W., Gillmor, C.S. and Scheible, W.R. (2000) Positional cloning in *Arabidopsis*. Why it feels good to have a genome initiative working for you. Plant Physiol. 123, 795-805.

Lütcke, H.A., Chow, K.C., Mickel, F.S., Moss, K.A., Kern, H.F. and Scheele, G.A. (1987) Selection of AUG initiation codons differs in plants and animals. EMBO J. 6, 43–48.

Manieri, W., Franchini, L., Raeber, L., Dai, S., Stritt-Etter, A.L. and Schürmann, P. (2003) N-terminal truncation of the variable subunit stabilizes spinach ferredoxin: thioredoxin reductase. FEBS Lett. 549, 167-170.

Martienssen, R.A. (1998) Functional genomics: probing plant gene function and expression with transposons Proc. Natl. Acad. Sci. USA 95, 2021-2026.

Martin, W. and Herrmann, R.G. (1998) Gene transfer from organelles to the nucleus: how much, what happens, and Why? Plant Physiol. 118, 9-17.

Martin, W. and Russell, M.J. (2003) On the origins of cells: a hypothesis for the evolutionary transitions from abiotic geochemistry to chemoautotrophic prokaryotes, and from prokaryotes to nucleated cells. Philos. Trans. R. Soc. Lond. B Biol. Sci. 358, 59-83.

Martin, W., Stoebe, B., Goremykin, V., Hapsmann, S., Hasegawa, M. and Kowallik, K.V. (1998) Gene transfer to the nucleus and the evolution of chloroplasts. Nature 393, 162-165.

Martinez-Zapater, J.M., Gil, P., Capel, J. and Somerville, C.R. (1992) Mutations at the Arabidopsis *CHM* locus promote rearrangements of the mitochondrial genome. Plant Cell 4, 889-899.

Maul, J.E., Lilly, J.W., Cui, L., dePamphilis, C.W., Miller, W., Harris, E.H. and Stern, D.B. (2002) The *Chlamydomonas reinhardtii* plastid chromosome: islands of genes in a sea of repeats. Plant Cell 14, 2659-2679.

McCormac, D.J. and Barkan, A. (1999) A nuclear gene in maize required for the translation of the chloroplast *atpB/E* mRNA. Plant Cell 11, 1709–1716.

McFadden, G.I. and van Dooren, G.G. (2004) Evolution: red algal genome affirms a common origin of all plastids. Curr. Biol. 14, 514-516.

McMaster, G.K. and Carmichael, G.G. (1977) Analysis of single and double-stranded nucleic acids on polyacrilamid and agarose gels by using glyoxal and acridine orange. Proc. Natl Acad. Sci. USA 74, 4835-4838.

Mehari, T., Qiao, F., Scott, M.P., Nellis, D.F., Zhao, J., Bryant, D.A. and Golbeck, J.H. (1995) Modified ligands to F_A and F_B in photosystem I. Part I. Structural constraints for the formation of iron sulfur clusters in free and rebound PsaC. J. Biol. Chem. 270, 28108-28117.

Mereschkowsky, C. (1905) Über Natur und Ursprung der Chromatophoren im Pflanzenreiche. Biol. Centralbl. 25, 593 – 604. [English translation in: Martin, W. and Kowallik, K.V. (1999) Annotated English translation of Mereschkowsky's 1905 paper 'Über Natur und Ursprung der Chromatophoren im Pflanzenreiche.' Eur. J. Phycol. 34, 287-295].

Meurer, J., Berger, A. and Westhoff, P. (1996a) A nuclear mutant of Arabidopsis with impaired stability on distinct transcripts of the plastid *psbB*, *psbD/C*, *ndhH*, and *ndhC* operons. Plant Cell 8, 1193–1207.

Meurer, J., Meierhoff, K. and Westhoff, P. (1996b) Isolation of high-chlorophyll-fluorescence mutants of *Arabidopsis thaliana* and their characterization by spectroscopy, immunoblotting and RNA gel hybridization. Planta 198, 385–396.

Meurer, J., Plücken, H., Kowallik, K.V. and Westhoff, P. (1998) A nuclear-encoded protein of prokaryotic origin is essential for the stability of photosystem II in *Arabidopsis thaliana*. EMBO J. 17, 5286–5297.

Michl, D., Karnauchov, I., Berghofer, J., Herrmann, R.G. and Klösgen, R.B. (1999) Phylogenetic transfer of organelle genes to the nucleus can lead to new mechanisms of protein integration into membranes. Plant J. 17, 31–40.

Mikuni, O., Kawakami, K. and Nakamura, Y. (1991) Sequence and functional analysis of mutations in the gene encoding peptide-chain-release factor 2 of *Escherichia coli*. Biochimie 73, 1509–1516.

Monde, R.A., Schuster, G. and Stern, D.B. (2000) Processing and degradation of chloroplast mRNA. Biochimie 82, 573–582.

Moseley, J.L., Page, M.D., Alder, N.P., Eriksson, M., Quinn, J., Soto, F., Theg, S.M., Hippler, M. and Merchant, S. (2002) Reciprocal expression of two candidate di-iron enzymes affecting photosystem I and light-harvesting complex accumulation. Plant Cell 14, 673-688.

Mullet, J.E. (1993) Dynamic regulation of chloroplast transcription. Plant Physiol. 103, 309–313.

Mullet, J.E., Klein, P.G. and Klein. R.R. (1990) Chlorophyll regulates accumulation of the plastid-encoded chlorophyll apoproteins CP43 and D1 by increasing apoprotein stability. Proc. Natl. Acad. Sci. USA 87, 4038-4042.

Munekage, Y., Hashimoto, M., Miyake, C., Tomizawa, K., Endo, T., Tasaka, M. and Shikanai, T. (2004) Cyclic electron flow around photosystem I is essential for photosynthesis. Nature 429, 579-582.

Munekage, Y., Hojo, M., Meurer, J., Endo, T., Tasaka, M. and Shikanai, T. (2002) PGR5 is involved in cyclic electron flow around photosystem I and is essential for photoprotection in *Arabidopsis*. Cell 110, 361-371.

Murashige, T. and Skoog, F. (1962) A revised medium for rapid growth and bioassays with tobacco tissue cultures. Physiol. Plant. 15, 473-497.

Nachin, L., Loiseau, L., Expert, D. and Barras, F. (2003) SufC: an unorthodox cytoplasmic ABC/ATPase required for [Fe-S] biogenesis under oxidative stress. EMBO J. 22, 427-437.

Nakamura, Y. and Ito, K. (2003) Making sense of mimic in translation termination. Trends Biochem. Sci. 28, 99-105.

Nakamura, Y., Ito, K. and Ehrenberg, M. (2000) Mimicry grasps reality in translation termination. Cell 101, 349–352.

Nakashima, H., Grahovac, M.J., Mazzarella, R., Fujiwara, H., Kitchen, J.R., Threat, T.A. and Ko, M.S. (1999) Two novel mouse genes - *Nubp2*, mapped to the t-complex on chromosome 17, and *Nubp1*, mapped to chromosome 16 - establish a new gene family of nucleotide-binding proteins in eukaryotes. Genomics 60, 152-160.

Nakazawa, M., Ichikawa, T., Ishikawa, A., Kobayashi, H., Tsuhara, Y., Kawashima, M., Suzuki, K., Muto, S. and Matsui, M. (2003) Activation tagging, a novel tool to dissect the functions of a gene family. Plant J. 34, 741-750.

Nickelsen, J. (1999) Transcripts containing the 5' untranslated regions of the plastid genes *psbA and psbB* from higher plants are unstable in *Chlamydomonas reinhardtii* chloroplasts. Mol. Gen. Genet. 262, 768-771.

Nickelsen, J. (2000) Mutations at three different nuclear loci of *Chlamydomonas* suppress a defect in chloroplast *psbD* mRNA accumulation. Curr. Genet. 37, 136-142.

Nickelsen, J. (2003) Chloroplast RNA-binding proteins. Curr. Genet. 43, 392-399.

Nickelsen, J., Fleischmann, M., Boudreau, E., Rahire, M. and Rochaix, J.D. (1999) Identification of *cis*-acting RNA leader elements required for chloroplast *psbD* gene expression in *Chlamydomonas*. Plant Cell 11, 957-970.

Nickelsen, J., van Dillewijn, J., Rahire, M. and Rochaix, J.D. (1994) Determinants for stability of the chloroplast *psbD* RNA are located within its short leader region in *Chlamydomonas reinhardtii*. EMBO J. 13, 3182-3191.

Nielsen, V.S., Scheller, H.V. and Moller, B.L. (1996) The photosystem I mutant *viridis-zb*^{63} of barley (*Hordeum vulgare*) contains low amounts of active but unstable photosystem I. Physiol. Plant. 98, 637-644.

Nierhaus, K.H. and Wittmann, H.G. (1980) Ribosomal function and its inhibition by antibiotics in prokaryotes. Naturwissenschaften 67, 234–250.

Nishio, K. and Nakai, M. (2000) Transfer of iron-sulfur cluster from NifU to apoferredoxin. J. Biol. Chem. 275, 22615-22628.

Ogawara, H., Urabe, H., Ohtaki, R. and Nakamura, Y. (1995) Properties of peptide chain release factor 2 from *Streptomyces coelicolor* A3(2): Conserved primary structure but no frameshift regulation. J. Bacteriol. 177, 5342–5345.

Ollagnier-de Choudens, S., Nachin, L., Sanakis, Y., Loiseau, L., Barras, F. and Fontecave, M. (2003) SufA from *Erwinia chrysanthemi*: characterization of a scaffold protein required for iron-sulfur cluster assembly. J. Biol. Chem. 278, 17993-18001.

Ossenbühl, F. and Nickelsen, J. (2000) *Cis*- and *trans*-acting determinants for translation of *psbD* mRNA in *Chlamydomonas reinhardtii*. Mol. Cell Biol. 20, 8134-8142.

Palmer, J.D. (2003) The symbiotic birth and spread of plastids: how many times and whodonit? J. Phycol. 39, 4-11.

Peltier, G. and Cournac, L. (2002) Chlororespiration. Annu. Rev. Plant. Biol. 53, 523-550.

Pesaresi, P., Varotto, C., Meurer, J., Jahns, P., Salamini, F. and Leister, D. (2001) Knock-out of the plastid ribosomal protein L11 in *Arabidopsis*: Effects on mRNA translation and photosynthesis. Plant J. 27, 179–189.

Petersen, L. and Downs, D.M. (1996) Mutations in *apbC* (*mrp*) prevent function of the alternative pyrimidine biosynthetic pathway in *Salmonella typhimurium*. J. Bacteriol. 178, 5676-5682.

Pfannschmidt, T., Nilsson, A. and Allen, J.F. (1999) Photosynthetic control of chloroplast gene expression. Nature 397, 625-628.

Pilon-Smits, E.A., Garifullina, G.F., Abdel-Ghany, S., Kato, S., Mihara, H., Hale, K.L., Burkhead, J.L., Esaki, N., Kurihara, T. and Pilon, M. (2002) Characterization of a NifS-like chloroplast protein from *Arabidopsis*. Implications for its role in sulfur and selenium metabolism. Plant Physiol. 130, 1309-1318.

Plücken, H., Müller, B., Grohmann, D., Westhoff, P. and Eichacker, L.A. (2002) The HCF136 protein is essential for assembly of the photosystem II reaction center in *Arabidopsis thaliana*. FEBS Lett. 532, 85-90.

Raghavendra, A.S. and Padmasree, K. (2003) Beneficial interactions of mitochondrial metabolism with photosynthetic carbon assimilation. Trends Plant. Sci. 8, 546-553.

Rangaraj, P., Shah, P. and Ludden, P. (1997) ApoNifH functions in iron-molybdenum cofactor synthesis and apodinitrogenase maturation. Proc. Natl. Acad. Sci. USA 94, 11250-11255.

Rapp, J.C., Baumgartner, B.J. and Mullet, J. (1992) Quantitative analysis of transcription and RNA levels of 15 barley chloroplast genes. Transcription rates and mRNA levels vary over 300-fold; predicted mRNA stabilities vary 30-fold. J. Biol. Chem. 267, 21404-21411.

Rattanachaikunsopon, P., Rosch, C. and Kuchka, M.R. (1999) Cloning and characterization of the nuclear AC115 gene of *Chlamydomonas reinhardtii*. Plant Mol. Biol. 9, 1-10.

Rawat, U.B., Zavialov, A.V., Sengupta, J., Valle, M., Grassucci, R.A., Linde, J., Vestergaard, B., Ehrenberg, M. and Frank, J. (2003) A cryo-electron microscopic study of ribosome-bound termination factor RF2. Nature 421, 87-90.

Redding, K., Cournac, L., Vassiliev, I.R., Golbeck, J.H., Peltier, G. and Rochaix, J.D. (1999) Photosystem I is indispensable for photoautotrophic growth, CO_2 fixation, and H_2 photoproduction in *Chlamydomonas reinhardtii*. J. Biol. Chem. 274, 10466-10473.

Régnier, P. and Arraiano, C.M. (2000) Degradation of mRNA in bacteria: emergence of ubiquitous features. Bioessays 22, 235-244.

Reiss, B., Klemm, M., Kosak, H. and Schell, J. (1996) RecA protein stimulates homologous recombination in plants. Proc. Natl. Acad. Sci. USA 93, 3094-3098.

Rhee, K.H. (2001) Photosystem II: the solid structural era. Annu. Rev. Biophys. Biomol. Struct. 30, 307-328.

Richly, E. and Leister, D. (2004) An improved prediction of chloroplast proteins reveals diversities and commonalities in the chloroplast proteomes of *Arabidopsis* and rice. Gene 329, 11-16.

Richly, E., Dietzmann, A., Biehl, A., Kurth, J., Laloi, C., Apel, K., Salamini, F. and Leister, D. (2003) Covariations in the nuclear chloroplast transcriptome reveal a regulatory master-switch. EMBO Rep. 4, 491-498.

Richmond, T. and Somerville, S. (2000) Chasing the dream: plant EST microarrays. Curr. Opin. Plant Biol. 3, 108-116.

Rochaix, J.D. (2004) Genetics of the biogenesis and dynamics of the photosynthetic machinery in eukaryotes. Plant Cell 16, 1650-1660.

Rochaix, J.D., Perron, K., Dauvillee, D., Laroche, F., Takahashi, Y. and Goldschmidt-Clermont, M. (2004) Post-transcriptional steps involved in the assembly of photosystem I in *Chlamydomonas*. Biochem. Soc. Trans. 32, 567-570.

Rodday, S.M., Webber, A.N., Bingham, S.E. and Biggins, J. (1995) Evidence that the F_X domain in photosystem I interacts with the subunit PsaC: site-directed changes in PsaB destabilize the subunit interaction in *Chlamydomonas reinhardtii*. Biochemistry 34, 6328-6334.

Rolland, N., Janosi, L., Block, M.A., Shuda, M., Teyssier, E., Miege, C., Cheniclet, C., Carde, J.P., Kaji, A. and Joyard, J. (1999) Plant ribosome recycling factor homologue is a chloroplastic protein and is bactericidal in *Escherichia coli* carrying temperature-sensitive ribosome recycling factor. Proc. Natl. Acad. Sci. USA 96, 5464–5469.

Roussell, D.L., Thompson, D.L., Pallardy, S.G., Miles, D. and Newton, K.J. (1991) Chloroplast structure and function is altered in the NCS2. Plant Physiol. 96, 232-238.

Roy, A., Solodovnikova, N., Nicholson, T., Antholine, W. and Walden, W.E. (2003) A novel eukaryotic factor for cytosolic Fe-S cluster assembly. EMBO J. 22, 4826-4835.

Ruf, S., Kossel, H. and Bock, R. (1997) Targeted inactivation of a tobacco intron-containing open reading frame reveals a novel chloroplast-encoded photosystem I–related gene. J. Cell Biol. 139, 95–102.

Russell, M.J., Hall, A.J. and Gize, A.P. (1990) Pyrite and the origin of life. Nature 344, 387.

Saenger, W., Jordan, P. and Krauss, N. (2002) The assembly of protein subunits and cofactors in photosystem I. Curr. Opin. Struct. Biol. 12, 244-254.

Sakamoto, W., Kondo, H., Murata, M. and Motoyoshi, F. (1996) Altered mitochondrial gene expression in a maternal distorted leaf mutant of Arabidopsis induced by chloroplast mutator. Plant Cell 8, 1377-1390.

Salvador, M.L. and Klein, U. (1999) The redox state regulates RNA degradation in the chloroplast of *Chlamydomonas reinhardtii*. Plant Physiol. 121, 1367-1374.

Salvador, M.L., Klein, U. and Bogorad, L. (1993) Light-regulated and endogenous fluctuations of chloroplast transcript levels in *Chlamydomonas*. Regulation by transcription and RNA degradation. Plant J. 3, 213-219.

Sambrook, J., Fritsch, E.F. and Maniatis, T. (1989) Molecular cloning – a laboratory manual. 2 ed. Cold Spring Harbor, New York, USA: Cold Spring Harbor Laboratory Press.

Saraste, M., Sibbald, P.R. and Wittinghofer, A. (1990) The P-loop - a common motif in ATP- and GTP binding proteins. Trends Biochem. Sci. 15, 430-434.

Scheller, H.V., Jensen, P.E., Haldrup, A., Lunde, C. and Knoetzel, J. (2001) Role of subunits in eukaryotic Photosystem I. Biochim. Biophys. Acta 1507, 41-60.

Schilke, B., Voisine, C., Beinert, H. and Craig, E. (1999) Evidence for a conserved system for iron metabolism in the mitochondria of *Saccharomyces cerevisiae*. Proc. Natl. Acad. Sci. USA 96, 10206-10211.

Schmid, K.J., Sorensen, T.R., Stracke, R., Torjek, O., Altmann, T., Mitchell-Olds, T. and Weisshaar, B. (2003) Large-scale identification and analysis of genome-wide single-nucleotide polymorphisms for mapping in *Arabidopsis thaliana*. Genome Res. 13, 1250-1257.

Schmitz-Linneweber, C., Regel, R., Du, T.G., Hupfer, H., Herrmann, R.G. and Maier, R.M. (2002) The plastid chromosome of *Atropa belladonna* and its comparison with that of *Nicotiana tabacum*: the role of RNA editing in generating divergence in the process of plant speciation. Mol. Biol. Evol. 19, 1602-1612.

Schnepf E. (1980) Types of plastids: their development and interconversions. In: Results and problems in cell differentiation. Vol. 10. Chloroplasts (Reinert, J., ed.). Berlin: Springer, pp. 1-27.

Schöneberg, U., Vahrson, W., Priedemuth, P. and Wittig, B. (1994) Analysis and interpretation of DNA and protein sequences using MacMolly Tetra. 3. ed. Bielefeld: Karoi-Verl. Bornemann.

Schubert, M., Petersson, U.A., Haas, B.J., Funk, C., Schroder, W.P. and Kieselbach, T. (2002) Proteome map of the chloroplast lumen of *Arabidopsis thaliana*. J. Biol. Chem. 277, 8354-8365.

Schultes, N.P., Sawers, R.J., Brutnell, T.P. and Krueger, R.W. (2000) Maize high chlorophyll fluorescent 60 mutation is caused by an Ac disruption of the gene encoding the chloroplast ribosomal small subunit protein 17. Plant J. 21, 317–327.

Schuster, G. and Bock, R. (2001) Editing, polyadenylation and degradation of mRNA in the chloroplast. In Regulation of Photosynthesis (Aro, E.-M. and Andersson, B., eds). Dordrecht: Kluwer Academic Publishers, pp. 121-136.

Schwabe, T.M. and Kruip, J. (2000) Biogenesis and assembly of photosystem I. Indian J. Biochem. Biophys. 37, 351-359.

Scolnick, E., Tompkins, R., Caskey, T. and Nirenberg, M. (1968) Release factors differing in specificity for terminator codons. Proc. Natl. Acad. Sci. USA 61, 768–774.

Selinger, D.W., Saxena, R.M., Cheung, K.J., Church, G.M. and Rosenow, C. (2003) Global RNA half-life analysis in *Escherichia coli* reveals positional patterns of transcript degradation. Genome Res. 13, 216-223.

Shahrestanifar, M., Saha, D.P., Scala, L.A., Basu, A. and Howells, R.D. (1994) Cloning of a human cDNA encoding a putative nucleotide-binding protein related to *Escherichia coli* MinD. Gene 147, 281-285.

Shen, G., Antonkine, M.L., van der Est, A., Vassiliev, I.R., Brettel, K., Bittl, R., Zech, S.G., Zhao, J., Stehlik, D., Bryant, D.A. and Golbeck, J.H. (2002) Assembly of photosystem I. Part II. Rubredoxin is required for the *in vivo* assembly of F_X in *Synechococcus* sp. PCC 7002 as shown by optical and EPR spectroscopy. J. Biol. Chem. 277, 20355-20366.

Shiina, T., Allison, L. and Maliga, P. (1998) *rbcL* transcript levels in tobacco plastids are independent of light: reduced dark transcription rate is compensated by increased mRNA stability. Plant Cell 10, 1713-1722.

Shikanai, T., Endo, T., Hashimoto, T., Yamada, Y., Asada, K. and Yokota, A. (1998) Directed disruption of the tobacco *ndhB* gene impairs cyclic electron flow around photosystem I. Proc. Natl. Acad. Sci. USA 95, 9705-9709.

Singh, M., Boutanaev, A., Zucchi, P. and Bogorad, L. (2001) Gene elements that affect the longevity of *rbcL* sequence-containing transcripts in *Chlamydomonas reinhardtii* chloroplasts. Proc. Natl. Acad. Sci. USA 98, 2289-2294.

Sizova, I.A., Lapina, T.V., Frolova, O.N., Alexandrova, N.N., Akopiants, K.E. and Danilenko, V.N. (1996) Stable nuclear transformation of *Chlamydomonas reinhardtii* with a *Streptomyces rimosus* gene as the selective marker. Gene 181, 13–18.

Skovran, E. and Downs, D.M. (2003) Lack of the ApbC or ApbE protein results in a defect in Fe-S cluster metabolism in *Salmonella enterica* serovar *Typhimurium*. J. Bacteriol. 185, 98-106.

Smart, L.B. and McIntosh, L. (1993) Genetic inactivation of the *psaB* gene in *Synechocystis* sp. PCC 6803 disrupts assembly of photosystem I. Plant Mol. Biol. 21, 177-180.

Smart, L.B., Anderson, S.L. and McIntosh, L. (1991) Targeted genetic inactivation of the photosystem I reaction center in the cyanobacterium *Synechocystis* sp. PCC 6803. EMBO J. 10, 3289-3296.

Smart, L.B., Warren, P.V., Golbeck, J.H. and McIntosh, L. (1993) Mutational analysis of the structure and biogenesis of the photosystem I reaction center in the cyanobacterium *Synechocystis* sp. PCC 6803. Proc. Natl. Acad. Sci. USA 90, 1132-1136.

Somerville, C.R., Somerville, S.C. and Ogren, W.L. (1981) Isolation of photosynthetically active protoplasts and chloroplasts from *Arabidopsis thaliana*. Plant Sci. Lett. 21, 89-96.

Song, H., Mugnier, P., Das, A.K., Webb, H.M., Evans, D.R., Tuite, M.F., Hemmings, B.A. and Barford, D. (2000) The crystal structure of human eukaryotic release factor eRF1: Mechanism of stop codon recognition and peptidyl-tRNA hydrolysis. Cell 100, 311–321.

Stampacchia, O., Girard-Bascou, J., Zanasco, J.L., Zerges, W., Bennoun, P., and Rochaix, J.D. (1997) A nuclear-encoded function essential for translation of the chloroplast *psaB* mRNA in *Chlamydomonas*. Plant Cell 9, 773-782.

Stern, D.B. and Gruissem, W. (1987) Control of plastid gene expression: 3' inverted repeats act as mRNA processing and stabilizing elements, but do not terminate transcription. Cell 51, 1145–1157.

Stroebel, D., Choquet, Y., Popot, J.L. and Picot, D. (2003) An atypical haem in the cytochrome b_6f complex. Nature 426, 413-418.

Strotmann, H., Shavit, N. and Leu, S. (1998) Assembly and function of the chloroplast ATP synthase. In: The molecular biology of chloroplast and mitochondria in *Chlamydomonas* (Rochaix, J.D., Goldschmidt-Clermont, M. and Merchant, S., eds). Norwell, MA: Kluwer Academic Publishers, pp. 477–500.

Stubbe, W. (1989) *Oenothera* - an ideal system for studying the interaction of genome and plastome. Plant Mol. Biol. Rep. 7, 245-257.

Sugita, M. and Sugiura, M. (1996) Regulation of gene expression in chloroplasts of higher plants. Plant Mol. Biol. 32, 315-326.

Sugiura, M., Hirose, T. and Sugita, M. (1998) Evolution and mechanism of translation in chloroplasts. Annu. Rev. Genet. 32, 437-459.

Summer, H., Pfannschmidt, T. and Link, G. (2000) Transcripts and sequence elements suggest differential promoter usage within the *ycf3-psaAB* gene cluster on mustard (*Sinapis alba* L.) chloroplast DNA. Curr. Genet. 37, 45-52.

Sutak, R., Doleza,l P., Fiumera, H.L., Hrdy, I., Dancis, A., Delgadillo-Correa, M., Johnson, P.J., Muller, M. and Tachezy, J. (2004) Mitochondrial-type assembly of FeS centers in the hydrogenosomes of the amitochondriate eukaryote *Trichomonas vaginalis*. Proc. Natl. Acad. Sci. USA 101, 10368-10373.

Szabados, L., Kovacs, I., Oberschall, A., Abraham, E., Kerekes, I., Zsigmond, L., Nagy, R., Alvarado, M., Krasovskaja, I., Gal, M., Berente, A., Redei, G.P., Haim, A.B. and Koncz, C. (2002) Distribution of 1000 sequenced T-DNA tags in the *Arabidopsis* genome. Plant J. 32, 233-242.

Tachezy, J., Sanchez, L.B. and Muller, M. (2001) Mitochondrial type iron-sulfur cluster assembly in the amitochondriate eukaryotes *Trichomonas vaginalis* and *Giardia intestinalis*, as indicated by the phylogeny of IscS. Mol. Biol. Evol. 18, 1919-1928.

Takahashi, Y. and Tokumoto, U. (2002) A third bacterial system for the assembly of iron-sulfur clusters with homologs in archaea and plastids. J. Biol. Chem. 277, 28380-28383.

Takahashi, Y., Goldschmidt-Clermont, M., Soen, S.Y., Franzen, L.G. and Rochaix, J.D. (1991) Directed chloroplast transformation in *Chlamydomonas reinhardtii*: insertional inactivation of the *psaC* gene encoding the iron sulfur protein destabilizes photosystem I. EMBO J. 10, 2033-2040.

Tanaka, K., Oikawa, K., Ohta, N., Kuroiwa, H., Kuroiwa, T. and Takahashi, H. (1996) Nuclear encoding of a chloroplast RNA polymerase sigma subunit in a red alga. Science 272, 1932-1935.

Thomas, E.J. and Ortiz, W. (1995) Loss of chloroplast transcripts for proteins associated with photosystem II: an early event during heat-bleaching in *Euglena gracilis*. Plant Mol. Biol. 27, 317-325.

Timmis, J.N., Ayliffe, M.A., Huang, C.Y. and Martin, W. (2004) Endosymbiotic gene transfer: organelle genomes forge eukaryotic chromosomes. Nat. Rev. Genet. 5, 123-135.

Tottey, S., Block, M.A., Allen, M., Westergren, T., Albrieux, C., Scheller, H.V., Merchant, S. and Jensen. P.E. (2003) *Arabidopsis* CHL27, located in both envelope and thylakoid membranes, is required for the synthesis of protochlorophyllide. Proc. Natl. Acad. Sci. USA 100, 16119-16124.

Touraine, B., Boutin, J.P., Marion-Poll, A., Briat, .J.F., Peltier, G. and Lobreaux, S. (2004) Nfu2: a scaffold protein required for [4Fe-4S] and ferredoxin iron-sulphur cluster assembly in *Arabidopsis* chloroplasts. Plant J. 40, 101-111.

Tovar, J., Leon-Avila, G., Sanchez, L.B., Sutak, R., Tachezy, J., van der Giezen, M., Hernandez, M., Muller, M. and Lucocq, J.M. (2003) Mitochondrial remnant organelles of *Giardia* function in iron-sulphur protein maturation. Nature 426, 172-176.

Turmel, M., Otis, C. and Lemieux, C. (1999) The complete chloroplast DNA sequence of the green alga *Nephroselmis olivacea*: Insights into the architecture of ancestral chloroplast genomes. Proc. Natl. Acad. Sci. USA 96, 10248–10253.

Unseld, M., Marienfeld, J.R., Brandt, P. and Brennicke, A. (1997) The mitochondrial genome of *Arabidopsis thaliana* contains 57 genes in 366,924 nucleotides. Nat. Genet. 15, 57–61.

Vaistij, F.E., Boudreau, E., Lemaire, S.D., Goldschmidt-Clermont, M. and Rochaix, J.D. (2000a) Characterization of Mbb1, a nucleus-encoded tetratricopeptide-like repeat protein required for expression of the chloroplast *psbB/psbT/psbH* gene cluster in *Chlamydomonas reinhardtii*. Proc. Natl. Acad. Sci. USA 97, 14813-14818.

Vaistij, F.E., Goldschmidt-Clermont, M., Wostrikoff, K. and Rochaix, J.D. (2000b) Stability determinants in the chloroplast *psbB/T/H* mRNAs of *Chlamydomonas reinhardtii*. Plant J. 21, 469-482.

van Hoof, A., Frischmeyer, P.A., Dietz, H.C., and Parker, R. (2002). Exosome-mediated recognition and degradation of mRNAs lacking a termination codon. Science 295, 2262–2264.

Vestergaard, B., Van, L.B., Andersen, G.R., Nyborg, J., Buckingham, R.H. and Kjeldgaard, M. (2001). Bacterial polypeptide release factor RF2 is structurally distinct from eukaryotic eRF1. Mol. Cell 8, 1375–1382.

Vitale, G., Fabre, E. and Hurt, E.C. (1996) NBP35 encodes an essential and evolutionary conserved protein *Saccharomyces cerevisiae* with homology to a superfamily of bacterial ATPases. Gene 178, 97-106.

von Heijne, G. (1990) Protein targeting signals. Curr. Opin. Cell Biol. 2, 604–608.

Voss, H., Tamames, J., Teodoru, C., Valencia, A., Sensen, C., Wiemann, S., Schwager, C., Zimmermann, J., Sander, C. and Ansorge, W. (1995) Nucleotide sequence and analysis of the centromeric region of yeast chromosome IX. Yeast 11, 61-78.

Vothknecht, U.C. and Westhoff, P. (2001) Biogenesis and origin of thylakoid membranes. Biochim. Biophys. Acta 1541, 91-101.

Wächtershäuser, G. (1992) Groundworks for an evolutionary biochemistry: the iron-sulphur world. Prog. Biophys. Mol. Biol. 58, 85-201.

Walker, J.E., Saraste, M., Runswick, M.J. and Gay, N.J. (1982) Distantly related sequences in the alpha- and beta-subunits of ATP synthase, myosin, kinases and other ATP-requiring enzymes and a common nucleotide binding fold. EMBO J. 1, 945-951.

Watanabe, T., Sugita, M. and Sugiura, M. (1998) Identification of 10Sa RNA (tmRNA) homologues from the cyanobacterium *Synechococcus* sp. strain PCC 6301 and related organisms. Biochim. Biophys. Acta 1396, 97-104.

Weigel, M., Pesaresi, P. and Leister, D. (2003) Tracking the function of the cytochrome c_6-like protein in higher plants. Trends Plant Sci. 8, 513-517.

Westhoff, P. and Herrmann, R.G. (1988) Complex RNA maturation in chloroplasts: The *psbB* operon from spinach. Eur. J. Biochem. 171, 551-564.

Westhoff, P., Offermann-Steinhard, K., Höfer, M., Eskins, K., Oswald, A., and Streubel, M. (1991) Differential accumulation of plastid transcripts encoding photosystem II components in the mesophyll and bundle-sheat cells of monocotyledonous NADP-malic enzyme-type C4 plants. Planta 184, 377-388.

Wilde, A., Lunser, K., Ossenbühl, F., Nickelsen, J. and Börner, T. (2001) Characterization of the cyanobacterial *ycf37*: mutation decreases the photosystem I. Biochem. J. 357, 211-216.

Wilson, R., Ainscough, R., Anderson, K., Baynes, C., Berks, M., Bonfield, J., Burton, J., Connell, M., Copsey, T. and Cooper, J. (1994) 2.2 Mb of contiguous nucleotide sequence from chromosome III of *C. elegans*. Nature 368, 32-38.

Wimberly, B.T., Brodersen, D.E., Clemons, W.M. Jr., Morgan-Warren, R.J., Carter, A.P., Vonrhein, C., Hartsch, T. and Ramakrishnan, V. (2000) Structure of the 30S ribosomal subunit. Nature 407, 327-339.

Wittwer, C.T., Herrmann, M.G., Moss, A.A. and Rasmussen, R.P. (1997a) Continuous fluorescence monitoring of rapid cycle DNA amplification. Biotechniques 22, 130-131, 134-138.

Wittwer, C.T., Ririe, K.M., Andrew, R.V., David, D.A., Gundry, R.A. and Balis, U.J. (1997b) The LightCycler: a microvolume multisample fluorimeter with rapid temperature control. Biotechniques 22, 176-181.

Wollman, F.A., Minai, L. and Nechushtai, R. (1999) The biogenesis and assembly of photosynthetic proteins in thylakoid membranes. Biochim. Biophys. Acta 1411, 21-85.

Wostrikoff, K., Girard-Bascou, J., Wollman, F.A. and Choquet, Y. (2004) Biogenesis of PSI involves a cascade of translational autoregulation in the chloroplast of *Chlamydomonas*. EMBO J. 23, 2696–2705.

Xiong, J., Fischer, W.M., Inoue, K., Nakahara, M. and Bauer, C.E. (2000) Molecular evidence for the early evolution of photosynthesis. Science 289, 1724-1730.

Yabe, T., Morimoto, K., Kikuchi, S., Nishio, K., Terashima, I. and Nakai, M. (2004) The *Arabidopsis* chloroplastic NifU-like protein CnfU, which can act as an iron-sulfur cluster scaffold protein, is required for biogenesis of ferredoxin and photosystem I. Plant Cell 16, 993–1007.

Yamaguchi, K. and Subramanian, A.R. (2000) The plastid ribosomal proteins. Identification of all the proteins in the 50 S subunit of an organelle ribosome (chloroplast). J. Biol. Chem. 275, 28466-28482.

Yamaguchi, K. and Subramanian, A.R. (2003) Proteomic identification of all plastid-specific ribosomal proteins in higher plant chloroplast 30S ribosomal subunit. Eur. J. Biochem. 270, 190-205.

Yang, J., Schuster, G. and Stern, D.B. (1996) CSP41, a sequence-specific chloroplast mRNA binding protein, is an endoribonuclease. Plant Cell 8, 1409-1420.

Yohn, C.B., Cohen, A., Danon, A. and Mayfield, S.P. (1998) A poly(A) binding protein functions in the chloroplast as a message-specific translation factor. Proc. Natl. Acad. Sci. USA 95, 2238-2243.

Yu, J., Vassiliev, I.R., Jung, Y.S., Golbeck, J.H. and McIntosh, L. (1997) Strains of *Synechocystis* sp. PCC 6803 with altered PsaC. I. Mutations incorporated in the cysteine ligands of the two [4Fe-4S] clusters F_A and F_B of photosystem I. J. Biol. Chem. 272, 8032-8039.

Yu, J.P., Smart, L.B., Jung, Y.S., Golbeck, J. and McIntosh, L. (1995) Absence of PsaC subunit allows assembly of photosystem I core but prevents the binding of PsaD and PsaE in *Synechocystis* sp. PCC 6803. Plant Mol. Biol. 29, 331–42.

Yuvaniyama, P., Agar, J.N., Cash, V.L., Johnson, M.K. and Dean, D.R. (2000) NifS-directed assembly of a transient [2Fe-2S] cluster within the NifU protein. Proc. Natl. Acad. Sci. USA 97, 599-604.

Zak, E. and Pakrasi, H.B. (2000) The BtpA protein stabilizes the reaction center proteins of photosystem I in the cyanobacterium *Synechocystis* sp. PCC 6803 at low temperature. Plant Physiol. 123, 215-222.

Zerges, W. (2000) Translation in chloroplasts. Biochimie 82, 583–601.

Zerges, W., Auchincloss, A.H. and Rochaix, J.D. (2003) Multiple translational control sequences in the 5' leader of the chloroplast *psbC* mRNA interact with nuclear gene products in *Chlamydomonas reinhardtii*. Genetics 163, 895-904.

Zhu, T. (2003) Global analysis of gene expression using GeneChip microarrays. Curr. Opin. Plant Biol. 6, 418-425.

Zou, Z., Eibl, C. and Koop, H.U. (2003) The stem-loop region of the tobacco *psbA* 5'UTR is an important determinant of mRNA stability and translation efficiency. Mol. Genet. Genomics 269, 340-349.

Zuker, M., Mathews, D.H. and Turner, D.H. (1999) Algorithms and thermodynamics for RNA secondary structure prediction: A practical guide. In: RNA biochemistry and biotechnology (Barciszewski, J. and Clark, B.F.C., eds) New York: Kluwer Academic Publishers, pp. 11–43.

Zuo, Y. and Deutscher, M.P. (2001) Exoribonuclease superfamilies: structural analysis and phylogenetic distribution. Nucl. Acids Res. 29, 1017-1026.

Acknowledgements

This work was performed at the Department I of the Botanical Institute of the Ludwig-Maximilians-University in Munich in the laboratory of Prof. Dr. R.G. Herrmann. I would like to thank Prof. Dr. Herrmann for providing me the possibility to perform my PhD work in his laboratory and excellent working conditions, for discussing the data, the financial support in the beginning of my PhD study and for reviewing this work.

I am very grateful to the supervisor of my study Dr. Jörg Meurer for introducing me into the plant molecular biology field and giving me exciting projects, for his ideas and critical discussions, permanent support and understanding, inexhaustible energy and sense of humour, which gave great motivation and made life more rich and exciting.

I am thankful to Prof. Dr. Scheer for reviewing this work.

I would like to thank especially Elli Gerick for her excellent technical assistance in the lab and for the possibility to have many nice lunch hours at nice places. I am grateful to Ingrid Duschaneck and Dr. Martina Silber for help with sequencing, Claudia Nickel for support with protein analyses and Uli Wißnet for taking care of the plants.

I am grateful to my colleague Katrin Amann for collaboration on the *hcf101* mutant and for the nice time we spent together also outside the lab. I thank Dr. Staver Bezhani for performing the AtprfB import experiment and Prof. Dr. Wanner for the electron micrographs.

Many thanks to all my colleagues, especially to Cristina, Jefferson, Won, Pavan, Stephan, Lada, Jarda, Manfred, Rainer, Christian, Julia, Sabine, Michi, Peter, Anja, Holger, Anna, Lena, Irina P. and Misha, Giusy, Irina G., Martin, Gabi, Jutta, Irmi, Cordelia, Pat, Petra for their help and support and creating nice atmosphere. I am thankful to Giusy also for coffee support, which helped me to stay in working form during difficult morning hours. I would like to thank Jutta for providing me the place to live in the beginning of my stay in Munich and for good time I could spend in her house.

I thank very much my family for care and support during all my study.

Curriculum vitae

Personal data

Family name:	Lezhneva
First name:	Lina
Home address:	Klugstr. 93, 80637 München
Date of birth:	18.07.1971
Place of birth:	Salesje/Grodnenskaja, Belarus
Marrial status:	single

School education

1978 – 1988
Secondary School, Machulishchi / Minsk, Belarus.
Graduation with a Gold Medal, *June 1988*

Academic education

August 1999 – March 2005
Post-graduate study at the Botanic Institute of the Ludwig-Maximilians-University, Munich

October 1998 – July 1999
DAAD (Deutscher Akademischer Austauschdienst) scholarship for the Friedrich-Schiller-University of Jena, Institute of General Botany

September 1988 – June 1993
Study of biology at the Biology Faculty of the Byelorussian State University, Minsk, Belarus.
Major - Plant Physiology and Biochemistry.
Graduated with Honors, *June 1993*

Experience

November 1993 - September 1998
Researcher, Institute of Photobiology, Minsk, Belarus

August 1993 - November 1993
Biology teacher, Secondary School, Machulishchi / Minsk, Belarus.

March 1992 - December 1992
Laboratory Assistant, Byelorussian State University, the Faculty of Biology, Minsk, Belarus.

Publications

1. Lezhneva, L. and Meurer, J. **(2004)** The nuclear factor HCF145 affects chloroplast *psaA-psaB-rps14* transcript abundance in *Arabidopsis thaliana*. **Plant J.** 38, 740-753.

2. Lezhneva, L., Amann, K. and Meurer, J. **(2004)** The universally conserved HCF101 protein is involved in assembly of [4Fe-4S]-cluster-containing complexes in *Arabidopsis thaliana* chloroplasts. **Plant J.** 37, 174-185.

3. Amann, K., Lezhneva, L., Wanner, G., Herrmann, R.G. and Meurer J. **(2004)** ACCUMULATION OF PHOTOSYSTEM ONE1, a member of a novel gene family, is required for accumulation of [4Fe-4S] cluster-containing chloroplast complexes and antenna proteins. **Plant Cell** 16, 3084-3097.

4. Dal Bosco, C., Lezhneva, L., Biehl, A., Leister, D., Strotmann, H., Wanner, G. and Meurer, J. **(2004)** Inactivation of the chloroplast ATP synthase gamma subunit results in high non-photochemical fluorescence quenching and altered nuclear gene expression in *Arabidopsis thaliana*. **J. Biol. Chem.** 279, 1060-1069.

5. Meurer, J., Lezhneva, L., Amann, K., Gödel, M., Bezhani, S., Sherameti, I. and Oelmüller, R. **(2002)** A peptide chain release factor 2 affects the stability of UGA-containing transcripts in Arabidopsis chloroplasts. **Plant Cell** 14, 3255-3269.

6. Usatov, A., Rassadina, V., Averina, N., Lezhneva, L., Dudko, Y., Mashkina, E., Prikhozhenko, E. and Kolokolova, N. **(2004)** Structural and functional characteristics of the mutant plastids from extranuclear variegated forms of sunflower. **Russ. J. Plant Physiol.** 51, 156-163.

7. Lezhneva, L., Rassadina, V., Yaronskaya, E., Radyuk, M., Taran, S. and Averina N. **(2001)** Activity of the Fe-branch of tetrapyrrole biosynthesis in the chlorophyll-deficient plastome mutant of sunflower. **Russ. J. Plant Physiol.** 48, 57-61.

8. Rassadina, V., Lezhneva, L., Yaronskaya, E., Taran, S. and Averina N. **(2001)** The biogenesis of the photosynthetic apparatus and the activity of chlorophyll biosynthesis in a plastome mutant of sunflower. **Russ. J. Plant Physiol.** 48, 148-154.

9. Vezitskii, A., Lezhneva, L., Shcherbakov, R., Rassadina, V., and Averina, N. **(1999)** Activity of chlorophyll synthetase and chlorophyll *b* reductase in the chlorophyll-deficient plastome mutant of sunflower. **Russ. J. Plant Physiol.** 46, 580–585.

Oral presentations at conferences and seminars

Phylogenetic integration of plastid transcript regulation into the compartmentalized genome of the eukaryote

- TR1-SFB meeting; Utting, 2001
- TR1-SFB meeting; Freising, 2004

Phylogeny and regulation of plastid ribosomal release

- ISE-G meeting; Blaubeuren, 2002

Photosystem I biogenesis in higher plants

- Seminar in the laboratory of Prof.Dr. Apel in ETH, Zürich, 2005
- FEBS Advanced Lecture Course on Origin and Evolution of Mitochondria and Chloroplasts, Wildbad Kreuth, 2005

Eidesstattliche Erklärung:

Hiermit versichere ich, daß ich die vorliegende Arbeit selbständig und nur unter Verwendung der angegebenen Hilfsmittel und Quellen angefertigt habe.

München, März 2005

Lina Lezhneva